Performance analysis of switching systems

Performance analysis of switching systems

Roel van den Berg

A catalogue record is available from the Eindhoven University of Technology Library
ISBN: 978-90-386-1344-4

Performance analysis of switching systems / by R.A. van den Berg – Eindhoven : Technische Universiteit Eindhoven, 2008

Reproduction: Universiteitsdrukkerij Technische Universiteit Eindhoven
Cover design: Marieke Steegh

Performance analysis of switching systems

PROEFSCHRIFT

ter verkrijging van de graad van doctor aan de
Technische Universiteit Eindhoven, op gezag van de
Rector Magnificus, prof.dr.ir. C.J. van Duijn, voor een
commissie aangewezen door het College voor
Promoties in het openbaar te verdedigen
op dinsdag 19 augustus 2008 om 16.00 uur

door

Roelof Alexander van den Berg

geboren te Roosendaal en Nispen

Dit proefschrift is goedgekeurd door de promotoren:

prof.dr.ir. J.E. Rooda
en
prof.dr. A.L. Fradkov

Copromotor:
dr. A.Y. Pogromsky

Preface

This thesis presents the results of four years of work in the Systems Engineering Group at the Eindhoven University of Technology. Looking back at these four years of my PhD project, I am proud that I have reached this milestone. I have learned many new things about both scientific and less scientific matters, and even though there were some moments at which I lacked the motivation (which PhD student does not recognize this?), I persevered in this challenge. There were also many great moments, such as the participation in several international conferences and workshops, and the achievement of new scientific results. In short, these four years have been a great and valuable experience.

From this place I would like to thank all the people who contributed, one way or the other, to the realization of this thesis. First of all, my gratitude goes to professor Koos Rooda, who gave me the opportunity to perform my PhD project in the Systems Engineering Group, and who was always there for me when I needed his opinion. Furthermore, a great word of thanks goes to my co-promotor Sasha Pogromsky, with whom I had many fruitful discussions. Without his constant support and advice, this thesis would not have appeared in its current form. I also would like to thank my second promotor, professor Alexander Fradkov, for his valuable comments on my thesis, and the pleasant cooperation during my visit in St. Petersburg.

I am grateful to professor Onno Boxma, doctor Bernard Brogliato, and professor Rodolphe Sepulchre for accepting to be in my PhD committee and for their valuable comments on my thesis.

Furthermore, a special thanks goes to Frans Soers and Henk van Rooy for their help with the construction of the experimental setup. I also want to thank all the students who made a contribution to my PhD project. In particular, I want to thank former graduate student William van den Bremer for his contribution to Chapter 5 of this thesis.

I am also grateful for the financial support of the Dutch-Russian program "Dynamics and Control of Hybrid Mechanical Systems" (NWO grant 047.017.018, co-leaders H. Nijmeijer and

G.A. Leonov) that I received for the participation in several conferences.

These years at the Systems Engineering Group have passed by very quickly, as ‘time flies when you are having fun’. I want to thank all my colleagues from the group for the pleasant working environment they created. A great word of thanks goes to my (former) roommates Joost van Eekelen, Bas Roset, and Mihály Petreczky, and to the ‘guys from the basement’ Ad Kock, Casper Veeger, Maarten Hendriks, Michiel Stoets, Ricky Andriansyah, and Simon Tosserams. Thank you for all the fun, the good and bad jokes, the lively discussions, and the experiences we shared. Thank you also, Mieke Lousberg, for your assistance in the many non-technical aspects of my PhD project.

Finally, I want to thank my family and friends for their interest and support during these years. A special word of gratitude goes to my wife Willemijn for her endless love and patience, especially in the last few months.

Roel van den Berg
Eindhoven, June 2008

Summary

Performance analysis of switching systems

Performance analysis is an important aspect in the design of dynamic (control) systems. Without a proper analysis of the behavior of a system, it is impossible to guarantee that a certain design satisfies the system's requirements. For linear time-invariant systems, accurate performance analyses are relatively easy to make and as a result also many linear (controller) design methods have appeared in the past. For nonlinear systems, on the other hand, such accurate performance analyses and controller design methods are in general not available. A main reason hereof is that nonlinear systems, as opposed to linear time-invariant systems, can have multiple steady-state solutions. Due to the coexistence of multiple steady-state solutions, it is much harder to define an accurate performance index. Some nonlinear systems, i.e. the so-called convergent nonlinear systems, however, are characterized by a *unique* steady-state solution. This steady-state solution may depend on the system's input signals (e.g. reference signals), but is independent of the initial conditions of the system. In the past, the notion of convergent systems has already been proven to be very useful in the performance analysis of nonlinear systems with inputs.

In this thesis, new results in the field of performance analysis of nonlinear systems with inputs are presented, based on the notion of convergent systems. One part of the thesis is concerned with the question "how to analyse the performance for a convergent system?" Since the behavior of a convergent system is independent of the initial conditions (after some transient time), simulation can be used to find the unique steady-state solution that corresponds to a certain input signal, but this can be very time-consuming. In this thesis, a computationally more efficient approach is presented to estimate the steady-state performance of harmonically forced Lur'e systems, in terms of nonlinear frequency response functions (nFRFs). This approach is based on the method of harmonic linearization. It provides both a linear approximation of the nFRF and an upper bound on the error between this linear approximation and the true nFRF. It is shown in several examples that the approximation of the nFRF is accurate, and that it provides more detailed information on the considered system than the often used '$\mathscr{L}_2$ gain' performance index. An additional observation that is made, is that the method of harmonic linearization can sometimes be ‘misleading’ for Lur’e systems with a saturation-like nonlinearity: for the case that the harmonic balance equation has a unique solution, it is shown that the corresponding nonlinear system can have multiple distinct steady-state solutions.

Another part of the thesis is concerned with the question “under what conditions is a system with inputs guaranteed to be convergent?” In particular two types of systems were investigated: switched linear systems and Lur’e systems with a saturation nonlinearity and marginally stable linear part.

For the switched linear systems, it is assumed that the dynamics of all the separate linear modes are given. For this setting, it was investigated if it is possible to find a switching rule (which defines when to switch between the available modes) such that the closed-loop system is convergent. Both a state-based, an observer-based, and a time-based switching rule are presented that guarantee a convergent system, assuming some conditions on the linear dynamics are met.

The second type of systems that are discussed, are Lur’e systems with a saturation nonlinearity and marginally stable linear part. For this type of systems, the goal was to find sufficient conditions under which the closed-loop system is convergent. Because of the marginally stable linear part, however, a quadratically convergent system cannot be obtained. Instead, sufficient conditions are discussed that guarantee uniform convergency of the system. The obtained theory is shown to be also applicable to a class of anti-windup systems with a marginally stable plant. For this class of systems, the results of the convergency-based performance analysis are compared with the analysis results of existing anti-windup methods. It is shown that the convergency-based performance analysis can in some cases provide more detailed information on the steady-state behavior of the system.

The results of uniform convergency for anti-windup systems are shown to be also applicable in the field of production and inventory control of discrete-event manufacturing systems. Since a manufacturing machine has a certain production capacity and cannot produce at a negative rate, it can be seen as an integrator plant (input: production rate, output: amount of finished products) preceded by a saturation function. For this marginally stable plant, a controller was constructed in such a way that the closed-loop system is uniformly convergent. The controller was also implemented in the discrete-event domain and the results from discrete-event simulations were compared with those of continuous-time simulations. Similarly, the controller was also applied for the production and inventory control of a line of four manufacturing machines. For both the single machine and the line of four machines, the resulting controlled discrete-event systems are shown to have the desired tracking properties.

Besides these theoretical and numerical results, also experimental results are presented in this thesis. By means of an electromechanical construction, several experimental results were obtained, and used to validate the theoretical results for both the switched linear systems and the anti-windup systems.

Contents

Preface **v**

Summary **vii**

1 Introduction **1**

1.1 Performance analysis of nonlinear systems with external inputs . . . 1

1.2 Notion of convergent systems . . . 3

1.3 Contribution of the thesis . . . 4

1.4 Outline of the thesis . . . 6

1.5 Summary of publications . . . 7

2 Mathematical Preliminaries **9**

2.1 Stability concepts . . . 9

2.2 S-procedure . . . 10

2.3 $\mathscr{L}_2$ gain . . . 11

2.4 Convergent systems . . . 13

2.5 Harmonic linearization . . . 16

3 Harmonic Linearization for Harmonically Forced Lur'e Systems **21**

3.1 Introduction . . . 21

3.2 Harmonic linearization . . . 22

3.3 Well-posedness . . . 26

3.4 Accuracy . . . 28

3.5 Illustrating examples 32
3.6 Discussion 37

4 Performance Analysis for Externally Forced Lur'e Systems with Saturation 39
4.1 Introduction 39
4.2 Uniform convergency for Lur'e systems with saturation and marginally stable linear part 41
4.3 Uniform convergency for anti-windup systems with a marginally stable plant . . 45
4.4 Case study 1: Performance analysis of an anti-windup system with an integrator plant 48
4.5 Case study 2: Performance analysis of an anti-windup system with a 'mass-spring-damper' plant 56
4.6 Discussion 61

5 Feedback Control of Manufacturing Machines 63
5.1 Introduction 63
5.2 Feedback control of a single machine 65
5.3 Feedback control of a line of machines 75
5.4 Discussion 80

6 Performance Analysis of Switched Linear Systems under Specific Switching Rule Design 83
6.1 Introduction 84
6.2 Convergent system design using switching rules 85
6.3 Case study: Performance analysis of a switched linear system 91
6.4 Discussion 98

7 Conclusions and Recommendations 101
7.1 Conclusions 101
7.2 Recommendations for future research 104

Bibliography 114

A Experimental Setup: System Identification 115

Samenvatting 117

Curriculum Vitae 121

Chapter 1

Introduction

Abstract In this chapter, a general introduction is given to the performance analysis of externally forced nonlinear systems. First, a picture is sketched of the problems that arise in the performance analysis of nonlinear systems with external inputs. Then, a brief introduction is presented to the notion of convergent systems, which is used as a cornerstone in this thesis to study nonlinear performance analysis. The second part of this chapter gives an overview of the contributions to the field that are made in this thesis, and presents an outline of the remainder of this thesis. In addition to the literature that is reviewed in this chapter, a more detailed overview of relevant literature is given in the introduction of each chapter for the research discussed in that chapter.

1.1 Performance analysis of nonlinear systems with external inputs

Performance analysis is an important aspect in decision-making and control, and is present in daily life in many different forms. For example, one can ask oneself: “am I still driving on the (correct) road and is this really the fastest way from Eindhoven to Amsterdam?” or “is the isolation of my house good enough to keep out the noise of the neighbors?” Every time such a question is asked, one is in fact analysing the performance of some system. Once the question has been answered, i.e. the performance has been analysed, one can decide to do nothing (if the result is satisfactory) or to take action to improve the performance.

In the field of design and control of dynamic systems, performance analysis is also very relevant. The (controller) design of such a system is often directly coupled to the performance of that system. That is, a controller is designed in such a way that the closed-loop system satisfies certain performance conditions. Or, if a certain task needs to be executed and several dynamic systems are available for this goal, then (probably) the dynamic system is selected which has the best performance with respect to that task.

But what is performance exactly? The notion of performance is not rigorously defined, but is often expressed by means of some performance indices that are selected to describe relevant behavior. In the field of dynamics and control the performance indices that are used to express the performance of a system can be roughly divided into three groups: performance indices for transient behavior (e.g. convergence rate), for steady-state behavior (e.g. how good is the reference tracking or disturbance rejection?), and for more general properties of a system (e.g. reachable set using certain inputs, or domain of attraction for a certain solution). For example, consider a manufacturing machine. Once warmed up, this machine is able to process 100 items per hour, which is an indication of the steady-state performance of the system. Furthermore, this machine requires 15 minutes to ramp up from idle to full production speed, which falls within the category of transient performance. A more general property of the system is for example that the machine can process three different types of items.

For linear time-invariant (LTI) systems, it is often easy to find performance indices that describe the exact behavior of the system. This is due to the property that all dynamics of this system are linear, and therefore (in a stable setting) solutions with different initial conditions eventually converge to a unique steady-state solution, which may depend on external inputs but is independent of the initial conditions of the system. As a result it is possible to uniquely describe both the transient and steady-state response of a system to a certain input signal in the time domain, or the steady-state response to a certain input signal in the frequency domain, see e.g. [21]. Due to the superposition principle for linear systems not only system responses to harmonic input signals can be determined, but also systems responses to all other input signals that can be written as a Fourier series can be constructed. Furthermore, as a result of this ease of analysis, many controller design methods have become available for linear systems, see e.g. [21, 87]. These design methods are also widely used in industry.

An important reason why nonlinear (control) systems are currently not popular in industry, even though they can provide a wider range of dynamics than linear systems, is the lack of proper performance analyses and controller design methods for nonlinear systems. A main reason why it is less straightforward to define performance indices for nonlinear systems, is that multiple steady-state solutions may coexist and the dynamics may depend on the initial condition of the system. For nonlinear systems with constant (or zero) inputs, one can in some cases still determine stability and (approximative) domain of attraction of equilibrium points, e.g. using Lyapunov theory, see [40, 81]. However, for nonlinear systems with time-varying inputs, it is much harder to describe the exact system behavior using performance indices. In literature, an often used performance index for the description of input-output behavior of such systems is the $\mathscr{L}_p$ gain for some $1 \leq p \leq \infty$. A disadvantage of this performance index is that it only provides a rough estimate on the 'worst-case' input-output behavior of the system. That is, since multiple steady-state solutions may coexist, the $\mathscr{L}_p$ gain only indicates the 'worst-case' behavior (i.e. the steady-state solution with the largest $\mathscr{L}_p$ norm), and provides no knowledge at all on whether or not other (more desirable) steady-state solutions exist as well. Also, a disadvantage of the $\mathscr{L}_p$ gain is that in the computation of this gain no specific properties of the input signal are involved except for its $\mathscr{L}_p$ norm. As a consequence, completely different input signals (e.g. a harmonic signal vs. white noise) with an identical $\mathscr{L}_p$ norm, result in the same estimate for the $\mathscr{L}_p$ norm of the output.

The main reason that the nonlinear system response to some input signal cannot be uniquely described in general, is that this response may depend on the initial conditions of the system. In view of this problem, it is interesting to note that there exists a subclass of nonlinear systems, i.e. the class of convergent systems, for which the steady-state solution does *not* depend on the initial conditions of the system. As a result of this property it is easier to describe the exact behavior, and hence to accurately evaluate the performance of such a system. In this thesis, the notion of convergent systems is therefore used as a cornerstone for the performance analysis of nonlinear systems with external inputs. This notion of convergent systems is discussed in the following section.

1.2 Notion of convergent systems

The most striking property that distinguishes convergent systems from general nonlinear systems is that the solutions of a convergent system 'forget' their initial conditions, and after some transient time the dynamics of the system only depends on the system's input signal(s). This property, which is a natural property for all asymptotically stable *linear* systems, is very attractive in the field of dynamics and control. It guarantees that the system has only one steady-state solution, and hence performance analysis of these convergent systems is much easier than for general nonlinear systems. Furthermore, it is also a useful property in synchronization problems, observer design, and reference tracking problems, see e.g. [64, 70] and references therein. In these cases, the system or controller is designed mainly to get rid of the solution's dependency on initial conditions.

The property that a solution of a nonlinear system 'forgets' its initial conditions has been addressed several times in literature. The notion of convergent systems was introduced in the 1960's by Demidovich, Pliss and Yakubovich [11, 12, 69, 109], see also [63]. In the same period, the idea of solutions that converge to each other, was also investigated by LaSalle and Lefschetz [43], and Yoshisawa [110]. In the 1990's, the interest in the convergent system property revived, and similar notions appeared, such as incremental stability and contraction analysis, see e.g. [3, 23, 52] and references therein. In recent years, new results in this field were obtained on so-called 'quadratic convergency' of piecewise affine (PWA) systems [65], and on performance analysis for convergent systems using nonlinear frequency response functions [66]. In this thesis, new results on convergent systems and performance analysis of nonlinear systems are presented, as explained in the following section. Formal definitions and properties of convergent systems are presented later on in this thesis.

In the past, the notion of convergent systems has already been shown to be useful in the performance analysis of nonlinear systems. However, more research on this subject is required to fully understand the possibilities of this notion. It may be used to 'fill the gap' between nonlinear (control) systems and well-understood linear (control) systems, such that in the future the rich dynamics of nonlinear systems can be exploited to the fullest.

1.3 Contribution of the thesis

The general objective of the research that is described in this thesis is to extend the results in the ongoing investigation on performance analysis of externally forced nonlinear systems, based on the notion of convergent systems. In line with this objective, four problems are considered in particular

- Under what conditions is a system guaranteed to be convergent?
- In what way can the performance of a convergent nonlinear system with inputs be evaluated?
- For what applications can the results that are obtained during the research be used?
- Can the theoretical results be validated using simulation and real-time experiments?

In this thesis, contributions are made to each of these problems. In the remainder of this section the specific contributions of this thesis are presented. Furthermore, at the introduction of each chapter (Chapters 3-6), the relationship of each contribution with existing results in literature is discussed in more detail.

In literature, already several results are available that provide sufficient conditions to guarantee convergency for several types of systems, see e.g. [63–65] and references therein. In this thesis, two types of externally forced 'switching' systems are investigated for which such a proof of convergency did not yet exist, i.e. switched linear systems and 'marginally stable' Lur'e systems with a saturation nonlinearity (the latter system can be seen as a 'switching' system, as it switches between a linear mode and saturated modes).

The considered switched linear systems consist of two or more linear subsystems and a switching rule that governs the switching between those subsystems. These systems are widely studied in literature, see e.g. [48, 59, 60, 82, 89], and have been shown to be especially useful in adaptive and robust control problems. Furthermore, it has been shown for these systems that by appropriate switching between the available linear subsystems, the performance (e.g. transient response) of the closed-loop system can be improved in comparison with the performance of the linear subsystems, see e.g. [16]. In this thesis, the dynamics of all separate linear modes are assumed to be given, and it is investigated if it is possible to find a switching rule such that the closed-loop system is convergent for a wide class of external inputs. If the system can be made convergent by proper switching, then also the steady-state performance of such systems with inputs can be evaluated and compared to the performance of the corresponding linear systems. In order to find a proof for convergency, both a state-based, an observer-based, and a time-based switching rule are considered. For each type of switching rule, sufficient conditions are sought under which the closed-loop system is convergent. A property of the considered switching rules is that they allow infinitely fast switching (sliding mode). In order to investigate how these switching rules behave in a real-time environment (with only a finite sample rate), the results of real-time experiments (performed on an experimental setup) are analysed.

The second class of systems that is discussed in this thesis is the class of externally forced Lur'e systems with a saturation nonlinearity and marginally stable linear part. Most results on general convergent systems in literature are aimed on proving quadratic convergency, see e.g. [63, 65], however, these results are not applicable for a system that is marginally stable. Therefore, in this thesis, sufficient conditions are sought for a weaker form of convergency, i.e. 'uniform' convergency.

An application area in which this uniform convergency property can be useful is the anti-windup design for linear control systems with actuator saturation and a marginally stable plant. Actuator saturation is a phenomenon that is ubiquitous in control systems, since actuators have only a limited range of operation, and can have disastrous consequences, such as the fighter crashes in 1992 [14] and 1993 [86]. The research on anti-windup compensation, see e.g. [21, 22, 41, 90], is focussed on preventing these consequences and restoring the original (linear) dynamics as much as possible. In this thesis, the obtained theory on uniform convergency is applied to these systems with anti-windup compensation, and the steady-state performance of the systems is analysed. Since several anti-windup methods exist in literature, see e.g. [39, 90], a comparison is made to clarify the exact differences between this convergent systems approach and existing anti-windup methods. Furthermore, simulations and real-time experiments (on an experimental setup) are performed to support the theoretical results.

Another application field that is considered, is the production and inventory control of manufacturing systems. These systems are often characterized by discrete-event behavior, which makes it difficult to construct a proper controller, especially for large systems. If, however, the system is approximated by a continuous flow model [2], then standard control theory can be applied to control the production and inventory of the system, see e.g. [28, 85, 105]. Since a manufacturing machine has a certain production capacity and cannot have a negative production rate, such a machine can be seen as an integrator preceded by a saturation nonlinearity. Using the obtained results on convergent anti-windup design for systems with a marginally stable plant, a controller is constructed for this machine in such a way that the closed-loop system is uniformly convergent. The controller is also implemented in the discrete-event domain and the results from discrete-event simulations are compared with those of continuous-time simulations. Similarly, the controller is also applied for the production and inventory control of a line of manufacturing machines.

With respect to the performance analysis of convergent nonlinear systems, some results are currently available in literature. For example, it is already known that for convergent systems, simulation can be used as a reliable analysis tool, and that by means of simulation also nonlinear frequency response functions (nFRFs) can be constructed, see e.g. [66]. This is a quite useful result, since it allows a performance analysis of nonlinear systems, which is very similar to a common performance analysis of linear systems, i.e. investigation of a system's steady-state response to harmonic excitations with different frequencies. A disadvantage, however, of this simulation-based analysis is that it can be very time-consuming. In this thesis, therefore, a more time-efficient alternative to the simulation-based analysis is investigated for the construction of nFRFs. This alternative is based on the method of harmonic linearization and results in an approximative nFRF together with an upper bound on the error between the approximative nFRF and the true nFRF. This alternative is applied together with the existing simulation-based analysis to evaluate the performance in terms of nFRFs of all considered systems in this thesis.

1.4 Outline of the thesis

This thesis is organized as follows. Chapter 2 contains the preliminaries that are used throughout the thesis. It recalls several concepts of stability of solutions and ultimate boundedness. It also recalls the S-procedure and the definition of $\mathscr{L}_2$ gain, and provides a way of computing this gain using linear matrix inequalities. Furthermore, it presents several definitions and properties of convergent systems. Finally, it gives a short description of the method of harmonic linearization for autonomous nonlinear systems of Lur'e type. This method is discussed further in Chapter 3.

Chapters 3-6 contain the main results of this thesis. These chapters all start with an introduction that gives a motivation for the research presented in that chapter and a comparison with related literature. Furthermore, each of these chapters ends with a 'Discussion'-section, in which the results presented in that chapter are summarized and final comments on these results are made.

In Chapter 3, the method of harmonic linearization is applied to analyse harmonically forced Lur'e systems in the frequency domain. For this purpose, the method of harmonic linearization as summarized in Chapter 2 is extended, and both the well-posedness and the accuracy of the resulting harmonic linearization are discussed. The presented theory is illustrated by means of three examples, in which it becomes clear that the nonlinear frequency response functions can often be accurately approximated using harmonic linearization. The results as presented in this chapter are also used for performance analysis in the remaining chapters.

In Chapter 4, a theorem is derived to establish uniform convergency for externally forced Lur'e systems with a saturation nonlinearity and marginally stable linear part. The result is also applied to the field of anti-windup systems with a marginally stable plant, where it is used to analyse the steady-state performance of such systems. After a discussion on the differences between this convergent systems approach and existing anti-windup methods, two case-studies are performed to illustrate the obtained theoretical result. The case-studies are supported by both simulation and experimental results.

In Chapter 5, the results of Chapter 4 on convergent anti-windup design are used for another application, i.e. for the production control of a discrete-event manufacturing system. Here, a manufacturing machine is interpreted as an integrator plant preceded by a saturation nonlinearity. An anti-windup controller is constructed that guarantees a convergent closed-loop system. The controller is also implemented in the discrete-event domain and simulations in both the continuous-time and discrete-event domain are compared. Finally, the controller is applied for the production rate control of a manufacturing line.

A different kind of 'switching' system is considered in Chapter 6. This chapter deals with switched linear systems, for which it is assumed that the dynamics of the separate linear modes are fixed. It is discussed if for such systems a switching rule and some accompanying conditions can be found so that the closed-loop system is guaranteed to be convergent. Both state-dependent, (observer-based) output-dependent, and time-dependent switching rules are considered. The theoretical results are supported by means of a case-study, in which both simulation and experimental results are presented.

Chapter 7 contains the conclusions of this thesis and recommendations for future research.

1.5 Summary of publications

This thesis is mostly based on conference and journal papers, either published or submitted. This section summarizes the relationship between the papers and the chapters in this thesis. Note that some papers are used in more than one chapter.

Chapter 3 contains results presented in:

- [71]: A.Y. Pogromsky, R.A. van den Berg, and J.E. Rooda. Performance analysis of harmonically forced nonlinear systems. *Proceedings of 3rd IFAC Workshop Periodic Control Systems, St.Petersburg, Russia,* 2007.

- [96]: R.A. van den Berg, A.Y. Pogromsky, and J.E. Rooda. Well-posedness and accuracy of harmonic linearization for Lur'e systems. *Proceedings of the 46th IEEE Conference on Decision and Control, New Orleans, USA,* 2007.
- [99]: R.A. van den Berg, A.Y. Pogromsky, and J.E. Rooda. Frequency domain performance analysis of marginally stable LTI systems with saturation. *Proceedings of the 6th EUROMECH Nonlinear Oscillations Conference (ENOC), St.Petersburg, Russia,* 2008.

Chapter 4 contains results presented in:

- [93]: R.A. van den Berg, A.Y. Pogromsky, G.A. Leonov, and J.E. Rooda. Design of convergent switched systems. In *Lecture Notes in Control and Information Sciences 336: Group Coordination and Cooperative Control,* pages 291-311. Springer Verlag, 2006.
- [94]: R.A. van den Berg, A.Y. Pogromsky, and J.E. Rooda. Convergent systems design: Anti-windup for marginally stable plants. *Proceedings of the 45th IEEE Conference on Decision and Control, San Diego, USA,* 2006.
- [100]: R.A. van den Berg, A.Y. Pogromsky, and J.E. Rooda. A new perspective on anti-windup design based on experimental results. *Proceedings of 17th IFAC World Congress, Seoul, Korea,* 2008.
- [98]: R.A. van den Berg, A.Y. Pogromsky, and J.E. Rooda. Uniform convergency for anti-windup systems with a marginally stable plant. *Submitted to a journal,* 2008.

Chapter 5 contains results presented in:

- [102]: W.A.P. van den Bremer, R.A. van den Berg, A.Y. Pogromsky, and J.E. Rooda. Anti-windup based approach to the control of manufacturing machines. *Proceedings of 17th IFAC World Congress, Seoul, Korea,* 2008.
- [72]: A.Y. Pogromsky, R.A. van den Berg, and J.E. Rooda. On cascade interconnections of convergent systems with application to control of manufacturing systems. *Submitted to the 47th IEEE Conference on Decision and Control, Cancun, Mexico,* 2008.

Chapter 6 contains results presented in:

- [93]: R.A. van den Berg, A.Y. Pogromsky, G.A. Leonov, and J.E. Rooda. Design of convergent switched systems. In *Lecture Notes in Control and Information Sciences 336: Group Coordination and Cooperative Control,* pages 291-311. Springer Verlag, 2006.
- [95]: R.A. van den Berg, A.Y. Pogromsky, and J.E. Rooda. Convergent design of switched linear systems. *Proceedings of 2nd IFAC Conference on Analysis and Design of Hybrid System, Alghero, Sardinia,* 2006.

Chapter 2

Mathematical Preliminaries

Abstract In this chapter, several mathematical notions and results are presented that are used throughout this thesis. Section 2.1 deals with the definition of stability for solutions and the definition of ultimate boundedness. Section 2.2 introduces the S-procedure. Section 2.3 gives a definition of $\mathscr{L}_2$ gain and describes how such an $\mathscr{L}_2$ gain can be computed for some systems using linear matrix inequalities (LMIs). Section 2.4 introduces the notion of convergent systems and describes several properties of such systems. Finally, Section 2.5 presents the basic concept of harmonic linearization.

2.1 Stability concepts

Consider the following nonlinear time-varying system

$$\dot{x} = f(x,t) \tag{2.1}$$

where $x \in \mathbb{R}^n$ represents the state of the system, $t \in \mathbb{R}$ represents time, and $f(x,t)$ satisfies some regularity assumptions to guarantee the existence of local solutions. In Definition 2.1, stability of a particular (or all) solution(s) of this system is defined. In this definition, and in the remainder of this thesis, $|\cdot|$ represents the Euclidean norm.

Definition 2.1 ([40]). Solution $\bar{x}$ of system (2.1), defined for all $t \in (t_*, +\infty)$, is said to be

- *stable* if for any $t_0 \in (t_*, +\infty)$ and $\varepsilon > 0$ there exists a $\delta = \delta(\varepsilon, t_0) > 0$ such that $|x(t_0) - \bar{x}(t_0)| < \delta$ implies $|x(t) - \bar{x}(t)| < \varepsilon$ for all $t \geq t_0$;

- *uniformly stable* if it is stable and the number δ in the definition of stability can be chosen independently of t_0;
- *asymptotically stable* if it is stable and for any $t_0 > t_*$ there exists a $\delta = \delta(t_0) > 0$ such that $|x(t_0) - \bar{x}(t_0)| < \delta$ implies $\lim_{t\to\infty} |x(t) - \bar{x}(t)| = 0$;
- *uniformly asymptotically stable* if it is uniformly stable and there exists a $\delta > 0$ (independent of t_0) such that for any $\varepsilon > 0$ there exists a $T = T(\varepsilon) > 0$ such that $|x(t_0) - \bar{x}(t_0)| < \delta$ implies $|x(t) - \bar{x}(t)| < \varepsilon$ for all $t \geq t_0 + T$;
- *exponentially stable* if there exist positive constants δ, C, β such that $|x(t_0) - \bar{x}(t_0)| < \delta$ implies
$$|x(t) - \bar{x}(t)| \leq Ce^{-\beta(t-t_0)}|x(t_0) - \bar{x}(t_0)|;$$
- *globally (uniformly/ asymptotically/ exponentially) stable* if it is (uniformly/ asymptotically/ exponentially) stable and attracts *all* solutions $x(t)$ starting in $(x_0, t_0) \in \mathbb{R}^n \times (t_*, +\infty)$.

Furthermore, global uniform ultimate boundedness of solutions is defined as follows.

Definition 2.2 ([40])**.** The solutions of system (2.1) are *globally uniformly ultimately bounded* with ultimate bound b if there exist a positive constant b, independent of $t_0 > t_*$, and for every $a \geq 0$ there is a $T = T(a,b) \geq 0$, independent of $t_0 > t_*$, such that $|x(t_0)| \leq a$ implies
$$|x(t)| \leq b, \ \ \forall t \geq t_0 + T.$$

For simplicity, in this thesis a *system* is called uniformly ultimately bounded, if its solutions are globally uniformly ultimately bounded.

2.2 S-procedure

The S-procedure is a method that is often used in the area of nonlinear control. A general description of the S-procedure can for example be found in [68]. In this section, the method is briefly recalled.

Let $G_0(x), G_1(x), \ldots, G_k(x)$ be real-valued functionals that are defined on an abstract space $\mathbb{X}$ (here, $\mathbb{X}$ can be $\mathbb{R}^n$ [6, 18], $\mathbb{C}^n$ [18, 19], or $\mathscr{L}_2([0,\infty), \mathbb{R}^n)$ [58, 83, 108]). Furthermore, let $\tau = [\ \tau_1 \ \ldots \ \tau_k\ ]$ be a vector of real numbers and define
$$S(\tau, x) = G_0(x) - \sum_{j=1}^{k} \tau_j G_j(x).$$

Now, consider the following two conditions

1. $G_0(x) \geq 0$ for all $x \in \mathbb{X}$ that satisfy the constraints $G_1(x) \geq 0, \ldots, G_k(x) \geq 0$.

2. There exist constants $\tau_1 \geq 0, \ldots, \tau_k \geq 0$ such that $\sum_{j=1}^{k} \tau_j > 0$ and $S(\tau, x) \geq 0$ for all $x \in \mathbb{X}$.

The term S-procedure refers to the procedure of replacing condition 1 with the stronger condition 2. Condition 2 clearly implies condition 1. However, the reverse is not always true: one can find examples were condition 1 does not imply condition 2. Nevertheless, if one imposes certain additional constraints on $G_0(x), G_1(x), \ldots, G_k(x)$, then condition 1 may also imply condition 2. In this case, the S-procedure is called *lossless*. For example, if $\mathbb{X} = \mathbb{R}^n$ and $G_0(x), G_1(x)$ are quadratic forms on $\mathbb{R}^n$ satisfying condition 1 (with $k = 1$), then there exist constants $\tau_0 \geq 0$ and $\tau_1 \geq 0$ such that $\tau_0 + \tau_1 > 0$ and $\tau_0 G_0(x) - \tau_1 G_1(x) \geq 0$ holds for all $x \in \mathbb{R}^n$, i.e. the S-procedure is lossless [107]. Note that the S-procedure can be similarly applied to strict inequalities, i.e. $G_0(x) > 0$ or $G_1(x) > 0, \ldots, G_k(x) > 0$.

2.3 $\mathscr{L}_2$ gain

Consider the following system

$$\begin{aligned} \dot{x} &= f(x, w), \;\; x(0) = 0 \\ z &= h(x, w) \end{aligned} \tag{2.2}$$

where state x, input w, and performance output z take respectively values in $\mathbb{R}^n$, $\mathbb{R}^m$, and $\mathbb{R}^p$. Furthermore, assume that w, $f(x, w)$ and $h(x, w)$ satisfy some regularity conditions to guarantee the existence of local solutions and local square-integrability of $z(t)$.

For each square-integrable vector-valued function $x \in \mathscr{L}_2([0, \infty), \mathbb{R}^n)$, let $||x||_2$ denote the usual $\mathscr{L}_2$ norm

$$||x||_2 = \left(\int_0^\infty |x(t)|^2 dt \right)^{1/2}.$$

Definition 2.3 ([40])**.** If there exists a nonnegative constant γ such that for any $w \in \mathscr{L}_2([0, \infty), \mathbb{R}^m)$, solution z of (2.2) satisfies

$$||z||_2 \leq \gamma ||w||_2,$$

then system (2.2) has $\mathscr{L}_2$ gain (from w to z) less than or equal to γ. The smallest value of γ for which the above inequality holds, is called the $\mathscr{L}_2$ gain from w to z.

In the remainder of this section, it is shown how an upper bound on the $\mathscr{L}_2$ gain can be computed for some systems using linear matrix inequalities (LMIs), see e.g. [6]. For this purpose, consider a system of Lur'e type

$$\begin{aligned} \dot{x} &= Ax + B\phi(y) + Fw \\ y &= Cx + Dw \\ z &= Hx \end{aligned} \tag{2.3}$$

where $x \in \mathbb{R}^n$ is the state, $w \in \mathbb{R}$ is the input, $y \in \mathbb{R}$ is the output (for feedback), $z \in \mathbb{R}$ is the performance output, and ϕ is a continuous scalar nonlinearity, which satisfies the sector condition

$$0 \leq \frac{\phi(y)}{y} \leq \mu, \ \ \forall y \neq 0, \tag{2.4}$$

for some finite constant μ. A more general result that also includes $\mu = +\infty$ can be derived using the standard results of passivity theory.

First note that if a differentiable storage function $V(x)$ with $V(0) = 0$ can be found for system (2.3) such that

$$\dot{V}(x) \leq \gamma^2 w^T w - z^T z \tag{2.5}$$

for some finite γ, then γ is an upper bound for the $\mathscr{L}_2$ gain of the system. To show this, (2.5) is integrated

$$\int_0^T \dot{V}(x)dt = V(x(T)) - V(x(0)) \leq \int_0^T \gamma^2 w(t)^T w(t)dt - \int_0^T z(t)^T z(t)dt,$$

where $V(x(0)) = 0$. Since $V(x)$ is a nonnegative function, $V(x(T)) \geq 0$ so that

$$0 \leq \int_0^T \gamma^2 w(t)^T w(t)dt - \int_0^T z(t)^T z(t)dt$$

or, equivalently

$$\int_0^T z(t)^T z(t)dt \leq \gamma^2 \int_0^T w(t)^T w(t)dt.$$

If $w \in \mathscr{L}_2([0,\infty),\mathbb{R})$, then one can prove that the limit

$$\lim_{T\to\infty} \int_0^T z(t)^T z(t)dt$$

also exists, i.e. $z \in \mathscr{L}_2([0,\infty),\mathbb{R})$. Taking the square root then results in

$$||z||_2 \leq \gamma ||w||_2$$

which implies that γ is an upper bound on the $\mathscr{L}_2$ gain of the system.

Now, for system (2.3) consider a quadratic storage function $V(x) = x^T P x$ with $P = P^T > 0$, such that inequality (2.5) becomes

$$x^T(PA + A^T P)x + 2x^T PB\phi(y) + 2x^T PFw - \gamma^2 w^T w + x^T H^T Hx \leq 0.$$

In order to find an upper bound on the $\mathscr{L}_2$ gain, this inequality should hold for (at least) all y that satisfy sector condition (2.4). To incorporate the sector condition in the above inequality, the S-procedure (see Section 2.2) is used. By rewriting the sector condition into

$$\phi(y)^2 - \mu\phi(y)y \leq 0$$

and applying the S-procedure, the resulting inequality is

$$x^T(PA+A^TP)x+2x^TPB\phi(y)+2x^TPFw-2\tau\phi(y)^2+2\tau\mu\phi(y)y-\gamma^2w^Tw+x^TH^THx\le 0.$$

This inequality can be written as

$$\begin{bmatrix} x \\ \phi \\ w \end{bmatrix}^T \begin{bmatrix} PA+A^TP+H^TH & PB+\tau\mu C^T & PF \\ B^TP+\tau\mu C & -2\tau & \tau D \\ F^TP & \tau D^T & -\gamma^2 \end{bmatrix} \begin{bmatrix} x \\ \phi \\ w \end{bmatrix} \le 0$$

and is satisfied if the following LMI holds

$$\begin{bmatrix} PA+A^TP+H^TH & PB+\tau\mu C^T & PF \\ B^TP+\tau\mu C & -2\tau & \tau D \\ F^TP & \tau D^T & -\gamma^2 \end{bmatrix} \le 0 \tag{2.6}$$

for some $P=P^T>0$, $\tau\ge 0$ and $\gamma>0$. Computationally efficient LMI solvers, as present in numerical toolboxes such as Yalmip [51], SeDuMi [84], and Matlab's LMI-lab [50], can be used to determine if this LMI is feasible, and to compute the minimal value of γ for which the LMI is still feasible. This minimal value of γ is an upper bound on the $\mathscr{L}_2$ gain of system (2.3).

Note that besides a quadratic storage function $V(x)$, other storage functions can be considered as well for the computation of such an upper bound, see e.g. [49, 75]. This, however, falls outside the scope of this thesis.

2.4 Convergent systems

In this section, first some basic definitions and properties of convergent systems are given that are used in the remainder of this thesis. Subsequently, it is explained why for convergent systems (in contrast to nonlinear systems in general) simulation can be used as a reliable analysis tool. Finally, the results of [66] on nonlinear frequency response functions for convergent systems are briefly discussed.

Consider the following system

$$\dot{x}(t)=f(x,w(t)) \tag{2.7}$$

with state $x\in\mathbb{R}^n$ and input $w\in\overline{\mathbb{PC}}_m$. Here, $\overline{\mathbb{PC}}_m$ is the class of bounded piecewise continuous inputs $w(t):\mathbb{R}\to\mathbb{R}^m$. Furthermore, assume that $f(x,w)$ satisfies some regularity conditions to guarantee that, for any input $w\in\overline{\mathbb{PC}}_m$, system (2.7) has well-defined solutions in the sense of Filippov.

Definition 2.4. System (2.7) is said to be

- *uniformly convergent* for a class of inputs $\mathscr{W}\subset\overline{\mathbb{PC}}_m$ if for every input $w(t)\in\mathscr{W}$ there is a solution $\bar{x}(t)=x(t,t_0,\bar{x}_0)$ satisfying the following conditions:

1. $\bar{x}(t)$ is defined and bounded for all $t \in (-\infty, +\infty)$,
2. $\bar{x}(t)$ is globally uniformly asymptotically stable.

- *exponentially convergent* for a class of inputs $\mathscr{W} \subset \overline{\mathbb{PC}}_m$ if
  1. it is uniformly convergent,
  2. $\bar{x}(t)$ is globally exponentially stable.

Solution $\bar{x}(t)$ is called a *limit solution*. As follows from the above definition, any solution of a uniformly or exponentially convergent system 'forgets' its initial condition and converges to a limit solution which is independent of the initial conditions. The following statements describe some properties of this limit solution.

Property 2.5 ([109]). Consider system (2.7) with a given input $w(t)$ defined for all $t \in \mathbb{R}$. Let $\mathscr{D} \subset \mathbb{R}^n$ be a compact set which is positively invariant with respect to system (2.7). Then there is at least one solution $\bar{x}(t)$, such that $\bar{x}(t) \in \mathscr{D}$ for all $t \in (-\infty, +\infty)$.

Note that in general, if there exists a globally asymptotically stable limit solution $\bar{x}(t)$ it may be non-unique, in the sense that there can exist another solution $\tilde{x}(t)$ bounded for all $t \in (-\infty, +\infty)$ that is also globally asymptotically stable. For any two such solutions it obviously follows that $||\bar{x}(t) - \tilde{x}(t)|| \to 0$ as $t \to \infty$. At the same time for *uniformly* convergent systems the limit solution is unique, as formulated in the following property.

Property 2.6 ([65]). For a uniformly convergent system, the limit solution is unique, i.e. it is the only solution bounded for all $t \in (-\infty, +\infty)$.

The following property of uniformly convergent systems provides insight in the behavior of the limit solution for systems with constant or periodic input signals.

Property 2.7 ([64]). Suppose system (2.7) is uniformly convergent. Then, if input $w(t)$ is constant, the corresponding limit solution $\bar{x}(t)$ is also constant. If input $w(t)$ is periodic with period T, then the corresponding limit solution $\bar{x}(t)$ is also periodic with the same period T.

Since any exponentially convergent system is also uniformly convergent, the above properties also hold for exponentially convergent systems.

Now consider a scalar continuously differentiable function $V(x)$ for system (2.7). The time derivative of this function along solutions of system (2.7) is defined as follows

$$\dot{V} = \frac{\partial V(x)}{\partial x}\dot{x}(t).$$

Since V is continuously differentiable and solution $x(t)$ is an absolutely continuous function of time, $\dot{V}$ exists almost everywhere. The upper derivative for function $V(x)$ is defined as follows

$$\dot{V}^*(x,t) = \sup_{\xi \in F(x,t)} \left(\frac{\partial V(x)}{\partial x} \xi \right)$$

with $F(x,t)$ a set-valued function, for which $\dot{x} \in F(x,t)$ is called a Filippov solution for system (2.7). For almost all t it holds that

$$\dot{V}(x(t)) \leq \dot{V}^*(x(t),t).$$

According to Filippov ([17], p.155), if $V(x)$ is continuously differentiable and $\dot{V}(x) \leq 0$ is satisfied in the domains of continuity of $F(x,t)$, then inequality $\dot{V}^*(x) \leq 0$ holds for all $(x,t) \in \mathbb{R}^{n+1}$. This leads to the following definition.

Definition 2.8. System (2.7) is called quadratically convergent if for any input $w \in \overline{\mathbb{PC}}_m$ there exists a positive definite matrix $P = P^T > 0$ and a scalar $\alpha > 0$ such that for function $V(x_1,x_2) = (x_1 - x_2)^T P(x_1 - x_2)$ it holds that

$$\dot{V}^*(x_1,x_2,t) \leq -\alpha V(x_1,x_2).$$

Quadratic convergency is a useful tool for establishing exponential convergency, as follows from the following property.

Property 2.9 ([65])**.** If system (2.7) is quadratically convergent, then it is exponentially convergent.

An important advantage of convergent nonlinear systems over general nonlinear systems is that, due to the fact that the limit solution of a convergent system only depends on the input and is independent of the initial conditions, *simulation* can be used to determine the limit solution of the system. That is, evaluation of one solution (one arbitrary initial state) suffices, whereas for general nonlinear systems all (i.e. an infinite number of) initial conditions need to be evaluated to obtain a reliable analysis. This means that for convergent systems simulation is a reliable tool for the analysis of the limit solution.

Furthermore, whereas steady-state performance evaluation for general nonlinear systems can be difficult due to the possibility of multiple steady-state solutions, convergent systems have a unique limit solution and therefore steady-state performance can also be defined in a unique way. Since for every input signal there is only one limit solution — as is the case for linear systems — it is for example possible to make a frequency domain analysis using nonlinear frequency response functions [66]. For example, for a uniformly (exponentially) convergent system with some T-periodic scalar input w and scalar limit output $\bar{y}$, the nonlinear complementary sensitivity function is defined as

$$\mathscr{T} = \sqrt{\frac{\int_0^T \bar{y}^2(t)dt}{\int_0^T w^2(t)dt}}$$

and the nonlinear sensitivity function is defined as

$$\mathscr{S} = \sqrt{\frac{\int_0^T (w(t) - \bar{y}(t))^2 dt}{\int_0^T w^2(t) dt}}.$$

Note that for *linear* systems with a harmonic input signal the nonlinear complementary sensitivity function is equal to the magnitude of the complementary sensitivity function as defined for linear systems. This equivalence, however, does not hold for the nonlinear sensitivity function and the magnitude of the 'linear' sensitivity function. The nonlinear sensitivity function is also affected by phase differences between w and $\bar{y}$, whereas in the 'linear' sensitivity function, gain and phase are separated.

The nonlinear frequency response functions as defined above can be derived using simulation, but this can become time-consuming, if the limit solution has to be determined for many different input signals (e.g. different frequencies for harmonic input signals). In Section 2.5 and Chapter 3 an alternative analysis method is presented for harmonically forced Lur'e systems.

2.5 Harmonic linearization

Generally speaking, the method of harmonic linearization (also known as the describing function method or the method of harmonic balance) is used to gain insight in the existence and dynamics of periodic solutions of nonlinear systems. Although it may provide a good impression about whether or not a certain nonlinear system has a periodic solution and what this solution looks like, it is only an approximative method, and cannot give conclusive results whether or not this periodic solution actually exists. Of course if, in addition to this method, convergent systems theory is used, stronger conclusions can be obtained.

The method of harmonic linearization is founded in the 1930s on work of Galerkin (see e.g. [61]), Van der Pol [103], Krylov and Bogoliubov [42]. Since the 1960s the method received a lot of attention in literature, see e.g. [27, 31, 55, 56] and references therein. The method has since then also been included in many textbooks, such as [33, 38, 40, 78].

In this section, the method of harmonic linearization is presented for autonomous nonlinear systems, following the line of [40]. In Chapter 3 the method as presented here is extended for analysis of nonlinear systems of Lur'e type with forced harmonic excitation.

Consider the nonlinear system given by the feedback connection in Figure 2.1 represented by

$$\begin{aligned} \dot{x} &= Ax + Bu \\ y &= Cx \\ u &= \phi(y) \end{aligned} \tag{2.8}$$

where $x \in \mathbb{R}^n$, $u, y \in \mathbb{R}$, matrices A, B, C are of corresponding dimensions, (A, B) is controllable, (A, C) is observable, and $G(s) = C(sI - A)^{-1}B$ is a strictly proper, rational transfer function.

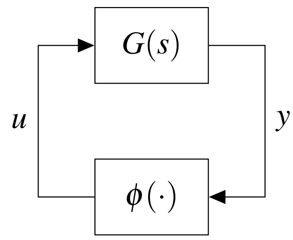

Figure 2.1: Autonomous nonlinear system.

Furthermore ϕ is a continuous scalar nonlinearity which is time-invariant and memoryless[1], i.e. $\phi(y)$ depends only on the current value of y.

In order to find out if system (2.8) has a periodic solution, the following reasoning is used. If there exists a periodic solution, then it should satisfy $y(t+T) = y(t)$ for some period $T = 2\pi/\omega$. The idea of the method of harmonic linearization is to represent this periodic solution by a Fourier series

$$y(t) = \frac{a_0}{2} + \sum_{k=1}^{\infty} a_k \cos(k\omega t) + \sum_{k=1}^{\infty} b_k \sin(k\omega t)$$

and seek a frequency ω and set of Fourier coefficients a_0, a_k, b_k such that they satisfy system equations (2.8). Since nonlinearity ϕ is time-invariant and memoryless, $\phi(y(t))$ is also T-periodic and can be written as

$$\phi(y(t)) = \frac{c_0}{2} + \sum_{k=1}^{\infty} c_k \cos(k\omega t) + \sum_{k=1}^{\infty} d_k \sin(k\omega t).$$

Note that Fourier coefficients c_k and d_k can also be written as a function of $\phi(y(t))$

$$c_k = \frac{\omega}{\pi} \int_0^{2\pi/\omega} \phi(y(t)) \cos(k\omega t) dt, \tag{2.9}$$

$$d_k = \frac{\omega}{\pi} \int_0^{2\pi/\omega} \phi(y(t)) \sin(k\omega t) dt. \tag{2.10}$$

If $y(t)$ is a solution of (2.8) it must satisfy the following equation

$$y(t) = G(s)\phi(y(t)) \tag{2.11}$$

where $s = \frac{d}{dt}$. Using the Fourier series of $y(t)$ and $\phi(y(t))$ this can be written as

$$\frac{a_0}{2} + \sum_{k=1}^{\infty} a_k \cos(k\omega t) + \sum_{k=1}^{\infty} b_k \sin(k\omega t) = G(s) \left(\frac{c_0}{2} + \sum_{k=1}^{\infty} c_k \cos(k\omega t) + \sum_{k=1}^{\infty} d_k \sin(k\omega t) \right).$$

From the above equation, one can deduce that (2.11) can only be satisfied if

$$\begin{aligned} a_0 - c_0 G(0) &= 0 \\ a_k - c_k G(ik\omega) &= 0 \\ b_k - d_k G(ik\omega) &= 0 \end{aligned} \tag{2.12}$$

[1]For harmonic linearization of time-varying nonlinearities or nonlinearities with memory, such as hysteresis and backlash, see [4, 35].

for all integers $k > 0$. Unfortunately, (2.12) is an infinite-dimensional equation, which is practically impossible to solve. Therefore, in the process of harmonic linearization, (2.12) is approximated by a finite-dimensional problem, in which it is required that (2.12) is only satisfied for $k < q$, where $q > 0$ is some finite integer. If the transfer function $G(s)$ has a sharp low-pass filter characteristic, then it is reasonable to approximate $G(ik\omega)$ by 0 for high values of k, and hence to make this finite-dimensional approximation of (2.12). However, since the frequency of oscillation ω is unknown, one can still not judge if this is a good approximation, even if $G(s)$ is a priori known. In the classical method of harmonic linearization one chooses $\tilde{y}(t) = a\sin(\omega t)$, i.e. $q = 1$ and $a_0 = a_1 = a_k = b_k = 0$ for all $k > 1$. If in addition it is assumed that the nonlinearity ϕ is an odd function[2], i.e. $\phi(\tilde{y}) = -\phi(-\tilde{y})$, then $a_0 = 0$ implies $c_0 = 0$, and the Fourier series of $\phi(\tilde{y})$ cannot contain cosines since they are even functions, i.e. $c_1 = 0$. This simplifies (2.12) to the following equation

$$a - d_1 G(i\omega) = 0. \tag{2.13}$$

Coefficient d_1 is the amplitude of the first harmonic of $\phi(\tilde{y}(t))$ when $\tilde{y}(t) = a\sin(\omega t)$. Using (2.10) this coefficient can be described by

$$d_1 = \frac{\omega}{\pi}\int_0^{2\pi/\omega} \phi(a\sin(\omega t))\sin(\omega t)dt.$$

Now a function $K(a)$, called the *describing function* of nonlinearity ϕ, is defined by

$$K(a) = \frac{d_1}{a} = \frac{2}{\pi a}\int_0^{\pi} \phi(a\sin\theta)\sin\theta d\theta$$

such that (2.13) can be rewritten as

$$[1 - K(a)G(i\omega)]a = 0.$$

Since a solution with $a = 0$ is not of interest, this simplifies to

$$1 - K(a)G(i\omega) = 0. \tag{2.14}$$

Equation (2.14) is known as the (first-order) *harmonic balance equation*. Solving this equation gives all possible combinations of (a, ω) for $\tilde{y}(t) = a\sin(\omega t)$ as approximative periodic solution of nonlinear system (2.8). Note however that the method of harmonic linearization states that if (2.14) has a solution (a^*, ω^*), then there is *probably* a periodic solution of (2.8) with amplitude and frequency close to (a^*, ω^*), but it cannot *guarantee* this. Conversely, if (2.14) has no solutions, then the system *probably* has no periodic solution. On the other hand, there exist rigorous conditions, see e.g. Theorem 7.4 in [40], that *are* able to guarantee the (non)existence of periodic solutions as found by the method of harmonic linearization.

Using the describing function $K(a)$, one can also formulate the system equations of the quasi-linear system

$$\begin{aligned} \dot{\xi} &= A\xi + BK(a)\zeta \\ \zeta &= C\xi \end{aligned}$$

[2] A generalization for the case in which ϕ is not odd can be found in [81].

that produces the periodic solution $\zeta(t) = \tilde{y}(t) = a\sin(\omega t)$ as approximation for the solution of the nonlinear system. Note that the only difference between these system equations and the equations of nonlinear system (2.8) is that nonlinear function ϕ is replaced by linear gain $K(a)$.

In Chapter 3 the method of harmonic linearization is discussed further for the case in which the system under consideration is a nonlinear system of Lur'e type with forced harmonic excitation.

Chapter 3

Harmonic Linearization for Harmonically Forced Lur'e Systems

Abstract In this chapter, a method is provided that can be used to analyse harmonically forced nonlinear systems of Lur'e type in the frequency domain. This method is based on harmonic linearization, and is an extension to the harmonic linearization method as summarized in Section 2.5. Both the well-posedness and the accuracy of the harmonic linearization are discussed. A frequency domain condition is provided that guarantees a unique positive real solution to the harmonic balance equation for a certain class of nonlinearities. Furthermore, an upper bound is found for the $\mathscr{L}_2$ norm of the error between the periodic solution of the Lur'e system and the corresponding harmonic linearization. The presented theory is illustrated by means of three examples. The examples show for three different Lur'e systems how this harmonic linearization approach can be used to obtain a frequency domain performance analysis of these systems. The results are compared to the often used $\mathscr{L}_2$ gain performance index.

3.1 Introduction

For asymptotically stable linear time-invariant (LTI) systems with a harmonic input signal, any solution converges to a unique harmonic solution, that only depends on the input signal and not on the initial conditions. Due to this property, it is possible to analyse the performance (in terms of gain and phase) of such a system in the frequency domain. Such an analysis can provide valuable insight in how good the system can follow a certain periodic reference signal, and how it reacts on disturbances of a certain frequency. For nonlinear systems with a harmonic input signal, a similar frequency domain analysis would be useful as well to evaluate the behavior of the system. However, such a frequency domain analysis is virtually impossible to perform for nonlinear systems *in general*, due to specific properties of a nonlinear system, such as the possibility of having multiple periodic solutions, or non-harmonic responses to harmonic input signals. Furthermore, whereas for LTI systems the periodic solution can be easily derived (e.g. by determining the transfer function of the system), for nonlinear systems this problem can be hard to tackle. Nonetheless, for *some* nonlinear systems a frequency domain analysis is possible. Here, a harmonic linearization method is used to obtain a frequency domain analysis for these nonlinear systems.

For already more than 70 years the method of harmonic linearization (or describing function method, see also Section 2.5) has been used to predict existence and dynamics of periodic solutions of mainly autonomous nonlinear systems (such as the Van der Pol equation), although it has also been used for analysis of periodically forced nonlinear systems (such as the Duffing equation), see e.g. [38].

In this chapter, harmonic linearization for Lur'e systems with forced harmonic excitation is investigated further. Well-posedness of this harmonic linearization is discussed and an upper bound is found for the $\mathscr{L}_2$ norm of the error between the unique T-periodic solution (T being the period of the harmonic excitation) of the Lur'e system and the corresponding harmonic linearization, using the notion of contraction. Ideas used in this chapter are similar to those in [33]. An alternative method, based on the circle criterion, which deals with existence and stability of periodic motions for periodically forced nonlinear systems and can provide some $\mathscr{L}_\infty$ bound on the system's periodic solution, is system analysis via (incremental) integral quadratic constraints, see e.g. [37, 57, 76]. This analysis, however, is not considered further here.

The remainder of this chapter is organized as follows. Section 3.2 introduces the considered Lur'e system and the extension of the existing harmonic linearization method. Sections 3.3 and 3.4, respectively, deal with the well-posedness and accuracy of this harmonic linearization. Section 3.5 provides three examples that illustrate the presented theory. Finally, Section 3.6 gives a discussion on the results obtained in this chapter.

3.2 Harmonic linearization

Consider a nonlinear system of Lur'e type (see Figure 3.1) that can be described by the following equations

$$\left\{ \begin{array}{rcl} \dot{x} & = & Ax + B\phi(y) + Fw \\ y & = & Cx + Dw \end{array} \right. \tag{3.1}$$

where $x \in \mathbb{R}^n$ is the state, $w \in \mathbb{R}$ is the input, $y \in \mathbb{R}$ is the output, ϕ is a continuous scalar nonlinear function and matrices A, B, C, D, F are of corresponding dimensions. It is assumed that nonlinear function ϕ satisfies the following incremental sector condition

$$0 \leq \frac{\phi(y_1) - \phi(y_2)}{y_1 - y_2} \leq \mu, \ \forall y_1, y_2, \ y_1 \neq y_2 \tag{3.2}$$

for some positive and finite μ. A more general result that also includes $\mu = +\infty$ can be derived using the standard methods of absolute stability theory. Note that condition (3.2) implies well-posedness (i.e. local existence and continuous dependence on initial conditions) of solutions to (3.1) for all essentially bounded measurable $w(t)$.

Let $\bar{x}$ be some solution of (3.1) with *harmonic* input w. In order to learn more about this solution, nonlinear system (3.1) is approximated by a linear system using harmonic linearization and the corresponding harmonic solution is evaluated.

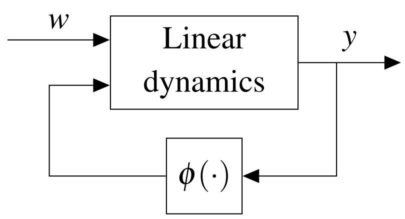

Figure 3.1: A Lur'e system.

The method of harmonic linearization for a Lur'e system with forced harmonic excitation is applied as follows. Solution $\bar{x}$ (resp. $\bar{y}$) of nonlinear system (3.1) is approximated by a periodic solution $\bar{\xi}$ (resp. $\bar{\zeta}$) of the linear system

$$\left\{ \begin{array}{lcl} \dot{\xi} & = & A\xi + BK\zeta + Fw \\ \zeta & = & C\xi + Dw \end{array} \right. \tag{3.3}$$

in which the scalar nonlinear function ϕ is replaced by a linear gain K. Here, gain K is to be determined. If matrix $A + BKC$ does not have eigenvalues on the imaginary axis then for a harmonic input $w(t) = b\sin(\omega t)$, with amplitude $b > 0$ and frequency $\omega > 0$, the linear system has a unique harmonic steady-state solution $\bar{\xi}(t)$, and thus a unique harmonic output $\bar{\zeta}(t)$, which can be described by

$$\bar{\zeta}(t) = a\sin(\omega t + \psi), \tag{3.4}$$

with amplitude $a = |H(i\omega)|$ and phase $\psi = \tan^{-1}\frac{\mathrm{Im}\ H(i\omega)}{\mathrm{Re}\ H(i\omega)}$, where $H(i\omega)$ is the transfer function of system (3.3). In the process of harmonic linearization gain K is chosen to minimize the following criterion

$$J := \frac{1}{T}\int_0^T [\phi(\bar{\zeta}(t)) - K\bar{\zeta}(t)]^2 dt,$$

where $\bar{\zeta}(t) = C\bar{\xi}(t) + Dw(t)$ and $T = 2\pi/\omega$ is the period of input w. The optimal gain can be found by solving the condition

$$\frac{dJ}{dK} = 0$$

and is given by

$$K = \left(\int_0^T \bar{\zeta}^2(t)dt \right)^{-1} \int_0^T \phi(\bar{\zeta}(t))\bar{\zeta}(t)dt.$$

If, in addition, nonlinear function ϕ is known to be an odd function, then $K(a)$ is its describing function

$$K(a) = \frac{2}{\pi a} \int_0^\pi \phi(a \sin\theta) \sin\theta d\theta. \tag{3.5}$$

Many examples of calculations of $K(a)$ for various ϕ can be found in many textbooks on the describing function method. For example, for the case that the nonlinear function is a saturation function $\phi(\cdot) = \mathrm{sat}(\cdot) = \mathrm{sign}(\cdot)\min(1, |\cdot|)$, the describing function is given by

$$K(a) = \begin{cases} 1, & a \le 1 \\ \frac{2}{\pi}\left(\sin^{-1}\left(\frac{1}{a}\right) + \frac{1}{a}\sqrt{1 - \frac{1}{a^2}} \right), & a > 1 \end{cases}$$

Note that for the computation of describing function $K(a)$ no knowledge of solution $\bar{x}$ is required. That is, an arbitrary solution $\bar{x}$ of nonlinear system (3.1) is approximated by a harmonic solution of linear system (3.3), and only this harmonic solution is used for the computation of $K(a)$. Later on in this chapter, the existence of a $2\pi/\omega$ periodic solution $\bar{x}$ is proven for the nonlinear system with input $w(t) = b\sin(\omega t)$, and the difference between this periodic solution and its harmonic approximation $\bar{\xi}$ is discussed.

So far, the described method of harmonic linearization for harmonically forced Lur'e systems is identical to the standard method as described in many textbooks. The extension lies in the following steps.

Once the describing function is known, amplitude a of the harmonic output $\bar{\zeta}(t)$ can be determined as a function of input amplitude b and frequency ω. Under the assumption that A does not have eigenvalues $\pm i\omega$, the value of amplitude a can be determined by solving the so-called harmonic balance equation, which for system (3.3) is computed as follows. Consider system (3.3) and let $s = \frac{d}{dt}$:

$$\begin{aligned} s\xi(t) &= A\xi(t) + BK\zeta(t) + Fw(t), \\ \zeta(t) &= C\xi(t) + Dw(t). \end{aligned}$$

After elimination of $\xi(s)$ this results in

$$\zeta(t) = C(sI - A)^{-1}BK(a)\zeta(t) + (C(sI - A)^{-1}F + D)w(t),$$

where I is an identity matrix of appropriate size. Since $\bar{\zeta}(t)$ is a harmonic signal of frequency ω and amplitude a, and the amplitude of $w(t)$ is b, the following harmonic balance equation is

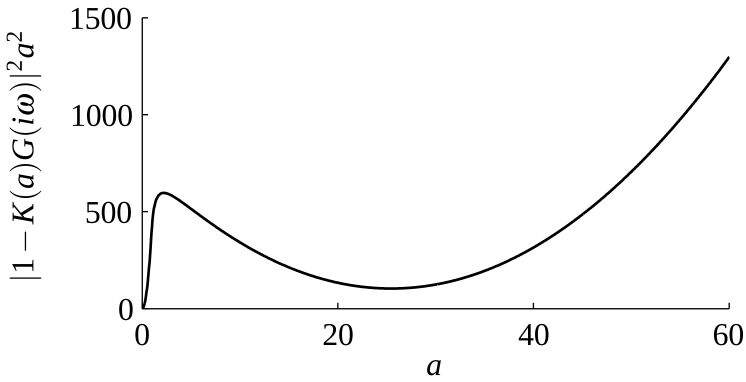

Figure 3.2: Left hand side of (3.6) for some Lur'e system with $G(i\omega) = (8i\omega + 20)/\omega^2$, $\phi(\cdot) = \mathrm{sat}(\cdot)$ and $\omega = 1$.

obtained

$$|1-K(a)G(i\omega)|^2a^2 = |C(i\omega I - A)^{-1}F + D|^2b^2 \tag{3.6}$$

where $G(i\omega) = C(i\omega I - A)^{-1}B$. For an autonomous system as usually considered for harmonic linearization, the right-hand side of (3.6) is equal to zero, as described in Section 2.5. For a Lur'e system with forced harmonic excitation, however, the right-hand side of (3.6) depends on the input amplitude b and input frequency ω. The left-hand side of (3.6) is a nonlinear function of a. Therefore, if this equation is solved for a, there may exist multiple solutions of a for one pair of (b,ω), see e.g. Figure 3.2. In this figure the left-hand side of (3.6) is plotted as a function of a, and if for example $|1-K(a)G(i\omega)|^2a^2 = |C(i\omega I - A)^{-1}F + D|^2b^2 = 300$ for some pair of (b,ω), then multiple solutions of a exist. If, on the other hand, there *is* a unique positive real solution $a(b,\omega)$ for a given pair of (b,ω), the steady-state solution $\bar{\xi}(t)$ can easily be computed by filling in $K(a(b,\omega))$ into (3.3) and applying standard analysis tools for linear systems.
If solution $a(b,\omega)$ is not unique positive and real for some pair of (b,ω), e.g. there are multiple solutions for a, then this approach is not applicable for finding a unique steady-state solution $\bar{\xi}(t)$ for *this* pair of (b,ω). Note however, that for other pairs of (b,ω) the approach may still be applicable.

In the remainder of this thesis, the harmonic linearization is called *well-posed* if there exists a unique positive real solution $a(b,\omega)$ to the harmonic balance equation (3.6). That is, if the harmonic linearization of a certain Lur'e system with forced harmonic linearization is well-posed, it is possible to find a unique linear approximation system with a unique steady-state solution $\bar{\xi}(t)$, which in turn can be used to find an approximative description of the frequency domain behavior of the Lur'e system. In Section 3.3 conditions are presented under which well-posedness of the harmonic linearization is guaranteed. Section 3.4 deals with the accuracy of this well-posed harmonic linearization and how this can be used to give a detailed bound on the frequency domain behavior of the Lur'e system.

3.3 Well-posedness

In order to find out whether a unique positive real solution $a(b,\omega)$ to the harmonic balance equation (3.6) does or does not exist for certain harmonic input signals, one can of course fill in all system data and determine graphically (e.g. using plots like Figure 3.2) or numerically if the solution is unique positive real for a given pair of (b,ω). However, this approach can be very time-consuming, especially when evaluating a large set of input signals. In this section a more time-efficient alternative is given, that is, a frequency domain condition is presented under which a unique positive real solution $a(b,\omega)$ is guaranteed.

Before presenting the theorem that introduces the frequency domain condition, first some characteristics of function $K(a)$ are specified. If nonlinear function $\phi(\cdot)$ is odd and satisfies either the *sector* or the *incremental sector* condition, then it is possible to characterize function $K(a)$ as given in the following lemmata.

Lemma 3.1. *Assume that the continuous scalar nonlinear function ϕ is odd and for some $\mu > 0$ satisfies*

$$0 \leq \frac{\phi(y)}{y} \leq \mu, \ \ \forall y \in \mathbb{R}/\{0\}.$$

Then

$$0 \leq K(a) \leq \mu, \quad \forall a \geq 0.$$

Proof. ([40], p285) Describing function $K(a)$ satisfies the lower bound

$$K(a) = \frac{2}{\pi a}\int_0^{\pi} \phi(a\sin\theta)\sin\theta d\theta = \frac{2}{\pi}\int_0^{\pi} \frac{\phi(a\sin\theta)}{a\sin\theta}\sin^2\theta d\theta \geq \frac{2}{\pi}\int_0^{\pi} 0 d\theta = 0$$

and the upper bound

$$K(a) = \frac{2}{\pi a}\int_0^{\pi} \phi(a\sin\theta)\sin\theta d\theta = \frac{2}{\pi}\int_0^{\pi} \frac{\phi(a\sin\theta)}{a\sin\theta}\sin^2\theta d\theta \leq \frac{2\mu}{\pi}\int_0^{\pi} \sin^2\theta d\theta = \mu.$$

□

Similarly:

Lemma 3.2. *Assume that the continuous scalar nonlinear function ϕ is odd and that for all $y_1, y_2 \in \mathbb{R}$ there is a $\mu > 0$ such that*

$$0 \leq \frac{\phi(y_1) - \phi(y_2)}{y_1 - y_2} \leq \mu, \ \ \forall y_1, y_2, \ y_1 \neq y_2.$$

Then

$$0 \leq \frac{K(a_1)a_1 - K(a_2)a_2}{a_1 - a_2} \leq \mu, \quad \forall a_1, a_2 \geq 0, a_1 \neq a_2. \tag{3.7}$$

Proof. Denote

$$L_K := \frac{K(a_1)a_1 - K(a_2)a_2}{a_1 - a_2}.$$

Then

$$\begin{aligned} L_K &= \frac{1}{a_1 - a_2}\left(\frac{1}{\pi}\int_0^{2\pi} \phi(a_1 \sin\theta)\sin\theta d\theta - \frac{1}{\pi}\int_0^{2\pi} \phi(a_2 \sin\theta)\sin\theta d\theta\right) \\ &= \frac{1}{\pi}\int_0^{2\pi} \frac{(\phi(a_1\sin\theta) - \phi(a_2\sin\theta))\sin^2\theta d\theta}{a_1\sin\theta - a_2\sin\theta} \\ &\le \frac{\mu}{\pi}\int_0^{2\pi} \sin^2\theta d\theta = \mu \end{aligned}$$

The left inequality is proven in the same way. □

Now consider again harmonic balance equation (3.6). The following result holds.

Theorem 3.3. *Suppose matrix A does not have eigenvalues $\pm i\omega$ on the imaginary axis and the frequency domain inequality*

$$\text{Re } G(i\omega) < \frac{1}{\mu} \tag{3.8}$$

is fulfilled for a given ω. Then for any function $K(a)$ satisfying (3.7) *and for any $b > 0$ there is a unique positive real solution $a(b,\omega)$ to harmonic balance equation* (3.6).

Proof. Consider the left hand side of equation (3.6)

$$\pi(a) = |a - K(a)aG(i\omega)|^2$$

The idea of the proof is to show that if frequency inequality (3.8) holds then $\pi(a)$ is a strictly increasing function. Condition (3.7) implies that $\pi(a)$ is a (Lipschitz) continuous function. Since $\pi(0) = 0$ and $\pi(\infty) = \infty$, existence and uniqueness of the positive real solution $a(b,\omega)$ of (3.6) follow.

For the sake of simplicity, the theorem is only proven under the assumption that $K(a)a$ is a differentiable function of a. The general case can be deduced from (3.7), taking into account that

$$0 \le \liminf_{a_1 \to a_2} \frac{K(a_1)a_1 - K(a_2)a_2}{a_1 - a_2} \le \limsup_{a_1 \to a_2} \frac{K(a_1)a_1 - K(a_2)a_2}{a_1 - a_2} \le \mu.$$

Differentiating $\pi(a)$ with respect to a yields

$$\begin{aligned} \frac{\pi(a)'}{a} &= (1 - (Ka)'G)(1 - KG^*) + (1 - KG)(1 - (Ka)'G^*) \\ &\ge 2\left(1 - \left(K + (Ka)'\right)\text{Re}G + K(Ka)'[\text{Re}G]^2\right) \\ &= 2(1 - K\text{Re}G)(1 - (Ka)'\text{Re}G) \end{aligned} \tag{3.9}$$

Here G^* stands for the complex conjugate of G. According to (3.7), $0 \le K(a) \le \mu$ and $0 \le (K(a)a)' \le \mu$. Together with (3.8) this implies that the right-hand side of expression (3.9) is positive. Thus, $\pi(a)$ is strictly increasing. □

Remark 3.4. Although the frequency domain inequality in Theorem 3.3 is a necessary condition to ensure a unique solution $a(b,\omega)$ to the harmonic balance equation for the *class* of functions $K(a)$ satisfying (3.7), it is possible that there exists a unique positive real solution $a(b,\omega)$ for a *given* nonlinearity ϕ while the frequency domain inequality is not met.

Remark 3.5. Condition (3.8) needs only to be satisfied for a *given* frequency ω, in contrast to the well-known circle criterion, see e.g. [40]. It is therefore possible that for a given system there exists a unique positive real solution $a(b,\omega)$ for some range of frequencies, while for another range of frequencies it does not exist. This is illustrated further in Example 3.11 in Section 3.5.

Remark 3.6. If condition (3.8) is satisfied for *all* frequencies, and in addition A is Hurwitz and $\{A,B,C,D\}$ is a minimal realization of G, i.e. the circle criterion holds, then system (3.1), (3.2) is quadratically convergent (as defined in Section 2.4).

The previous result allows one to complete the procedure of harmonic linearization for system (3.1). Indeed, if frequency condition (3.8) holds, there is a unique positive real solution $a(b,\omega)$, given the pair of (b,ω). Then substituting $K(a(b,\omega))$ in (3.3) gives a system that is linear in ξ. For this system one can calculate the unique harmonic solution $\bar{\xi}(t)$ using only algebraic calculations. Like in the harmonic linearization method, one can expect that $\bar{\xi}(t)$ is sufficiently close to $\bar{x}(t)$. In Section 3.4 a bound is derived that estimates the difference between the two solutions with an $\mathscr{L}_2$ norm.

3.4 Accuracy

In this section the accuracy of the harmonic linearization procedure is discussed. After the considered definition of accuracy is given, a theorem is derived that provides sufficient conditions to find the accuracy of the harmonic linearization.

To formulate the desired definition of accuracy it is assumed that for a given harmonic input $w(t) = b\sin\omega t$ system (3.1) has a $2\pi/\omega$-periodic solution $\bar{x}(t)$. Later on, this assumption is verified, i.e. sufficient conditions are given that ensure a unique $2\pi/\omega$-periodic solution of (3.1). Now consider together with system (3.1) and the corresponding linear system (3.3) the performance outputs

$$\begin{aligned} \bar{z}(t) &= H\bar{x}(t), \quad \bar{z} \in \mathbb{R} && (3.10) \\ \bar{\eta}(t) &= H\bar{\xi}(t), \quad \bar{\eta} \in \mathbb{R} && (3.11) \end{aligned}$$

with an appropriate matrix H. In order to describe the accuracy of the harmonic linearization, an upper bound is sought for the following $\mathscr{L}_2$ norm

$$\left(\frac{\omega}{2\pi} \int_0^{2\pi/\omega} [\bar{z}(t) - \bar{\eta}(t)]^T [\bar{z}(t) - \bar{\eta}(t)]\, dt \right)^{\frac{1}{2}}. \tag{3.12}$$

Note that in order to investigate the entire state instead of an arbitrary one-dimensional performance output, matrix H can be replaced by the identity matrix I, although in this case some small but straightforward adaptations have to be made in the following approach.

Let e be the difference $\bar{x} - \bar{\xi}$. Then

$$\begin{aligned} \dot{e} &= Ae + B\left[\phi(\bar{y}) - \phi(\bar{\zeta})\right] - B\Delta(t) \\ \bar{y} &= C\bar{x} + Du \\ \bar{\zeta} &= C\bar{\xi} + Du \end{aligned} \tag{3.13}$$

where

$$\Delta(t) = K(a(b,\omega))\bar{\zeta}(t) - \phi(\bar{\zeta}(t)).$$

Substituting (3.4) in the previous expression gives

$$\Delta(t) = K(a(b,\omega))a\sin(\omega t + \psi) - \phi(a\sin(\omega t + \psi)),$$

where $a(b,\omega)$ is the solution of (3.6). Let

$$v(a(b,\omega)) = \left(\frac{\omega}{2\pi}\int_0^{2\pi/\omega} \Delta^2(t)dt\right)^{\frac{1}{2}}.$$

Filling in $\Delta(t)$ and (3.5) results in

$$v(a) = \left(\frac{1}{2\pi}\int_0^{2\pi}\left[\frac{2}{\pi}\int_0^{\pi}\phi(a\sin\theta)\sin\theta d\theta\cdot\sin\vartheta - \phi(a\sin\vartheta)\right]^2 d\vartheta\right)^{\frac{1}{2}},$$

of which the value can be computed if ϕ and $a(b,\omega)$ are known.

Denote

$$\rho_1 := \sup_{k=\pm3,\pm5,\ldots} |C(ik\omega I - A - \frac{\mu}{2}BC)^{-1}B|$$

$$\rho_2 := \sup_{k=\pm3,\pm5,\ldots} |H(ik\omega I - A - \frac{\mu}{2}BC)^{-1}B|$$

and

$$\gamma = \frac{2\rho_2}{2-\mu\rho_1}$$

to be used in the following theorem.

Theorem 3.7. *Consider system* (3.1) *with periodic input* $w(t) = b\sin(\omega t)$ *and assume the following conditions are met*

1. (A,B) *is controllable,* (A,C) *is observable,*
2. *harmonic balance equation* (3.6) *has a unique positive real solution* $a(b,\omega)$*,*

3. *frequency domain condition* Re $G(ik\omega) < 1/\mu$ *is satisfied for* $k = \pm 3, \pm 5, \pm 7, \ldots$,

4. ϕ *is an odd function.*

Then system (3.1) *has a unique* $2\pi/\omega$*-periodic solution* $\bar{x}(t)$ *and the error between the* $2\pi/\omega$*-periodic output* $\bar{z}(t)$ *and* $\bar{\eta}(t)$ *is bounded by:*

$$\left(\frac{\omega}{2\pi}\int_0^{2\pi/\omega} [\bar{z}(t) - \bar{\eta}(t)]^T [\bar{z}(t) - \bar{\eta}(t)]\, dt\right)^{\frac{1}{2}} \leq \gamma v(a(b,\omega)). \tag{3.14}$$

Proof. The proof of this result for the case $H = C$ goes along the lines of proof of Lemma 7.1 in [40].

Consider the space $\mathscr{S}$ of all half-wave symmetric periodic signals of fundamental frequency ω, which have finite energy. A signal $y \in \mathscr{S}$ can be represented by its Fourier series

$$y(t) = \sum_{k \text{ odd}} a_k \exp(ik\omega t), \quad \sum_{k \text{ odd}} |a_k|^2 < \infty.$$

Let $\mathscr{S}_h \subset \mathscr{S}$ be a set of signals y represented by its Fourier series

$$y(t) = \sum_{k \text{ odd}, |k| \neq 1} a_k \exp(ik\omega t).$$

The harmonic balance equation has a unique positive solution a, therefore any periodic solution of the nonlinear system, if it exists, should satisfy

$$\bar{y} = \bar{\zeta} + Ce, \quad Ce \in \mathscr{S}_h$$

where, as before $e = \bar{x} - \bar{\xi}$.

First, it is proven that under the given conditions the linear approximation system (3.3) has a unique solution $\bar{\xi}(t)$, and that the nonlinear system (3.1) has a unique $2\pi/\omega$-periodic solution $\bar{x}(t)$.

Since the harmonic balance equation has a nonzero solution a it follows that

$$1 - K(a(b,\omega))G(i\omega) \neq 0,$$

with as before $G(i\omega) = C(i\omega I - A)^{-1}B$. This implies that the closed-loop transfer function of (3.3), i.e. $G/(1-KG)$, has no poles $\pm i\omega$ on the imaginary axis. Since system (3.3) can be rewritten as $\dot{\xi} = (A + BKC)\xi + (F + BKD)w$ and (A,B) is controllable and (A,C) is observable (i.e. $\{A,B,C,D\}$ is a minimal realization of G), this also implies that matrix $A + BKC$ has no eigenvalues $\pm i\omega$ on the imaginary axis. Therefore, the linear approximation system has a unique solution $\bar{\xi}(t)$, which has the same period $T = 2\pi/\omega$ as the input signal.

In order to prove that the nonlinear system (3.1) also has a unique $2\pi/\omega$-periodic solution, consider the nonlinear operator $\mathscr{T}$, defined on space $\mathscr{S}$

$$\mathscr{T}y = G(i\omega)\phi(y) = W(i\omega)(\phi(y) - \frac{\mu}{2}y),$$

where $W = G/(1-\mu G/2)$. Let $y_1, y_2 \in \mathscr{S}$ be two periodic functions such that $y_1 - y_2 \in \mathscr{S}_h$. Taking the $\mathscr{L}_2$ norm of $\mathscr{T}y_1 - \mathscr{T}y_2$ gives

$$\begin{aligned} ||\mathscr{T}y_1 - \mathscr{T}y_2||_2 &= ||W(i\omega)(\phi(y_1) - \frac{\mu}{2}y_1) - W(i\omega)(\phi(y_2) - \frac{\mu}{2}y_2)||_2 \\ &\leq ||W(i\omega)||_2 \cdot ||\phi(y_1) - \frac{\mu}{2}y_1 - \phi(y_2) + \frac{\mu}{2}y_2||_2 \end{aligned}$$

and, since $\phi(y_1) - \frac{\mu}{2}y_1 - \phi(y_2) + \frac{\mu}{2}y_2$ belongs to $\mathscr{S}_h$ this simplifies to

$$||\mathscr{T}y_1 - \mathscr{T}y_2||_2 \leq \sup_{k=\pm 3, \pm 5, \ldots} |W(ik\omega)| \cdot ||\phi(y_1) - \frac{\mu}{2}y_1 - \phi(y_2) + \frac{\mu}{2}y_2||_2.$$

Applying the incremental sector condition (3.2) gives

$$||\mathscr{T}y_1 - \mathscr{T}y_2||_2 \leq \sup_{k=\pm 3, \pm 5, \ldots} |W(ik\omega)| \cdot \frac{\mu}{2}||y_1 - y_2||_2.$$

Furthermore, since

$$|W(ik\omega)|^2 = \frac{G^*(ik\omega)G(ik\omega)}{(1-\frac{\mu}{2}G^*(ik\omega))(1-\frac{\mu}{2}G(ik\omega))} = \frac{G^*(ik\omega)G(ik\omega)}{(1-\mu\mathrm{Re}(G(ik\omega)) + \frac{\mu^2}{4}G^*(ik\omega)G(ik\omega))}$$

and condition 3 of Theorem 3.7 holds:

$$\begin{aligned} |W(ik\omega)|^2 &< \frac{G^*(ik\omega)G(ik\omega)}{\frac{\mu^2}{4}G^*(ik\omega)G(ik\omega)} \quad \text{for all } k = \pm 3, \pm 5, \ldots \\ |W(ik\omega)| &< \frac{2}{\mu} \quad \text{for all } k = \pm 3, \pm 5, \ldots \end{aligned} \tag{3.15}$$

this results in

$$||\mathscr{T}y_1 - \mathscr{T}y_2||_2 < ||y_1 - y_2||_2,$$

from which the existence of a unique $2\pi/\omega$-periodic solution $\bar{x}(t)$ follows according to the contraction mapping argument and observability of (A, C).

To estimate (3.12), i.e. $||He||_2$, rewrite system (3.13) as

$$\begin{aligned} \dot{e} &= (A + \frac{\mu}{2}BC)e + B\left[\phi(\bar{y}) - \frac{\mu}{2}\bar{y} - \phi(\bar{\zeta}) + \frac{\mu}{2}\bar{\zeta}\right] - B\Delta(t) \\ \bar{y} - \bar{\zeta} &= C\bar{e} \\ \bar{z} - \bar{\eta} &= H\bar{e} \end{aligned}$$

and notice that

$$\sup_{k=\pm3,\pm5,\ldots} |W(ik\omega)| = \sup_{k=\pm3,\pm5,\ldots} |C(ik\omega I - A - \frac{\mu}{2}BC)^{-1}B| = \rho_1.$$

Then, by analogy with the previous part of the proof, it follows that

$$||Ce||_2 \leq \frac{\rho_1\mu}{2}||Ce||_2 + \rho_1||\Delta||_2$$

and

$$||He||_2 \leq \frac{\rho_2\mu}{2}||Ce||_2 + \rho_2||\Delta||_2$$

and finally,

$$||He||_2 \leq \frac{2\rho_2}{2-\mu\rho_1}||\Delta||_2 = \gamma\nu(a).$$

Since $\rho_1 = \sup_{k=\pm3,\pm5,\ldots} |W(ik\omega)| < \frac{2}{\mu}$ as shown in (3.15), γ is finite. □

Remark 3.8. Due to Theorem 3.3, conditions 2 and 3 of Theorem 3.7 can be replaced by a stronger condition: Re $G(ik\omega) < 1/\mu$ for $k = \pm1, \pm3, \pm5, \ldots$.

Note that under the conditions in Theorem 3.7, the system is not necessarily convergent. Although the system is guaranteed to have a unique $2\pi/\omega$-periodic solution $\bar{x}(t)$ under the given conditions, periodic solutions with a different period may coexist. A situation in which all conditions of Theorem 3.7 are satisfied, but multiple periodic solutions exist, is given in Example 3.11 in Section 3.5. In order to make sure that linear approximation (3.3) and error bounds (3.14) actually describe the *only* solution of the nonlinear system, one needs to prove in a different way that the system is convergent. The topic of convergent systems, as described in Section 2.4, is discussed further in Chapters 4-6.

3.5 Illustrating examples

In this section, the theory as presented in this chapter is illustrated by means of three examples. All examples are based on a Lur'e system with a saturation nonlinearity, of which the system equations are given by

$$\begin{cases} \dot{x} &= Ax + B\text{sat}(y) + Fw \\ y &= Cx + Dw \\ z &= Hx \end{cases} \tag{3.16}$$

with $w = b\sin(\omega t)$. In the examples it is made clear how the obtained theoretical results can be used for frequency domain analysis of harmonically forced Lur'e systems. Furthermore the results of this frequency domain analysis are compared with the $\mathscr{L}_2$ gain, which is an often used performance index for nonlinear systems.

Example 3.9. In this example, a system of type (3.16) is considered for which matrix A is Hurwitz and the frequency domain condition (3.8) is satisfied for all frequencies. The system matrices are given by

$$A = \begin{bmatrix} -5 & 0 \\ 4 & -10 \end{bmatrix}, \quad B = \begin{bmatrix} 1 \\ 0.5 \end{bmatrix}, \quad F = \begin{bmatrix} 0 \\ -4 \end{bmatrix}, \quad C = \begin{bmatrix} -10 & 20 \end{bmatrix}, \quad D = \begin{bmatrix} 10 \end{bmatrix}, \quad H = \begin{bmatrix} 1 & 0 \end{bmatrix}.$$

Note that the saturation function satisfies the (incremental) sector condition with $\mu = 1$. From Figure 3.3, which shows the Nyquist plot for $G(i\omega) = C(i\omega I - A)^{-1}B$, it can be seen that Re $G(i\omega)$ is indeed smaller than $\frac{1}{\mu} = 1$, i.e. condition (3.8) is met for all frequencies ω, thus the harmonic linearization is well-posed for all harmonic inputs w with arbitrary $b > 0$ and $\omega > 0$.

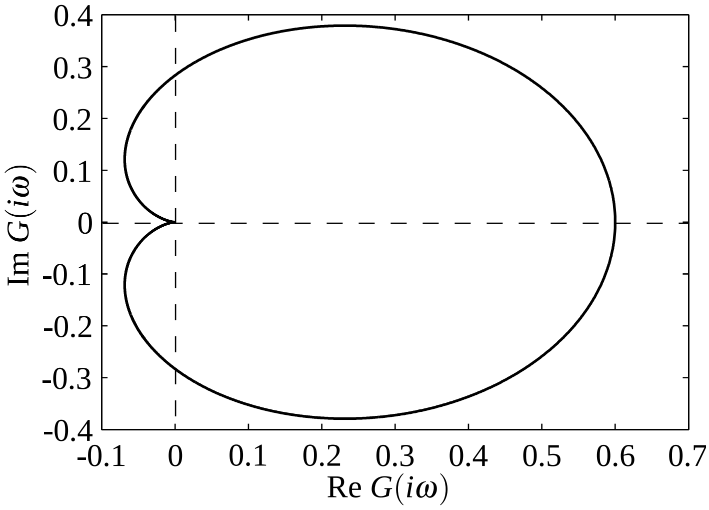

Figure 3.3: Nyquist plot for $G(i\omega)$.

The performance of this system, in terms of nonlinear complementary sensitivity function (nCSF) $||z||_2/||w||_2$, can now be established using Theorem 3.7 for any $b > 0$ and an arbitrary range of frequencies ω. This approach results in an nCSF for the harmonic linearization, and an upper- and lower bound, between which the nCSF of the nonlinear system is known to be. Furthermore, since the system is quadratically convergent (see Remark 3.6) simulation-based analysis as proposed in Section 2.4 can also be used to find the exact nCSF of the nonlinear system, although this approach is more time-consuming than the harmonic linearization approach. Finally, for system (3.16) with Hurwitz matrix A, also (an upper bound on) the $\mathscr{L}_2$ gain can be computed using LMIs, as explained in Section 2.3. In Figure 3.4 the results of all these approaches are plotted for $b = 1$ and $\omega \in [10^{-2}, 10^2]$.

As can be seen in Figure 3.4, the true nCSF as computed using the simulation-based analysis for convergent systems (dots) is approximated quite well by the nCSF of the harmonic linearization (solid line), and lies well between the computed upper- and lower bound (dotted lines). The (upper bound on the) $\mathscr{L}_2$ gain is simply a horizontal line in this figure, and contains no information on the dependence of the system's behavior on the frequency ω.

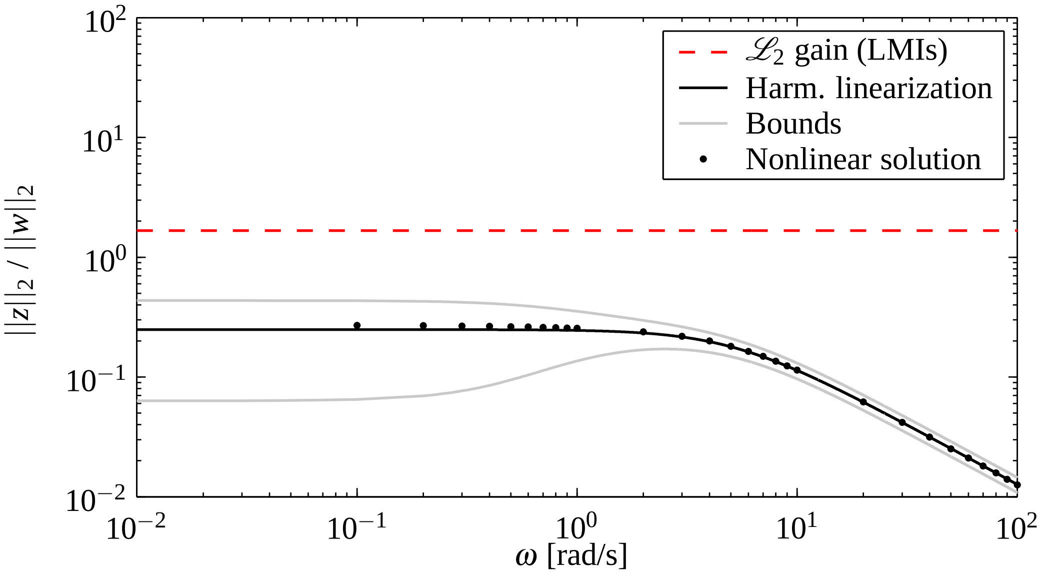

Figure 3.4: Frequency domain analysis for system (3.16), Example 3.9.

△

Example 3.10. In this example, a marginally stable system is considered (matrix A has one eigenvalue 0 and one eigenvalue -5), while the frequency domain condition (3.8) is still satisfied for all frequencies $\omega \neq 0$. The system matrices for the considered system (3.16) are as follows

$$A = \begin{bmatrix} 0 & 0 \\ 1 & -5 \end{bmatrix}, \quad B = \begin{bmatrix} 1 \\ 0.5 \end{bmatrix}, \quad F = \begin{bmatrix} 0 \\ -1 \end{bmatrix}, \quad C = \begin{bmatrix} -4 & 10 \end{bmatrix}, \quad D = \begin{bmatrix} 4 \end{bmatrix}, \quad H = \begin{bmatrix} 1 & 0 \end{bmatrix}.$$

Since the system is marginally stable, no finite $\mathscr{L}_2$ gain estimate can be found from w to z for $H = [1,\ 0]$ using a quadratic storage function as described in Section 2.3. The results of [49, 75] suggest that to find a finite $\mathscr{L}_2$ gain in this case, one can try to use nonquadratic storage functions. However, even if such a gain can be found, it only corresponds to the worst-case behavior of the system. Furthermore, since matrix A is not Hurwitz, the system is not quadratically convergent. Nevertheless, in Chapter 4 it is shown that this system is *uniformly* convergent, and hence it would be possible to determine the exact nCSF of the nonlinear system. However, for now it is assumed that only the results of the harmonic linearization approach are available. One can verify that frequency domain condition (3.8) holds for all frequencies $\omega \neq 0$. The results of this approach are plotted in Figure 3.5 for $b = 1$ and $\omega \in [10^{-2}, 10^{2}]$.

In this figure, the nCSF for the harmonic linearization and the bounds on the accuracy are plotted. Even though the exact nCSF of the nonlinear system is not plotted in this figure, the harmonic linearization results still give a very good idea about what this exact nCSF should look like, since the bounds are very tight. For this case, the distance between the upper- and lower bound, i.e. the 'uncertainty' on the exact nCSF, goes to zero for low frequencies. This can be explained by the fact that for low frequencies the value of y remains within the bounds of the saturation, and hence the system behaves in a linear way.

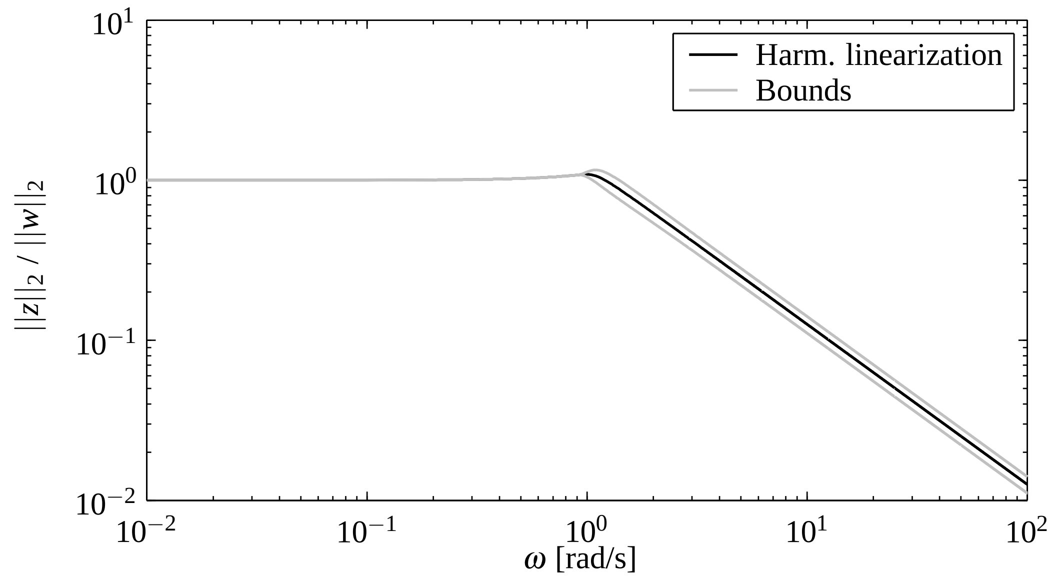

Figure 3.5: Frequency domain analysis for system (3.16), Example 3.10.

$\triangle$

Example 3.11. In this example, again a marginally stable system is considered, but now the frequency domain condition is not satisfied for all frequencies, which implies that the harmonic linearization may not be well-posed for all frequencies. Consider system (3.16) with system matrices

$$A = \begin{bmatrix} 0 & 0 \\ -1 & 0 \end{bmatrix}, \quad B = \begin{bmatrix} 1 \\ 0 \end{bmatrix}, \quad F = \begin{bmatrix} 0 \\ 1 \end{bmatrix}, \quad C = \begin{bmatrix} -10 & 20 \end{bmatrix}, \quad D = \begin{bmatrix} 10 \end{bmatrix}, \quad H = \begin{bmatrix} 0 & 1 \end{bmatrix}.$$

Since the system is marginally stable, no finite $\mathscr{L}_2$ gain estimate can be found from w to z for $H = [0,\ 1]$ using a quadratic storage function, and the system is not quadratically convergent. In fact, this system is not even (uniformly) convergent for the class of harmonic inputs, i.e. for some harmonic input signals the system has multiple stable periodic solutions. Nevertheless, Theorem 3.7 can be used to estimate the performance of the system for *some* harmonic input signals, as is shown in Figure 3.6 for $b = 5$ and $\omega \in [10^0, 10^2]$.

As one can see, Figure 3.6 contains only data for $\omega \geq 1.4908$ [rad/s]. For $\omega < 1.4908$ condition 3 of Theorem 3.7 is not satisfied, and hence uniqueness of the $T = 2\pi/\omega$-periodic solution cannot be guaranteed, and an upper bound for (3.12) cannot be computed. Although frequency domain condition (3.8) is only satisfied for $\omega \geq 4.4724$ (which makes sense since this is 3×1.4908), one can verify that for $\omega \in [1.4908, 4.4724]$ the harmonic balance equation (3.6) still has a unique solution $a(b, \omega)$ and hence the harmonic linearization is well-posed. Nevertheless, since there is no proof in this case that the $T = 2\pi/\omega$-periodic solution is the *only* periodic solution of this system, the result in Figure 3.6 must be handled with caution: it only holds for the $T = 2\pi/\omega$-periodic solution.

Indeed, for a harmonic input with $b = 5$ and $\omega = 2$, the system has stable periodic solutions

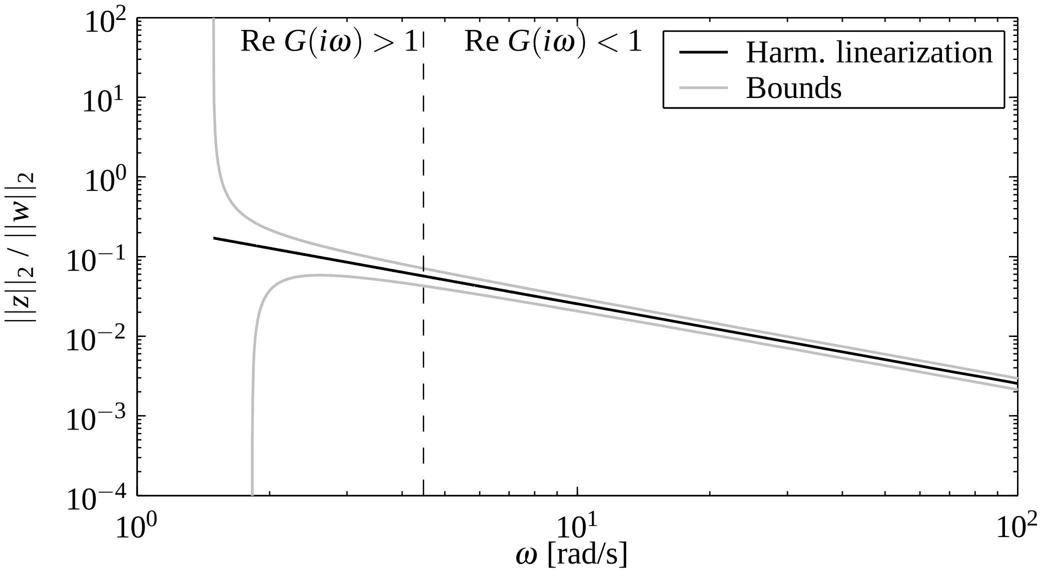

Figure 3.6: Frequency domain analysis for system (3.16), Example 3.11.

with a different period, as shown in Figure 3.7, while all conditions of Theorem 3.7 are satisfied. The three steady-state solutions, respectively T-periodic, $5T$-periodic and $7T$-periodic, have been obtained for the initial conditions $x_0 = [-0.4401,\ -2.7056]$, $x_0 = [2.2638,\ 2.7504]$, and $x_0 = [4.0096,\ 4.6892]$. Note that even more periodic solutions may exist than the ones plotted in Figure 3.7.

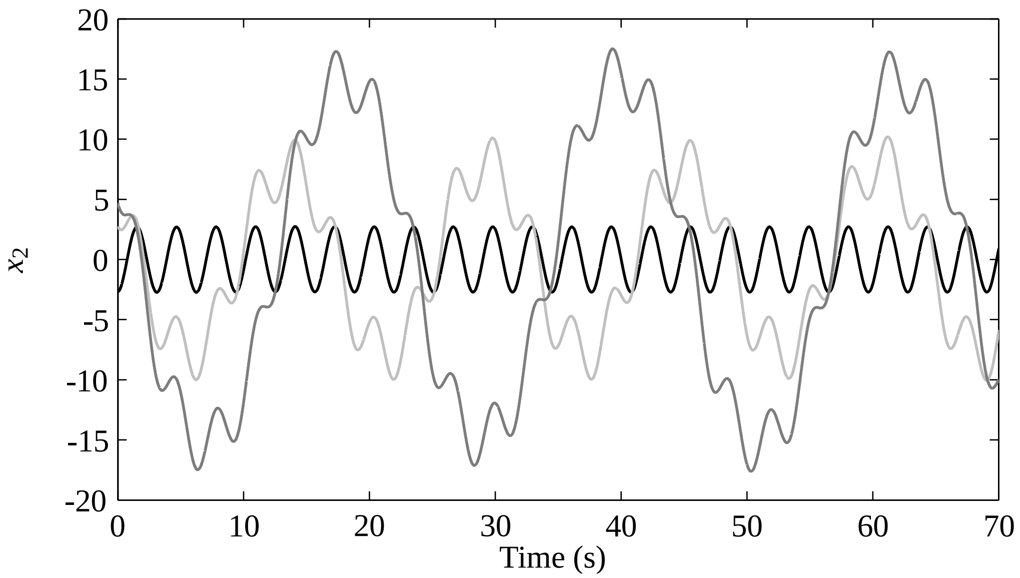

Figure 3.7: Multiple steady-state solutions with different period.

In line with the result in Figure 3.7, it is interesting to note that for a long time it was a common belief that periodically forced nonlinear systems should have a unique periodic steady-state response. In 1927, Van der Pol and Van der Mark [104] demonstrated that this is not the case, even for a simple second order system. Nevertheless, in 1945, Cartwright and Littlewood [8] remarked that their belief in their own results was at that time only sustained by the experimental evidence that stable subharmonics of two different orders did occur. Currently, it is well known, by Melnikov's method, see e.g. [106], that a periodically forced system can exhibit chaotic behavior. $\triangle$

For the three examples given in this section, the harmonic linearization approach has been illustrated and compared with the exact results (if available) and with the $\mathscr{L}_2$ gain, an often used performance index for nonlinear systems. The examples showed that although (an upper bound on) the $\mathscr{L}_2$ gain can be computed very fast using LMIs (see Section 2.3), it only provides a rough estimate on frequency domain performance of the system. For some cases, i.e. for marginally stable systems, a (finite) $\mathscr{L}_2$ gain estimate cannot even be found using a quadratic storage function.

Furthermore, it was observed that the harmonic linearization approach is a computationally efficient method to get an impression on a Lur'e system's frequency domain behavior, in comparison to the simulation-based analysis for convergent systems. An advantage of the simulation-based analysis for convergent systems, however, is that the system behavior can be investigated for a much wider class than only harmonic input signals. The results of the harmonic linearization approach should be used with caution, since other stable periodic solutions may exist with a different period. Convergent systems theory may be used to assure that the $T = 2\pi/\omega$-periodic solution is actually the only stable solution of the system.

A final remark is made on the fact that the error bound (3.12) for the system with Hurwitz matrix A (Example 3.9) does not go to zero for small frequencies, while for the marginally stable system (Example 3.10) it does go to zero. This is caused by the fact that for the marginally stable system $a(b,\omega) < 1$ for small frequencies, and thus $\nu(a) = 0$. For the system with Hurwitz matrix A and $b = 1$, on the other hand, amplitude a remains larger than 1 for all frequencies. For smaller values of b or a different choice of system parameters, however, a may also become smaller then 1.

3.6 Discussion

In this chapter, a computationally efficient approach was presented, based on the method of harmonic linearization, to analyse the frequency domain performance of nonlinear systems of Lur'e type with forced harmonic excitation. To the best of the author's knowledge, the existing harmonic linearization technique was not suitable for the approximation of this type of nonlinear systems, because the harmonic balance equation could have multiple solutions. In this chapter, a frequency domain condition was provided which, if satisfied, ensures a unique positive real solution to the harmonic balance equation. Furthermore, an upper bound was found for the $\mathscr{L}_2$ norm of the error between the solutions of the Lur'e system and its approximation obtained by harmonic linearization.

By means of three examples the obtained theory was illustrated. These examples showed that the proposed frequency domain analysis based on harmonic linearization often provides more detailed information on the considered system than the often used $\mathscr{L}_2$ gain. It was also shown that for some systems, such a (finite) $\mathscr{L}_2$ gain estimate cannot even be found using a quadratic storage function (as described in Section 2.3), while the harmonic linearization approach still can provide detailed results.
In the examples it also became clear that although simulation-based analysis can predict exact behavior for convergent systems, the approximative analysis based on harmonic linearization is a good alternative, which is much more time-efficient.

It is worth mentioning that the frequency domain analysis by means of the harmonic linearization approach as presented in this chapter has already been used for a practical application [67], i.e. analysis of a nonlinearly controlled optical storage drive.

Although the presented harmonic linearization approach already provides useful results, some interesting issues remain for future work. As mentioned in Section 3.4, the conditions in Theorem 3.7 are only used to prove existence and uniqueness of a $2\pi/\omega$-periodic solution. Existence of solutions with a different period is not excluded, as is shown in Example 3.11 in Section 3.5. However, it is conjectured that if condition 3 of Theorem 3.7 is extended to include also frequency ω, i.e. the frequency domain condition (3.8) is satisfied for $\omega, 3\omega, 5\omega, 7\omega, \ldots$, then the conditions of Theorem 3.7 may also be sufficient to prove that the $T = 2\pi/\omega$-periodic solution is the *only* bounded solution of the system with harmonic input $b\sin(\omega t)$. Future research must point out if this conjecture is true.
Another interesting issue for future work is that besides using the presented approach to evaluate frequency domain behavior of nonlinear systems of Lur'e type, it is suspected that this approach can also be used to *design* such a nonlinear system to meet certain performance requirements. Using the efficient way of computing performance and estimation error, one can try to develop an efficient procedure to find suitable system parameters in the linear approximation and minimize the corresponding estimation error.

In the remainder of this thesis, the harmonic linearization approach as presented in this chapter is used together with the simulation-based analysis for the frequency domain performance analysis of convergent systems.

Chapter 4

Performance Analysis for Externally Forced Lur'e Systems with Saturation

Abstract In this chapter, a theorem is derived to establish uniform convergency for externally forced Lur'e systems with a saturation nonlinearity and marginally stable linear part. This result is shown to be also applicable in the field of anti-windup systems, where it provides a means to analyse the steady-state performance of these systems. Furthermore it is discussed how the notion of convergent systems can be used in combination with existing anti-windup design methods, and what the added value of the convergency property is in this case. Various examples are given, which include results from both simulation and real-time experiments, to illustrate the developed theory and to show how this theory can be used to analyse a system's performance.

4.1 Introduction

In Section 2.4 definitions and some properties have been given for both quadratically convergent and uniformly convergent systems. In the past, several results have been found to prove quadratic convergency for different types of nonlinear systems, see e.g. [63, 65]. These results, however, are not applicable for a nonlinear system of Lur'e type with a marginally stable linear part. To prove that such a system is *uniformly* convergent, on the other hand, no constructive results were available so far. In this chapter, such a result is derived for Lur'e systems with a saturation nonlinearity and marginally stable linear part. That is, sufficient (constructive) conditions are found under which this type of systems is guaranteed to be uniformly convergent.

An application area in which the convergency property can be useful is the anti-windup design for linear control systems with actuator saturation. The presence of actuator saturation in an otherwise linear closed-loop system can dramatically degrade the performance of that system. This performance degradation is caused by the so-called 'controller windup': an integral action or relatively slow mode in the controller causes the control signal to grow (windup) while saturation occurs. A terrifying example of the effects that controller windup can cause is given by the pilot induced oscillations that caused the YF-22 crash in April 1992 [14] and the Gripen crash in August 1993 [86]. The study of anti-windup design deals with synthesizing an additional controller that compensates for this performance degradation. This study received a lot of attention during the last decades and has resulted in many proposals for both linear and nonlinear anti-windup designs (see e.g. [22, 24, 25, 29, 41, 77, 90]). A relatively simple introduction to the field of anti-windup design can be found in [21].

In this chapter, the theory on uniform convergency is applied to the field of anti-windup systems with a marginally stable plant, in order to analyse the steady-state performance of these systems. Although there exist in literature some anti-windup techniques (e.g. [39, 90]) that are able to guarantee global anti-windup for such systems, the convergent systems approach applied here is new. That is, whereas the existing anti-windup methods focus on guaranteeing some form of (incremental) $\mathscr{L}_2$ stability of the system, this convergent systems approach focusses on ensuring a unique limit solution. Since in some cases the anti-windup methods also lead to convergent system behavior, a comparison is made that clarifies the exact differences between the convergent systems approach and the existing anti-windup methods. This comparison also clarifies that new insights can be gained from the convergent systems approach.

For anti-windup systems with an *asymptotically* stable plant, quadratic convergency can be proven using the theory of V.A. Yakubovich [109], see also [65]. A similar result has been obtained in [22]. However, for systems with a *marginally* stable plant as discussed in this chapter, quadratic convergency cannot be obtained and hence the focus lies on establishing uniform convergency.

The remainder of this chapter is organized as follows. Section 4.2 introduces the considered Lur'e system with saturation nonlinearity and provides a theorem with sufficient conditions under which this system is uniformly convergent. Section 4.3 describes how the obtained theoretic results can be applied in the field of anti-windup design, and provides a comparison with existing anti-windup design methods. In the second part of this chapter, the convergent systems approach is applied to analyse the system's performance in two case studies. The first case study (Section 4.4) deals with the performance analysis of an anti-windup system with an integrator plant, while in the second case study (Section 4.5) similar results are obtained for a second (more complex) anti-windup system with a marginally stable plant. For both case studies, simulation and experimental results are used to illustrate the convergent systems approach. Finally, Section 4.6 gives a discussion on the results obtained in this chapter.

4.2 Uniform convergency for Lur'e systems with saturation and marginally stable linear part

Consider a Lur'e system with saturation nonlinearity as given by the following equations

$$\begin{aligned} \dot{x} &= Ax + B\mathrm{sat}(u) + Fw \\ u &= Cx + Dw \\ y &= Hx \end{aligned} \tag{4.1}$$

where $x \in \mathbb{R}^n$ is the state, $u \in \mathbb{R}$ is the control input, $w \in \mathbb{R}^m$ is the external input (e.g. reference, disturbance), $y \in \mathbb{R}^p$ is the output, and the saturation function is defined as $\mathrm{sat}(u) = \mathrm{sign}(u)\min(1, |u|)$. Matrix A is marginally stable, i.e. there exists a $P = P^T > 0$ such that $PA + A^T P \leq 0$. Furthermore, it is assumed that matrix A has at least one eigenvalue equal to 0. Without loss of generality assume that $x = [\, x_1,\, x_2\,]^T$ with $x_1 \in \mathbb{R}^1$, $x_2 \in \mathbb{R}^{n-1}$ and

$$A = \begin{bmatrix} 0 & 0 \\ 0 & A_2 \end{bmatrix}, \quad B = \begin{bmatrix} B_1 \\ B_2 \end{bmatrix}, \quad F = \begin{bmatrix} F_1 \\ F_2 \end{bmatrix}, \tag{4.2}$$

where obviously B_1 is a scalar. If system (4.1) does not satisfy (4.2), a similarity transformation can be performed to obtain the desired form (4.2). Note that the convergency property for a system is coordinate independent, and thus it holds under a similarity transformation. External input w is assumed to belong to class $\mathscr{W}$ which is defined below.

Definition 4.1. A continuous function $t \mapsto w(t)$, $w(t) \in \mathbb{R}^m$ is said to belong to class $\mathscr{W}$ if $w(t)$ is bounded and if it satisfies the following conditions
1. $Dw(t)$ is uniformly continuous,
2. $\forall t \in \mathbb{R}$, $|F_1 w(t)| < \alpha_1 |B_1|$ for some constant $\alpha_1 < 1$.

The remainder of this section is written towards Theorem 4.3 which states under which conditions system (4.1) with $w \in \mathscr{W}$ is uniformly convergent.

Consider a system consisting of two copies of (4.1) with identical inputs:

$$\dot{x}_{\mathrm{AB}} = \begin{bmatrix} A & 0 \\ 0 & A \end{bmatrix} x_{\mathrm{AB}} + \begin{bmatrix} B & 0 \\ 0 & B \end{bmatrix} \begin{bmatrix} \mathrm{sat}(u_A) \\ \mathrm{sat}(u_B) \end{bmatrix} + \begin{bmatrix} F \\ F \end{bmatrix} w, \tag{4.3}$$

with $x_{\mathrm{AB}} = [\, x_{\mathrm{A}},\, x_{\mathrm{B}}\,]^T = [\, x_{1\mathrm{A}},\, x_{2\mathrm{A}},\, x_{1\mathrm{B}},\, x_{2\mathrm{B}}\,]^T$, $u_{\mathrm{A}} = Cx_{\mathrm{A}} + Dw$ and $u_{\mathrm{B}} = Cx_{\mathrm{B}} + Dw$. Define the function $\xi(t)$ as follows

$$\xi(t) = \begin{cases} \frac{\mathrm{sat}(u_{\mathrm{B}}) - \mathrm{sat}(u_{\mathrm{A}})}{u_{\mathrm{B}} - u_{\mathrm{A}}} & \text{if } u_{\mathrm{A}}(t) \neq u_{\mathrm{B}}(t); \\ 1 & \text{if } u_{\mathrm{A}}(t) = u_{\mathrm{B}}(t),\ |u_{\mathrm{A}}(t)| < 1 \text{ and } |u_{\mathrm{B}}(t)| < 1; \\ 0 & \text{otherwise.} \end{cases}$$

Furthermore, since the function $\mathrm{sat}(\cdot)$ satisfies the incremental sector condition it follows that $0 \leq \xi(t) \leq 1$ for all t.

Lemma 4.2. *Assume system* (4.1) *with* $w \in \mathscr{W}$ *is uniformly ultimately bounded (as defined in Section 2.1). Then, given a* $w \in \mathscr{W}$*, there is a* $\delta > 0$ *such that for any solution* $x_{AB}(t, t_0, x_{AB,0})$ *of* (4.3) *starting from some compact set* Ω *there exist a* $\bar{T} = \bar{T}(\Omega) > 0$*, such that for all* $t \geq t_0$ *it follows that*

$$\int_t^{t+\bar{T}} \xi(s)ds \geq \delta.$$

Proof. First, it is assumed that the initial conditions are taken from Ω_+, where Ω_+ is a positively invariant set with respect to system (4.1) with $w \in \mathscr{W}$, that exists due to the uniform ultimate boundedness of the system.

From (4.1), (4.2) it follows that

$$\dot{x}_{1\mathrm{A}} = B_1 \mathrm{sat}(u_{\mathrm{A}}) + F_1 w$$

and therefore for any $t \geq t_0$, $T > 0$

$$x_{1\mathrm{A}}(t+T) - x_{1\mathrm{A}}(t) = \int_t^{t+T} B_1 \mathrm{sat}(u_{\mathrm{A}}(s))ds + \int_t^{t+T} F_1 w(s)ds. \tag{4.4}$$

Dividing both sides of (4.4) by T and taking the absolute value gives

$$\begin{aligned} \left| \frac{B_1}{T} \int_t^{t+T} \mathrm{sat}(u_{\mathrm{A}}(s))ds \right| &= \left| \frac{x_{1\mathrm{A}}(t+T) - x_{1\mathrm{A}}(t)}{T} - \frac{1}{T} \int_t^{t+T} F_1 w(s)ds \right| \\ &\leq \left| \frac{x_{1\mathrm{A}}(t+T) - x_{1\mathrm{A}}(t)}{T} \right| + \left| \frac{1}{T} \int_t^{t+T} F_1 w(s)ds \right|. \end{aligned}$$

Note that due to Definition 4.1 and the assumption that system (4.1) is uniformly ultimately bounded, it follows that second term of the right hand side is strictly smaller than $|B_1|$, and that by making T sufficiently large, one can make the first term of the right hand side arbitrarily small. In other words, for a sufficiently large $\bar{T} = \bar{T}(\Omega_+)$ there is a constant $\alpha < 1$, that can be chosen independently of t_0 such that

$$\left| \frac{1}{\bar{T}} \int_t^{t+\bar{T}} \mathrm{sat}(u_{\mathrm{A}}(s))ds \right| \leq \alpha < 1. \tag{4.5}$$

Due to the mean value theorem, it follows from (4.5) that there is an $\eta \in (t, t+\bar{T}]$ such that $|\mathrm{sat}(u_{\mathrm{A}}(\eta))| \leq \alpha < 1$, i.e. in the time interval $(t, t+\bar{T}]$ there is always a moment in which 'one copy' of (4.3) is in the linear mode ($|u_{\mathrm{A}}| < 1$). From the assumption of uniform ultimate boundedness it follows that $\dot{x}_{\mathrm{A}}(t)$ is bounded and thus $x_{\mathrm{A}}(t)$ is uniformly continuous. Using also Definition 4.1 it can be concluded that function $\mathrm{sat}(u_{\mathrm{A}}(t))$ is uniformly continuous on $[t_0, \infty)$. Now choose some $\varepsilon > 0$ such that $\alpha + \varepsilon < 1$. Since $\mathrm{sat}(u_{\mathrm{A}}(t))$ is uniformly continuous there is a number $\Delta t > 0$, independent of t_0, such that

$$|\mathrm{sat}(u_{\mathrm{A}}(\tau))| \leq \alpha + \varepsilon < 1, \;\; \forall \tau \in [\eta - \Delta t, \; \eta + \Delta t].$$

Among the possible values, choose Δt such that $[\eta - \Delta t,\ \eta + \Delta t] \subset (t, t+\bar{T}]$. Now, integrating nonnegative ξ from t till $t+\bar{T}$ yields

$$\int_t^{t+\bar{T}} \xi(s)ds \geq \int_{\eta-\Delta t}^{\eta+\Delta t} \xi(s)ds \geq 2\Delta t \xi_{\min},$$

where

$$\xi_{\min} = \min_{\tau \in [\eta-\Delta t,\ \eta+\Delta t]} \xi(\tau).$$

For this case, in which $\mathrm{sat}(u_{\mathrm{A}}) = u_{\mathrm{A}} \leq \alpha + \varepsilon < 1$, the minimum value of $\xi(\tau)$ is obtained for a maximal value of u_{B}, i.e.

$$\xi_{\min} = \frac{\mathrm{sat}(u_{\mathrm{B}}) - \mathrm{sat}(u_{\mathrm{A}})}{u_{\mathrm{B}} - u_{\mathrm{A}}} \geq \frac{1-(\alpha+\varepsilon)}{u_{\mathrm{B,max}} - (\alpha+\varepsilon)} > 0$$

where $u_{\mathrm{B,max}}$ is the maximum value of $|u_{\mathrm{B}}|$ that can be obtained for a given $w \in \mathcal{W}$ and any $x_{\mathrm{B}} \in \Omega_+$. Note that also for the case in which $u_{\mathrm{B,max}} < 1$ (and thus $\mathrm{sat}(u_{\mathrm{B}}) < 1$) it holds that $\xi_{\min} > 0$. Therefore,

$$\int_t^{t+\bar{T}} \xi(s)ds \geq 2\Delta t \frac{1-\alpha-\varepsilon}{u_{\mathrm{B,max}} - \alpha - \varepsilon} > 0.$$

The last inequality implies the inequality from Lemma 4.2 with

$$\delta = 2\Delta t \frac{1-\alpha-\varepsilon}{u_{\mathrm{B,max}} - \alpha - \varepsilon}.$$

To prove the lemma, recall the definition of uniform ultimate boundedness (Section 2.1) and, for an arbitrary compact set Ω, take $\bar{T}(\Omega) = \bar{T}(\Omega_+) + T(\Omega)$, where $T(\Omega)$ is from the definition of uniform ultimate boundedness. Note that δ is independent of the initial conditions from Ω, and only depends on the positively invariant set Ω_+ and input $w \in \mathcal{W}$. □

In the following theorem the main result of this chapter is presented.

Theorem 4.3. *If system* (4.1) *with $w \in \mathcal{W}$ is uniformly ultimately bounded, and in addition there exists a Lyapunov matrix $P = P^T > 0$ such that*

$$PA + A^T P \leq 0 \tag{4.6}$$

and

$$P(A+BC) + (A+BC)^T P < 0, \tag{4.7}$$

then system (4.1) *is uniformly convergent for every input $w \in \mathcal{W}$.*

Note that if there is a Lyapunov matrix $P = P^T > 0$ such that $PA + A^T P < 0$ (instead of condition (4.6)) and $P(A+BC) + (A+BC)^T P < 0$ hold, then the corresponding system can be proven to be quadratically convergent. However, matrix A in system (4.1) is marginally stable thus $PA + A^T P < 0$ cannot be satisfied. The proof of Theorem 4.3 is given below.

Proof. Consider for system (4.3) the Lyapunov-like function

$$V(x_{\mathrm{AB}}) = x_{\mathrm{AB}}^T \begin{bmatrix} P & -P \\ -P & P \end{bmatrix} x_{\mathrm{AB}} \geq 0,$$

with $x_{\mathrm{AB}} = [\, x_{\mathrm{A}},\, x_{\mathrm{B}}]^T$. Denote $e = x_{\mathrm{A}} - x_{\mathrm{B}}$ and $\varphi = \mathrm{sat}(u_{\mathrm{A}}) - \mathrm{sat}(u_{\mathrm{B}})$. Then the derivative of V satisfies

$$\begin{aligned} \dot{V} &= e^T(PA + A^TP)e + 2e^TPB\varphi \\ &= e^T(PA + A^TP)e + 2e^TPBCe\xi \\ &= e^T(PA + A^TP)e(1-\xi) \\ &\quad + e^T(P(A+BC) + (A+BC)^TP)e\xi \\ &\leq e^T(P(A+BC) + (A+BC)^TP)e\xi. \end{aligned}$$

It follows then that V satisfies the following inequality

$$\dot{V} \leq \lambda_{\max}\xi(t)V,$$

in which $\lambda_{\max} < 0$ is the largest solution of the following generalized eigenvalue problem

$$\det\big(P(A+BC) + (A+BC)^TP - \lambda P\big) = 0.$$

Hence $\int_{t_0}^{t_0+\bar{T}} \lambda_{\max}\xi(t)dt \leq \lambda_{\max}\delta < 0$ with δ from the statement of Lemma 4.2. Using the Gronwall-Bellman lemma (see e.g. [1]) one can see that $V \to 0$ as $t \to \infty$ uniformly in time and uniformly in the initial conditions from Ω. Since the system is uniformly ultimately bounded, Ω is an arbitrary compact set, and all solutions are globally uniformly asymptotically stable. Due to Property 2.5 there is a bounded solution $\bar{x}(t)$ defined on the whole time interval $(-\infty, +\infty)$ and thus system (4.1) is uniformly convergent for every $w \in \mathscr{W}$. Note that due to Property 2.7 this solution $\bar{x}(t)$ is the unique solution bounded on $(-\infty, +\infty)$. □

As one can see, this proof is based on a PE-like (persistency of excitation) property that follows from Lemma 4.2. More advanced results in this direction can be found in [53, 62].

Remark 4.4. If the input of system (4.1) is a periodic function of time, then the proof of Theorem 4.3 can be simplified if one employs an extension of the LaSalle principle for periodic time-varying systems, see e.g. [79]. The approach used here is more general, yet requires the regularity assumption imposed on Dw.

In the following section, it is shown that the presented theorem can also be applied to prove uniform convergency of anti-windup systems with a marginally stable plant, and it is explained how this result can be used in addition to the existing synthesis methods for anti-windup systems.

4.3 Uniform convergency for anti-windup systems with a marginally stable plant

Consider the system in Figure 4.1 with plant dynamics

$$\begin{aligned} \dot{x}_\mathrm{p} &= A_\mathrm{p} x_\mathrm{p} + B_\mathrm{p}\left(\mathrm{sat}(u) + w_1\right) \\ y_\mathrm{p} &= C_\mathrm{p} x_\mathrm{p} \end{aligned} \tag{4.8}$$

where A_p is marginally stable with at least one eigenvalue 0. The controller dynamics are given by

$$\begin{aligned} \dot{x}_\mathrm{c} &= A_\mathrm{c} x_\mathrm{c} + B_\mathrm{c}(w_2 - y_\mathrm{p}) + L_\mathrm{aw}\left(\mathrm{sat}(u) - u\right) \\ u &= C_\mathrm{c} x_\mathrm{c} + D_\mathrm{c}(w_2 - y_\mathrm{p}) \end{aligned} \tag{4.9}$$

in which L_aw is a *static* anti-windup gain.

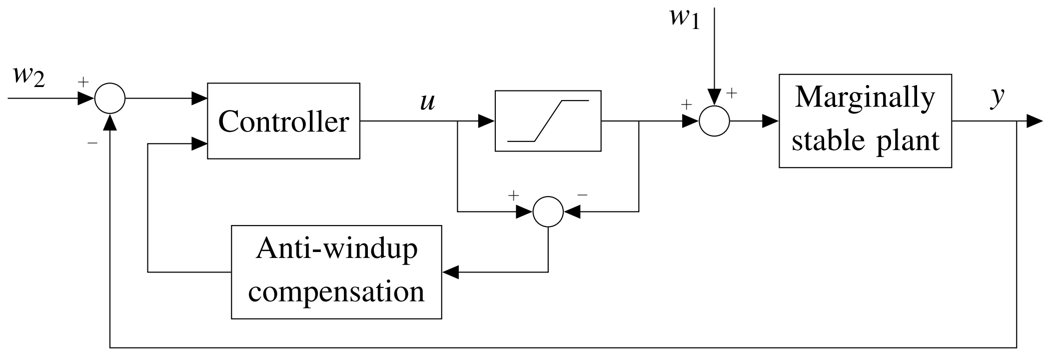

Figure 4.1: Anti-windup scheme with marginally stable plant.

For the given system the closed-loop dynamics can be written in Lur'e form (4.1) with $x = [\,x_\mathrm{p},\ x_\mathrm{c}\,]^T \in \mathbb{R}^n$, $w = [\,w_1,\ w_2\,]^T \in \mathscr{W}$, and

$$A = \begin{bmatrix} A_\mathrm{p} & 0 \\ L_\mathrm{aw} D_\mathrm{c} C_\mathrm{p} - B_\mathrm{c} C_\mathrm{p} & A_\mathrm{c} - L_\mathrm{aw} C_\mathrm{c} \end{bmatrix},$$

$$B = \begin{bmatrix} B_\mathrm{p} \\ L_\mathrm{aw} \end{bmatrix}, \quad F = \begin{bmatrix} B_\mathrm{p} & 0 \\ 0 & B_\mathrm{c} - L_\mathrm{aw} D_\mathrm{c} \end{bmatrix},$$

$$C = \begin{bmatrix} -D_\mathrm{c} C_\mathrm{p} & C_\mathrm{c} \end{bmatrix}, \quad D = \begin{bmatrix} 0 & D_\mathrm{c} \end{bmatrix}, \quad H = \begin{bmatrix} C_\mathrm{p} & 0 \end{bmatrix}.$$

After a similarity transform, this system fits the form (4.2), and hence Theorem 4.3 can be applied to establish uniform convergency of this system. In Section 4.4 it is demonstrated for a relatively simple system how the static anti-windup gain L_aw can be chosen in such a way that the system is convergent.

Note that also for *dynamic* anti-windup compensation, for example as proposed in [90], with plant dynamics (4.8) and controller dynamics given by

$$
\begin{aligned}
\dot{x}_{\mathrm{c}} &= A_{\mathrm{c}}x_{\mathrm{c}} + B_{\mathrm{c}}(w_2 - y_{\mathrm{p}} - v_2) \\
u &= C_{\mathrm{c}}x_{\mathrm{c}} + D_{\mathrm{c}}(w_2 - y_{\mathrm{p}} - v_2) + v_1 \\
\\
\dot{x}_{\mathrm{aw}} &= A_{\mathrm{p}}x_{\mathrm{aw}} + B_{\mathrm{p}}\left(\mathrm{sat}(u) - u + v_1\right) \\
v_1 &= k(x_{\mathrm{aw}}) \\
v_2 &= -C_{\mathrm{p}}x_{\mathrm{aw}}
\end{aligned}
\tag{4.10}
$$

with some linear function $k(x_{\mathrm{aw}})$, the closed-loop system equations can be written in Lur'e form (4.1), and hence Theorem 4.3 can be applied.

In order to clarify the difference between a convergent systems approach for anti-windup synthesis and the $\mathscr{L}_2$ anti-windup synthesis in e.g. [39, 90], first consider the definition by Teel and Kapoor [90] of the global (nominal) anti-windup problem. Loosely speaking, this definition states that the problem is to find a (static, dynamic) anti-windup modification of a predefined linear system with actuator saturation such that

1. if the control signal never saturates, then the closed-loop trajectories of the system with saturation and anti-windup equal those of the corresponding linear system (without saturation and anti-windup), i.e. if $\mathrm{sat}(u(t)) \equiv u(t)$ then $x(t) \equiv x_{\mathrm{lin}}(t)$
2. if $(\mathrm{sat}(u_{\mathrm{lin}}(t)) - u_{\mathrm{lin}}(t)) \in \mathscr{L}_2$ then $(x(t) - x_{\mathrm{lin}}(t)) \in \mathscr{L}_2$.

Here, x and u represent respectively the state and control input of the system with actuator saturation and anti-windup compensation, whereas x_{lin} and u_{lin} represent the state and control input of the corresponding linear system (i.e. without saturation and anti-windup compensation).

If $||\mathrm{sat}(u_{\mathrm{lin}}) - u_{\mathrm{lin}}||_2$ is finite then, by the result of [39, 90], $||x - x_{\mathrm{lin}}||_2$ is also finite, but it is not guaranteed that $x(t)$ converges to $x_{\mathrm{lin}}(t)$. If in addition to the assumptions in [39, 90] it is known that the nonlinear system is uniformly ultimately bounded and input w is bounded, it follows that $\dot{x} - \dot{x}_{\mathrm{lin}}$ is bounded and hence $x - x_{\mathrm{lin}}$ is uniformly continuous. By Barbalat's lemma (see e.g. [40]), it then follows that $x(t)$ eventually converges to $x_{\mathrm{lin}}(t)$. Since $x_{\mathrm{lin}}(t)$ is the solution of a linear system, it converges to a unique limit solution (provided that matrix $A + BC$ is Hurwitz), and hence $x(t)$ eventually converges to a unique limit solution, which is independent of the initial conditions, and only depends on the external input signals.

If, on the other hand, $||\mathrm{sat}(u_{\mathrm{lin}}) - u_{\mathrm{lin}}||_2$ is not finite, then based on the assumptions in [39, 90], no conclusions can be drawn about whether the system has a unique limit solution or not, and only an upper bound on the performance of the system may be found (using e.g. the extended $\mathscr{L}_2^e$ norm). Using a convergent systems approach, however, one can prove the existence of a unique limit solution, even for the case in which $||\text{sat}(u_{\text{lin}}) - u_{\text{lin}}||_2$ is not finite. This limit solution can then be determined exactly using simulation, as mentioned in Section 2.4.

It is interesting to note that the marginally stable plant (4.8) with the dynamic anti-windup design (4.10) and $k(x_{\text{aw}}) = -B_{\text{p}}^T P x_{\text{aw}}$ as proposed in [90], can be proven to be uniformly convergent, if $A_{\text{p}} - B_{\text{p}} B_{\text{p}}^T P$ is Hurwitz (this is always the case if $A_{\text{p}}, B_{\text{p}}$ is stabilizable), the system is uniformly ultimately bounded, and the external input signals satisfy Definition 4.1. Since the full proof of this claim is not interesting within the scope of this chapter, only the rough directions of this proof are given and technical details are omitted:
Using system equations (4.8) and (4.10) one can construct the following relation:

$$u = H_3 \text{sat}(u) + \frac{H_3 H_2 H_1 - H_2 H_1}{1 + H_2 H_1} w_1 + \frac{H_2 - H_3 H_2}{1 + H_2 H_1} w_2$$

with $H_1 = C_{\text{p}}(sI - A_{\text{p}})^{-1} B_{\text{p}}$, $H_2 = C_{\text{c}}(sI - A_{\text{c}})^{-1} B_{\text{c}} + D_{\text{c}}$, $H_3 = -B_{\text{p}}^T P (sI - A_{\text{p}})^{-1} B_{\text{p}}$, and $s = \frac{d}{dt}$. The dynamics of H_3 can for example be described by the following state-space representation:

$$\begin{aligned} \dot{\zeta} &= A_{\text{p}} \zeta + B_{\text{p}} \text{sat}(u), \\ u &= -B_{\text{p}}^T P \zeta. \end{aligned}$$

Matrix $P = P^T > 0$ is such that $P A_{\text{p}} + A_{\text{p}}^T P \leq 0$ and $P(A_{\text{p}} - B_{\text{p}} B_{\text{p}}^T P) + (A_{\text{p}}^T - P B_{\text{p}} B_{\text{p}}^T) P < 0$. If in addition the system is ultimately bounded and input w satisfies Definition 4.1, then all conditions of Theorem 4.3 are satisfied, and hence the system with the dynamic anti-windup as proposed in [90] is uniformly convergent.
From this result one can conclude that based on the convergent systems approach, an additional result can be obtained for the same anti-windup design, i.e. a result that can also be applied if $||\text{sat}(u_{\text{lin}}) - u_{\text{lin}}||_2$ is not finite.

Note that for anti-windup systems with an asymptotically stable plant, the convergent systems approach can also be used, using existing results on quadratic convergency of Lur'e systems, see e.g. [109] or [65]. In order to find an anti-windup compensator that optimizes the performance of the convergent closed-loop system, one can use some simulation-based optimization scheme that optimizes the steady-state trajectory of the system for some performance index. Also, the existing static and dynamic anti-windup synthesis methods (possibly with extension to $\mathscr{L}_2^e$) can be used in combination with the convergent system approach to obtain a more detailed performance analysis.

Concluding, one can observe that the convergent system approach is an alternative approach to the anti-windup problem. Whereas existing anti-windup methods, as discussed in [39, 90], focus on the *design* of anti-windup compensators, this convergent system approach focusses on performance *analysis* of systems with anti-windup compensation. It does not directly result in new anti-windup designs, but provides new performance insights for existing anti-windup designs, especially when $||\text{sat}(u_{\text{lin}}) - u_{\text{lin}}||_2$ is not finite, for which most existing anti-windup synthesis methods provide no performance analysis. The case in which $||\text{sat}(u_{\text{lin}}) - u_{\text{lin}}||_2$ is not finite for example occurs for (periodic) reference signals, which now and then keep forcing the control signal to saturate. If the fraction of time that the control signal saturates is small enough, one can argue not to use a (more expensive) actuator with saturation bounds that are less tight, but use an appropriate anti-windup compensator instead.

The following two sections contain several examples that demonstrate the convergent systems approach for a static anti-windup design for systems with a marginally stable plant.

4.4 Case study 1: Performance analysis of an anti-windup system with an integrator plant

In this section, the performance of the system in Figure 4.2 is investigated using the theory described in the previous two sections. For that purpose, first it is shown that this system is uniformly convergent if the anti-windup gain k_A satisfies a specific condition. Then, by means of simulation and experimental results, the behavior of the system is illustrated for both the case in which this condition is not met, and the case in which the condition is met. Finally, a frequency-domain performance analysis of the uniformly convergent system is presented, using both simulation and experimental results and the harmonic balance method as presented in Chapter 3.

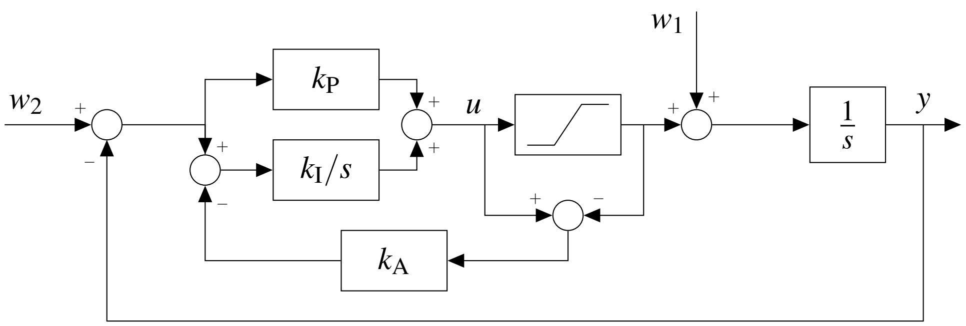

Figure 4.2: Anti-windup scheme with integrator plant.

Consider the system in Figure 4.2, consisting of an integrator plant, a proportional-integral (PI) feedback controller, actuator saturation and static anti-windup compensation. The dynamics of this system can be written in Lur'e form (4.1)

$$\begin{aligned}\dot{x} &= Ax + B\text{sat}(u) + Fw\\ u &= Cx + Dw\\ y &= Hx\end{aligned}$$

where $w = [\, w_1,\ w_2\,]^T \in \mathscr{W}$ and

$$A = \begin{bmatrix} 0 & 0 \\ -(1-k_A k_P) & -k_I k_A \end{bmatrix}, \quad B = \begin{bmatrix} 1 \\ k_A \end{bmatrix},$$

$$F = \begin{bmatrix} 1 & 0 \\ 0 & 1 - k_A k_P \end{bmatrix}, \quad C = \begin{bmatrix} -k_P & k_I \end{bmatrix},$$
$$D = \begin{bmatrix} 0 & k_P \end{bmatrix}, \quad H = \begin{bmatrix} 1 & 0 \end{bmatrix}.$$

Here, k_I and k_P are given positive constants, and k_A is a nonnegative constant to be designed. The following corollary states what condition k_A should satisfy to guarantee uniform convergency of the system.

Corollary 4.5. *If $k_A > 1/k_P$ then the system given in Figure 4.2 is uniformly convergent for all $w \in \mathscr{W}$.*

Proof. This corollary can be proved using the theory developed in Section 4.2. First, it is shown that the system is uniformly ultimately bounded. Under the given assumption, it is possible to perform a similarity transformation $[\, x_1,\, x_2\,]^T = Tx$ with

$$T = \begin{bmatrix} 1 & 0 \\ \frac{k_A k_P - 1}{k_I k_A} & 1 \end{bmatrix}$$

so that the given system can be rewritten into:

$$\begin{aligned} \begin{bmatrix} \dot{x}_1 \\ \dot{x}_2 \end{bmatrix} &= \begin{bmatrix} 0 & 0 \\ 0 & A_2 \end{bmatrix} \begin{bmatrix} x_1 \\ x_2 \end{bmatrix} + \begin{bmatrix} B_1 \\ B_2 \end{bmatrix} \mathrm{sat}(u) + \begin{bmatrix} F_1 \\ F_2 \end{bmatrix} w \\ u &= C_1 x_1 + C_2 x_2 + Dw \end{aligned} \tag{4.11}$$

with

$$\begin{aligned} A_2 &= -k_I k_A, \quad B_1 = 1, \quad B_2 = \frac{1 - k_A k_P + k_I k_A^2}{k_I k_A}, \\ F_1 &= [\, 1,\, 0\,], \quad F_2 = [\, \frac{1 - k_A k_P}{k_I k_A},\, 1 - k_A k_P\,], \\ C_1 &= -\frac{1}{k_A}, \quad C_2 = k_I, \quad D = [\, 0,\, k_P\,]. \end{aligned}$$

Since $\dot{x}_2 = A_2 x_2 + \ldots$ can be interpreted as an LTI system with bounded inputs and A_2 is Hurwitz, it follows that $\limsup_{t\to\infty} |x_2(t)|$ exists. Now consider the first subsystem of (4.11) together with the Lyapunov function $V = x_1^2/2$. The derivative of this function is given by

$$\dot{V} = x_1 \left[\mathrm{sat}(-\frac{1}{k_A} x_1 + k_I x_2 + k_P w_2) + w_1 \right].$$

Taking into account that $\limsup_{t\to\infty} |x_2(t)|$ exists, $|w_1| \le \alpha_1 < 1$, and $|w_2|$ is bounded it follows that

$$\mathrm{sat}(-\frac{1}{k_A} x_1 + k_I x_2 + k_P w_2) = \mathrm{sign}(-\frac{1}{k_A} x_1) \quad \text{if} \quad |x_1| > k_A(k_I |x_2| + k_P |w_2| + 1)$$

and thus

$$\dot{V} \le -|1 - \alpha_1|\, |x_1| < 0 \quad \text{if} \quad |x_1| > k_A(k_I |x_2| + k_P |w_2| + 1)$$

which (similarly to the Yoshizawa theorem, see e.g. [30]) implies that system (4.11) is uniformly ultimately bounded.

The fact that the system is uniformly ultimately bounded in turn implies that Lemma 4.2 holds for large enough $\bar{T}$. Finally, for $k_{\mathrm{A}} > 1/k_{\mathrm{P}}$ and for example

$$P = \begin{bmatrix} (k_{\mathrm{A}}k_{\mathrm{P}} - 1) + k_{\mathrm{I}}k_{\mathrm{A}}^2 & 0 \\ 0 & k_{\mathrm{I}}^2 k_{\mathrm{A}}^2 \end{bmatrix} > 0$$

inequalities (4.6) and (4.7) are satisfied. Thus Theorem 4.3 holds and the system in Figure 4.2 is uniformly convergent. □

Remark 4.6. Note that if $k_{\mathrm{A}} > 1/k_{\mathrm{P}}$, then also frequency domain inequality (3.8) holds for all frequencies $\omega \neq 0$. This is a standard result from the Kalman-Yakubovich-Popov lemma, see e.g. [40].

In the remainder of this section, the results of several simulations and experiments are shown and evaluated, in order to analyse the behavior of the system in Figure 4.2. The simulations have been performed in Matlab using an ODE-solver or Simulink model, while the experiments have been performed using the experimental setup as described below. For all the simulations and experiments, the following values have been chosen for the system parameters: $k_{\mathrm{P}} = 10$ and $k_{\mathrm{I}} = 20$, since these values provide a satisfactory closed-loop performance of the system without saturation. Furthermore, disturbance input w_1 is assumed to be 0 for simplicity.

Experimental setup

In order to investigate the behavior of the system in Figure 4.2 in practice, an experimental setup has been constructed, which is shown schematically in Figure 4.3. The experimental setup consists of a PI controlled integrator plant with actuator saturation and a static anti-windup (AW) gain k_{A}. As indicated in Figure 4.3, the hardware of this setup (see Figure 4.4) consists of an actuator (brushless DC motor) an integrator plant and a sensor (incremental encoder, 8192 counts/revolution). The hardware is connected (at sample rate: 1kHz) using a TUeDACS device [91] to a computer with a Matlab Simulink model (Real Time Workshop), which contains the software elements described in Figure 4.3. Both the reference and disturbance signal, and the controller parameters are defined in this model. The actuator is driven by a velocity controller (not shown in Figure 4.3), which receives its reference value v from the Simulink model. The settling time of the velocity controller is negligible, so that it can be assumed that the actuator exactly follows the reference velocity v. The actuator rotates a rigid body at the given speed, and the rotation angle of the body is measured by the incremental encoder and fed back to the Simulink model. This transition from angular velocity to rotation angle forms the integrator plant.

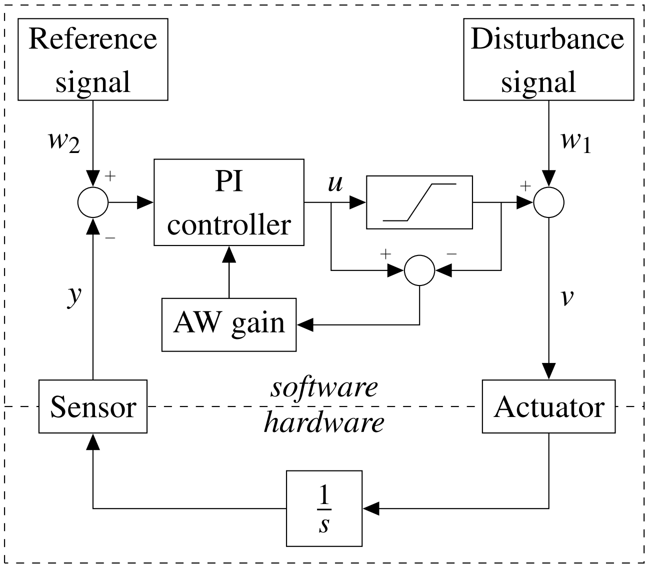

Figure 4.3: Schematic representation of the experimental setup.

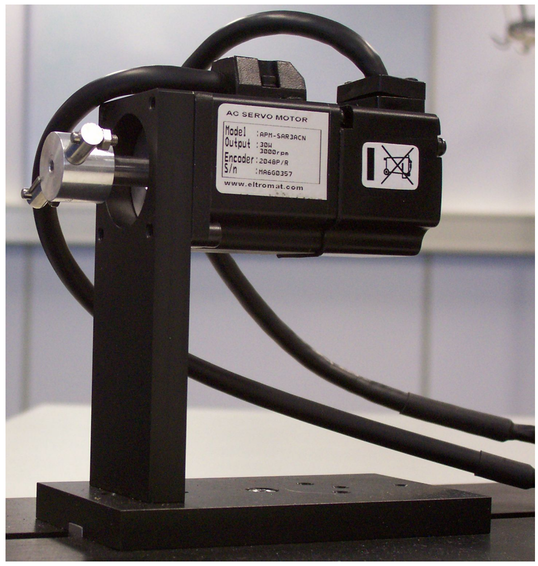

Figure 4.4: Photo of the hardware construction.

Simulation and experimental results for $k_A = 0$

First consider the case in which $k_A = 0$, i.e. condition $k_A > 1/k_P$ is not satisfied and hence the system is not guaranteed to be convergent. Figure 4.5 shows system output y as a function of time, when the reference input is $w_2(t) = b\sin(\omega t)$, with amplitude $b = 1$ and frequency $\omega = 1$. The two solutions depicted in the figure are obtained for respectively initial conditions $y(0) = 3$ and $y(0) = 4$, and the initial value of the integrator state in the controller is 0. As one can observe, the simulation results correspond very well to the experimental results. More important, one can also observe that after some transient time, two stable periodic solutions exist, which confirms that the system is not convergent. One solution follows the reference signal quite well, while the other solution resembles a sawtooth. This sawtooth indicates that control output u constantly hits upper and lower saturation as a result of integrator windup, which leads to this undesired behavior.

The fact that multiple steady-state solutions exist for this system is undesirable, even though one of the steady-state solutions displays desirable tracking behavior: a small disturbance can be enough to cause the system to switch from one solution to the other [100]. This also becomes clear from the next experiment, which is motivated by the following thought. Since the amplitude of control signal u becomes larger if amplitude b (or frequency ω) of the reference signal increases, one would suspect that for a relatively large amplitude b the sinusoid-like steady-state solution no longer exists. This is indeed the case, as can be seen in Figure 4.6. For this experiment, again a reference input $w_2(t) = b\sin(t)$ is used, but now with the amplitude slowly varying from $b = 0.1$ to $b = 1.5$ and back again. Every 200π seconds the amplitude is slightly increased/decreased, so that after each change, steady-state is reached again. Figure 4.6 displays the resulting amplitude of controller output u versus amplitude b of the reference signal,

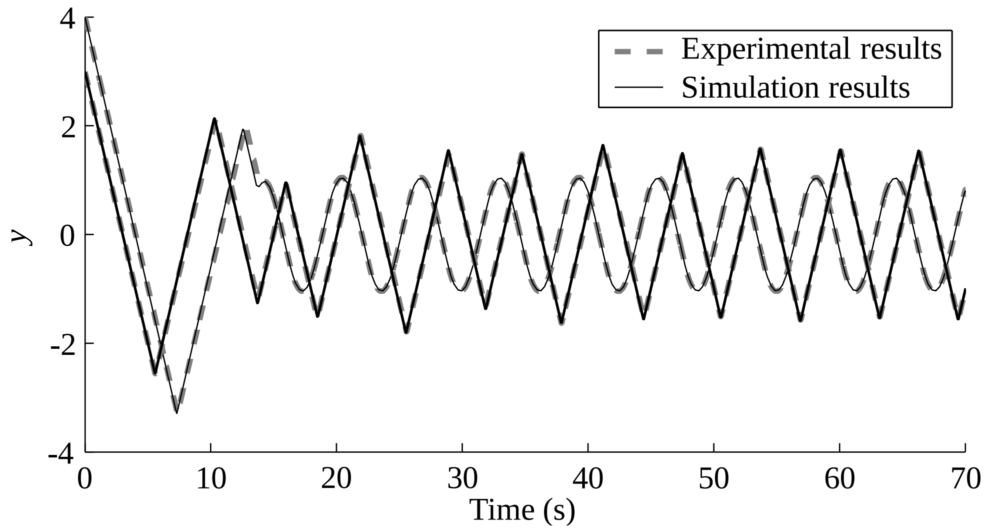

Figure 4.5: System output for $k_A = 0$ and $w_2 = \sin(t)$.

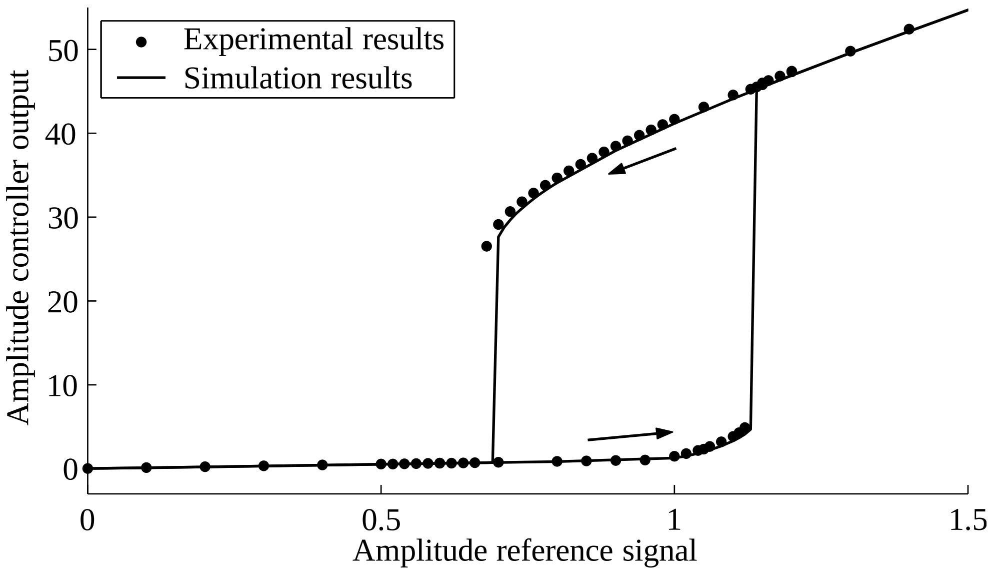

Figure 4.6: 'Hysteresis' for $k_A = 0$ and $w_2 = b\sin(t)$ with $b \in [0, 1.5]$.

once steady-state is reached. One can observe that for a small amplitude b, controller output u has only one amplitude, which suggests that there is only one steady-state solution. For b approximately between 0.69 and 1.13, u can have two different amplitudes, and thus there are (at least) two coexisting steady-state solutions. Finally, if b is larger then approximately 1.13 then again only one amplitude is left for u. Note, however, that this result does not guarantee that there exist no other steady-state solutions. In fact it can be shown using simulation that for this system also multi-periodic steady-state solutions exist (similar to Figure 3.7) for various values of b.

Another observation that can be made from Figure 4.6 is that by slowly increasing b, starting from $b = 0.1$, the amplitude of controller output u also slowly increases but does not switch to the other steady-state solution, until it makes a large jump at $b = 1.13$ and then slowly in-

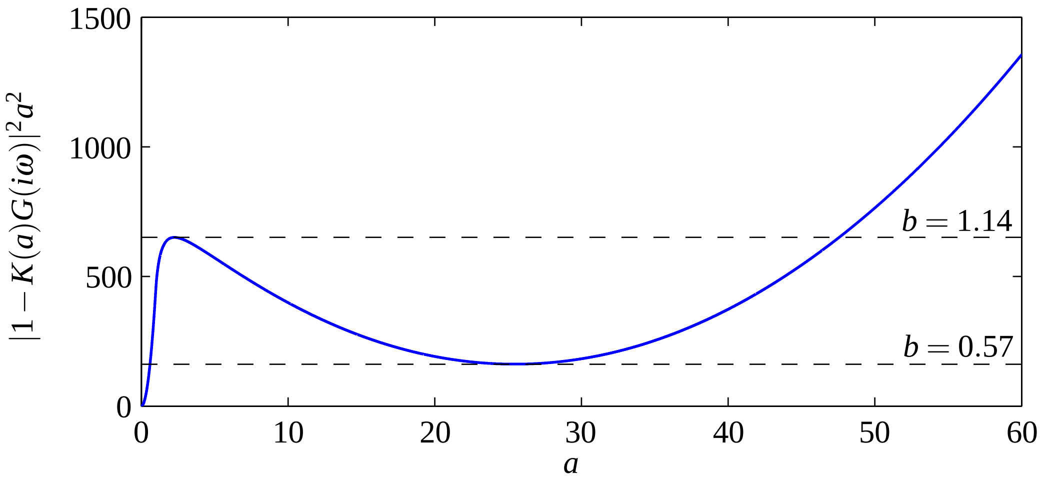

Figure 4.7: Left-hand side of harmonic balance equation for $k_A = 0$ and $\omega = 1$.

creases further. Then, if b is decreased again, the amplitude of u only slowly decreases and does not switch back to the other steady-state solution until $b = 0.69$. This gives Figure 4.6 a hysteresis-like shape. During the experiment it was also noted that the closer the increasing amplitude gets to $b = 1.13$, the smaller the required effort to switch from the desirable solution to the undesirable solution becomes (and vice versa for decreasing $b \to 0.69$). This suggests that the region of attraction of the desirable steady-state solution (small amplitude) decreases with increasing b, while the region of attraction of the undesired steady-state solution (large amplitude) decreases with decreasing b.

Finally, it is interesting to compare the results of Figure 4.6 with the results of a harmonic analysis, as discussed in Section 3.3. Figure 4.7 shows the left-hand side of the harmonic balance equation $|1-K(a)G(i\omega)|^2a^2 = |C(i\omega I - A)^{-1}F + D|^2b^2 = 500b^2$, and indicates the values of b which form the border between one and three solutions a of $|1-K(a)G(i\omega)|^2a^2 = 500b^2$. As one can observe, these values $b = 0.57$ and $b = 1.14$ are close to the values found in Figure 4.6, and also the values of a (small amplitude: < 5, large amplitude: > 30) correspond quite well to the amplitude of u for the different steady-state solutions.

Simulation and experimental results for $k_A k_P > 1$

Now consider the case where $k_A = 0.5 > 1/k_P$ and thus the system is uniformly convergent. The experiment with $w_2(t) = \sin(t)$ and initial conditions $y(0) = 3$ and $y(0) = 4$ is repeated for this value of k_A and the result is given in Figure 4.8. As was expected, the solutions with different initial conditions converge to a unique limit solution.

Since the system is uniformly convergent one can use simulation or experiments to determine the exact steady-state performance of the system, for example in terms of a nonlinear frequency response function (nFRF), or one can use harmonic linearization to estimate this nFRF, see

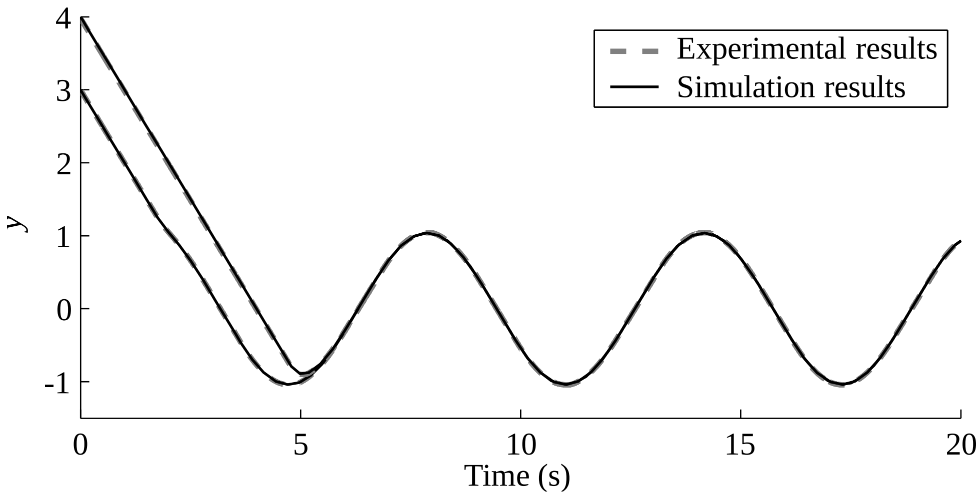

Figure 4.8: System output for $k_\mathrm{A} = 0.5$ and $w_2 = \sin(t)$.

Chapter 3. For a reference signal $w_2(t) = \sin(\omega t)$ with $\omega \in [10^{-1}, 10^2]$, and $k_\mathrm{A} = 0.5$ this nFRF is given in Figure 4.9. Both the results from the harmonic linearization, and the simulation results and the experimental results are given. The experimental results (open circles in Figure 4.9) show a large deviation from the simulation results for frequencies above 10 rad/s. This deviation is caused by the fact that the periodic output signal y of the experimental system has a certain constant offset (in the order of 0.01 revolutions), which is different for each trial. The cause of this offset is not yet clear, it could be unmodeled dynamics, measurement errors, or another cause. Nevertheless, if this offset is subtracted from the solution, such that the average of the steady-state solution is 0, then these corrected experimental results (asterisks in Figure 4.9) follow the simulation results quite well. Furthermore, it can be seen that the simulation and corrected experimental results lie well within the bounds as determined by the harmonic linearization approach, i.e. the harmonic linearization approach is able to give a quite accurate description of the frequency domain behavior of this system. For comparison the FRF for the linear system (i.e. without saturation and anti-windup) is also plotted in this figure. Note that for this system no finite estimate of the $\mathscr{L}_2$ gain from w to y can be found using a quadratic storage function, which makes the result in Figure 4.9 even more valuable from a practical point of view.

Similar nFRFs can be found for different values of k_A, but since they are almost identical to the steady-state results in Figure 4.9, these results are not shown here. On the other hand, whereas the value of k_A hardly affects the steady-state result, it does have a large influence on the transient behavior of the system, especially for relatively high frequencies, as is shown in Figure 4.10 for $w_2 = \sin(10t)$ and various values of k_A. The higher the value of k_A is, the longer the transient period becomes, although for high values of k_A this difference becomes again negligible. The difference between the solutions with $k_\mathrm{A} = 2$ and $k_\mathrm{A} = 20$ is already hardly visible in Figure 4.10.

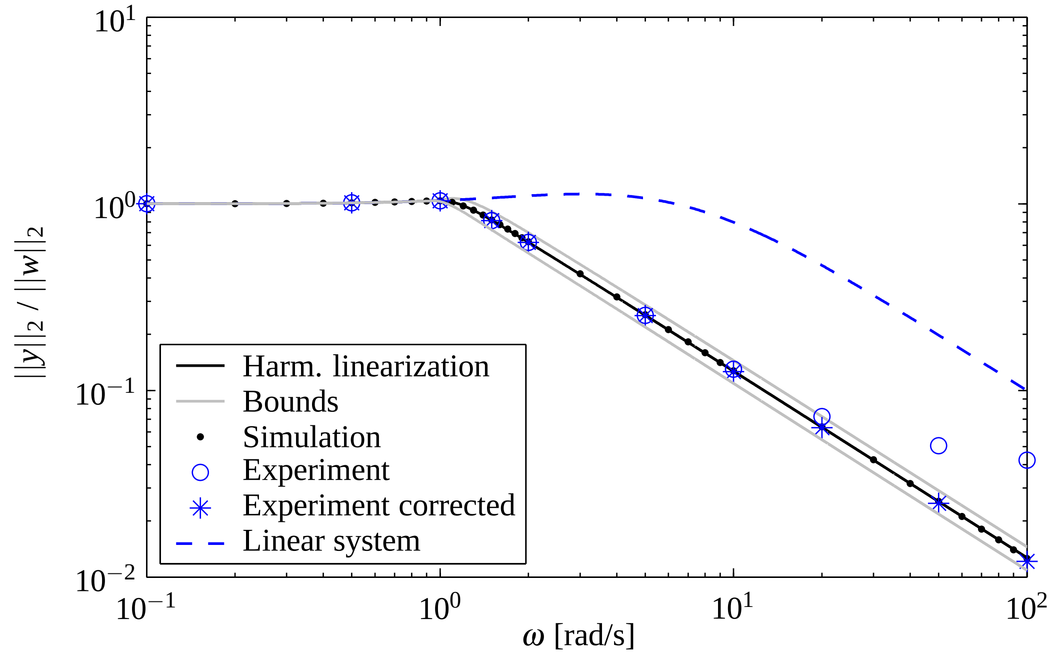

Figure 4.9: Frequency response function for $k_\mathrm{A} = 0.5$ and $w_2(t) = \sin(\omega t)$ with $\omega \in [10^{-1}, 10^{2}]$.

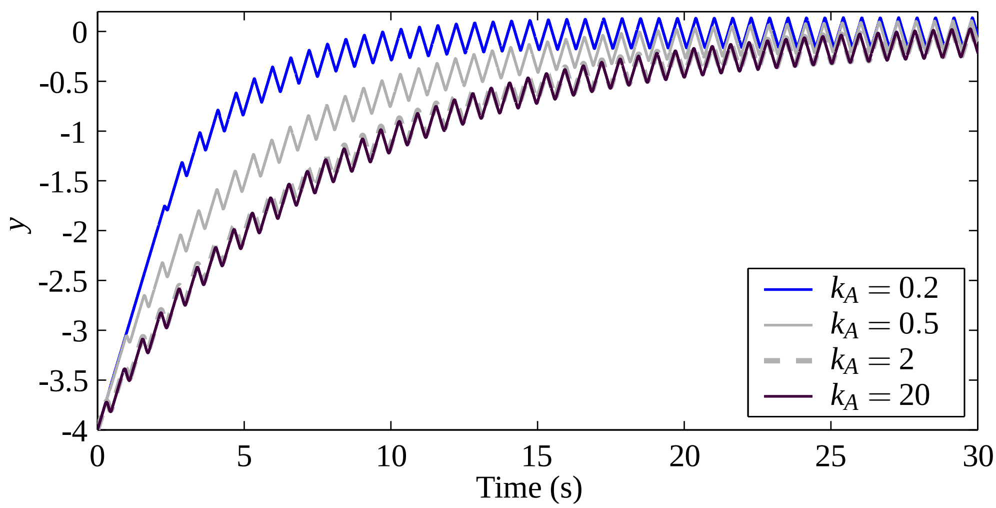

Figure 4.10: Transient behavior of solution for $w_2(t) = \sin(10t)$ and various values of k_A.

The results shown in Figures 4.9 and 4.10 provide much information on the behavior of the system. Results like these can also be used for example to determine the 'best' value of k_{A} for this system. The subject of optimization, however, lies outside the scope of this thesis and is left for future research.

Finally note that the results in Figure 4.9 only hold for harmonic reference signals with amplitude $b = 1$. For other amplitudes, similar graphs can be constructed. In Chapter 5, the effect of amplitude b on the nFRF of an anti-windup system with an integrator plant is discussed further, in the context of manufacturing systems.

4.5 Case study 2: Performance analysis of an anti-windup system with a 'mass-spring-damper' plant

In this case study, instead of an integrator plant, a plant with extra dynamics is investigated. The plant considered here emanates from the mass-spring-damper construction in the experimental setup as discussed later in this section. For the control of this plant again a PI controller with static anti-windup augmentation is applied. The dynamics of the resulting closed-loop system (Figure 4.11) can be described by the following equations

$$\begin{aligned} \dot{x} &= Ax + B\mathrm{sat}(u) + Fw \\ u &= Cx + Dw \\ y &= Hx \end{aligned}$$

where $w = [\, w_1,\ w_2 \,]^T \in \mathscr{W}$ and

$$A = \begin{bmatrix} 0 & 0 & 0 & 0 \\ 0 & 0 & 1 & 0 \\ 3.9 \cdot 10^3 & -3.9 \cdot 10^3 & -10.7 & 0 \\ 0 & -(1 - k_{\mathrm{A}} k_{\mathrm{P}}) & 0 & -k_{\mathrm{I}} k_{\mathrm{A}} \end{bmatrix}, \quad B = \begin{bmatrix} 1 \\ 0 \\ 10.7 \\ k_{\mathrm{A}} \end{bmatrix}, \quad F = \begin{bmatrix} 1 & 0 \\ 0 & 0 \\ 10.7 & 0 \\ 0 & 1 - k_{\mathrm{A}} k_{\mathrm{P}} \end{bmatrix},$$

$$C = \begin{bmatrix} 0 & -k_{\mathrm{P}} & 0 & k_{\mathrm{I}} \end{bmatrix}, \quad D = \begin{bmatrix} 0 & k_{\mathrm{P}} \end{bmatrix}, \quad H = \begin{bmatrix} 0 & 1 & 0 & 0 \end{bmatrix}.$$

Again, k_{I} and k_{P} are given positive constants, and k_{A} is a nonnegative constant to be designed.

As this system has extra dynamics in comparison to the system in Section 4.4, it is harder to analytically find a bound on k_{A} which is sufficient to guarantee uniform convergency of the system. However, it is possible to prove uniform ultimate boundedness of this system and to guarantee uniform convergency for certain *given* values of k_{I}, k_{P} and k_{A}, when $w \in \mathscr{W}$. Since matrix A has one eigenvalue 0, and the other eigenvalues have negative real part, uniform ultimate boundedness of this system can be proven for $k_{\mathrm{A}} > 0$ in the same way as was done in the proof of Corollary 4.5. If the values of k_{I}, k_{P} and k_{A} are such that there exists a $P = P^T > 0$ that satisfies LMIs (4.6) and (4.7) of Theorem 4.3, then the system is uniformly convergent.

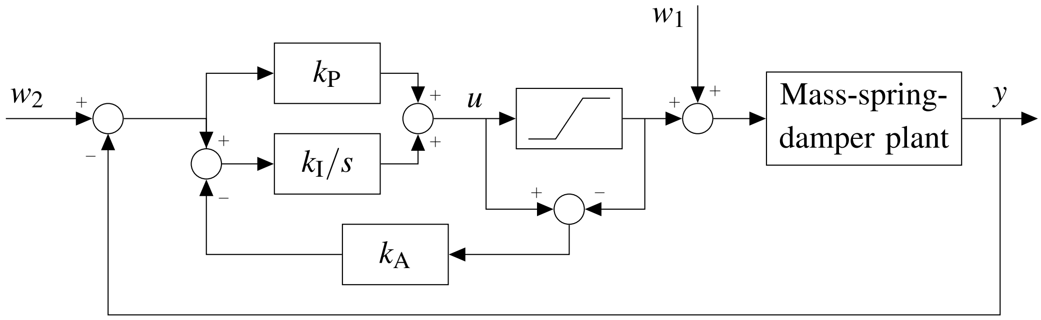

Figure 4.11: Anti-windup scheme with 'mass-spring-damper' plant.

Although it is hard to find an analytic bound on k_A that guarantees uniform convergency of the system for given values of k_P and k_I, it is possible to define a 'sufficient' interval for k_A once two values of k_A have been found for which LMIs (4.6), (4.7) can be solved. That is, since matrix A affinely depends on k_A, and there exists a $P = P^T > 0$ such that (4.6), (4.7) are solvable for $k_A = \underline{k_A}$ and $k_A = \overline{k_A}$, then the LMIs are also solvable for all k_A in the interval $[\underline{k_A}, \overline{k_A}]$. In that case, the system is uniformly convergent for all $k_A \in [\underline{k_A}, \overline{k_A}]$. The considered 'mass-spring-damper' system with $k_I = 20$ and $k_P = 8$ is uniformly convergent if $k_A \in [0.125, 6]$. A larger interval may exist, but is not pursued here.

The remainder of this section is dedicated to some simulation and experimental results that have been obtained for this system. The experimental results have been obtained from the experimental setup as described below.

Experimental setup

The experimental setup considered for this case study, which is schematically shown in Figure 4.13, is similar to the experimental setup discussed in Section 4.4. The only difference is that instead of the integrator plant, now a plant is used that consists of two rotating rigid bodies (masses) connected by an element that has a certain stiffness and damping, see Figure 4.12. The first body is driven by an actuator (brushless DC motor) and the rotation of the second body is measured by a sensor (incremental encoder, 8192 counts/revolution). The connection of the hardware to the software and the design of the software are the same as with the experimental setup in Section 4.4. The system identification, which was required to identify the dynamics of the mass-spring-damper elements, is described in Appendix A.

Simulation and experimental results

Consider the system in Figure 4.11 with $k_I = 20$ and $k_P = 8$. Similar to the system in Section 4.4, one can visualize that this system is not convergent for $k_A = 0$ (Figure 4.14) and that it is convergent for $k_A = 0.5$ (Figure 4.15). Again, it can be observed in these figures that the

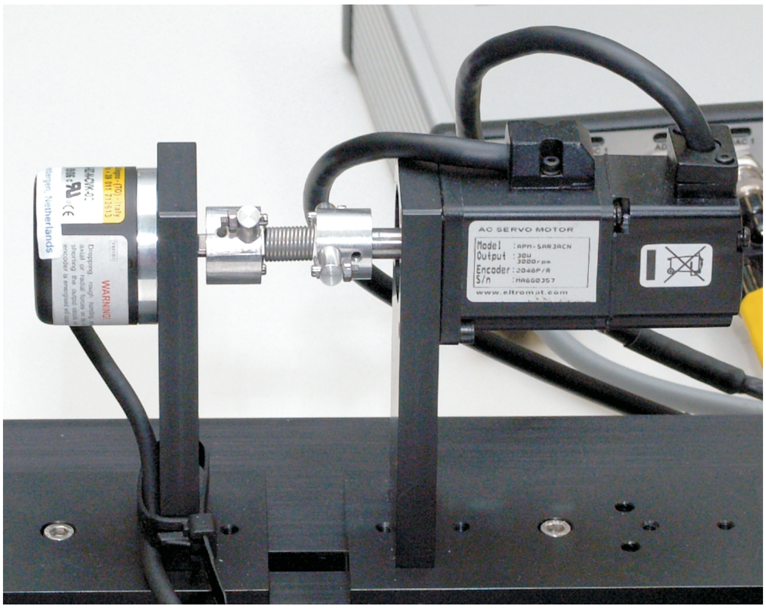

Figure 4.12: Photo of the hardware construction.

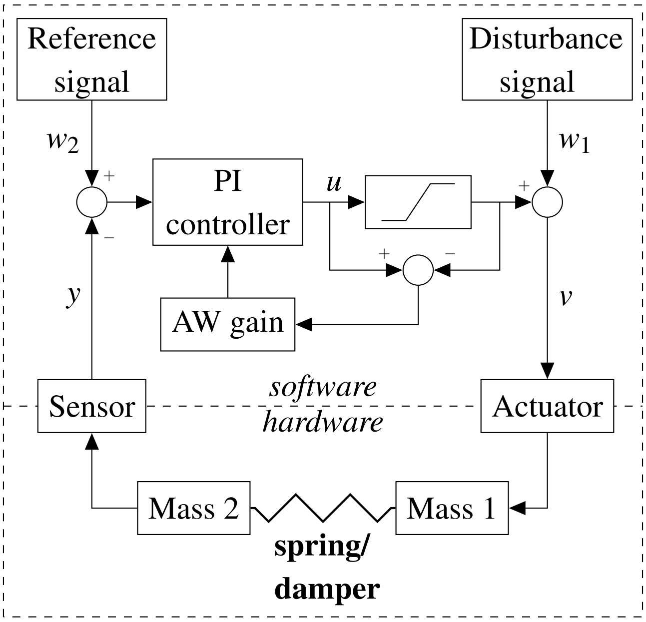

Figure 4.13: Schematic representation of the experimental setup.

simulation and experimental results match very well. Since these results are very similar to those in Figures 4.5 and 4.8, no further attention is paid to them here. A result which shows multi-periodic solutions (as in Figure 3.7) for this system with $k_\text{A} = 0$ can be found in [99]. In the remainder of this section, the uniformly convergent system (with $k_\text{A} = 0.5$) is examined further.

In Figure 4.16 an nFRF plot is shown based on both simulation and experimental results of the convergent system with $k_\text{A} = 0.5$. This plot has been obtained by evaluating solution y once

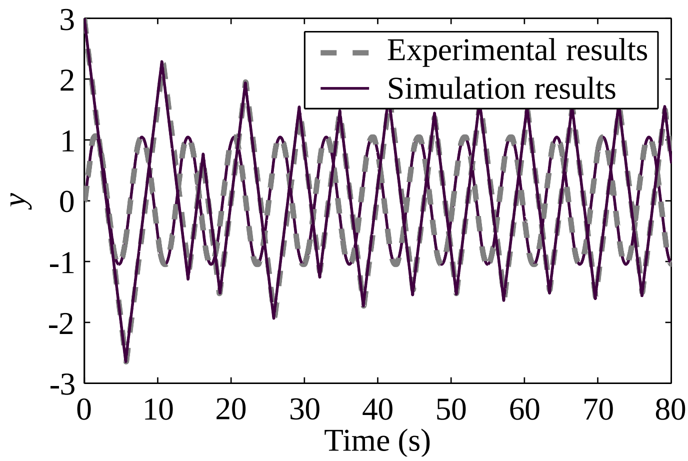

Figure 4.14: System output for $w_2 = \sin(t)$ and $k_A = 0$.

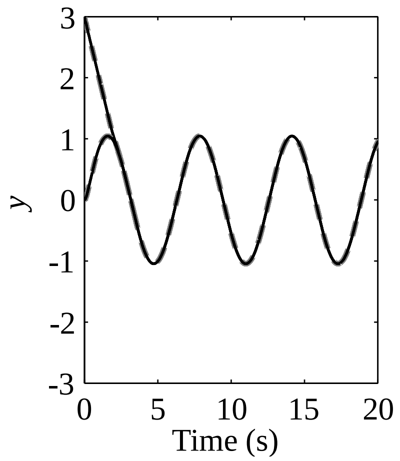

Figure 4.15: System output for $w_2 = \sin(t)$ and $k_A = 0.5$.

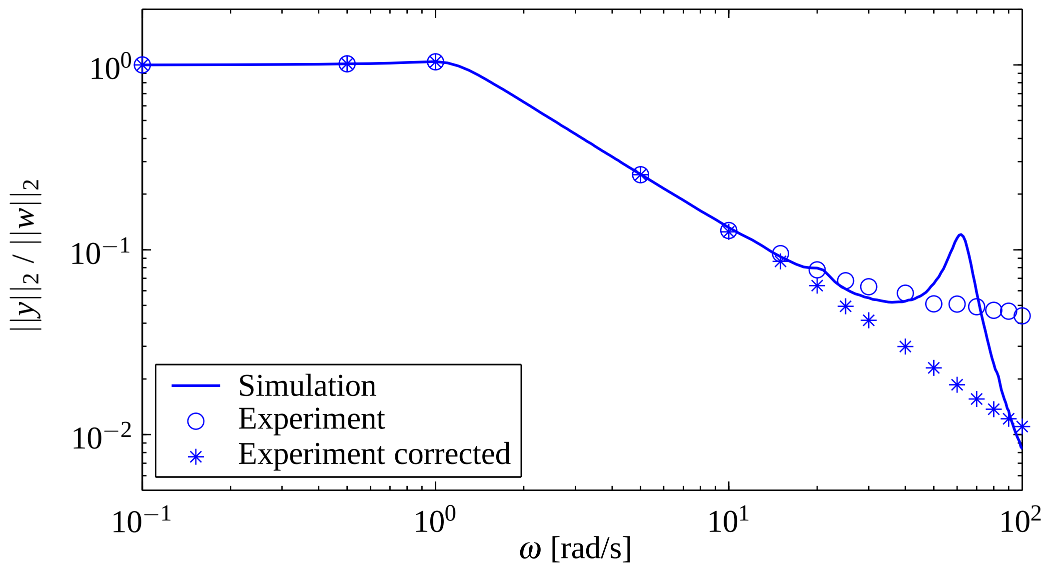

Figure 4.16: Nonlinear FRF for $k_A = 0.5$ and $w_2(t) = \sin(\omega t)$.

steady-state has been reached, for an input signal $w_2 = \sin(\omega t)$ with $\omega \in [10^{-1}, 10^2]$. Since the system is convergent, the initial conditions for this experiment are not relevant. It can be seen in Figure 4.16 that for $\omega > 10$ rad/s, the experiments and simulation give different results. In the original experimental results again an offset was present as discussed in Section 4.4. After removing this offset, however, these 'corrected' experimental results still do not match the simulation results for $\omega > 10$ rad/s. The identification of the experimental system, as described in Appendix A, indicate that there should be a resonance peak around 60 rad/s, however, this resonance does not occur in the performed experiment. This deviation is not fully understood yet, but might be caused by unmodeled (nonlinear) dynamics or measurement errors.

In Figure 4.17, the nFRF results (complementary sensitivity) are compared with the harmonic linearization results and the FRF of the corresponding linear system (i.e. without saturation and

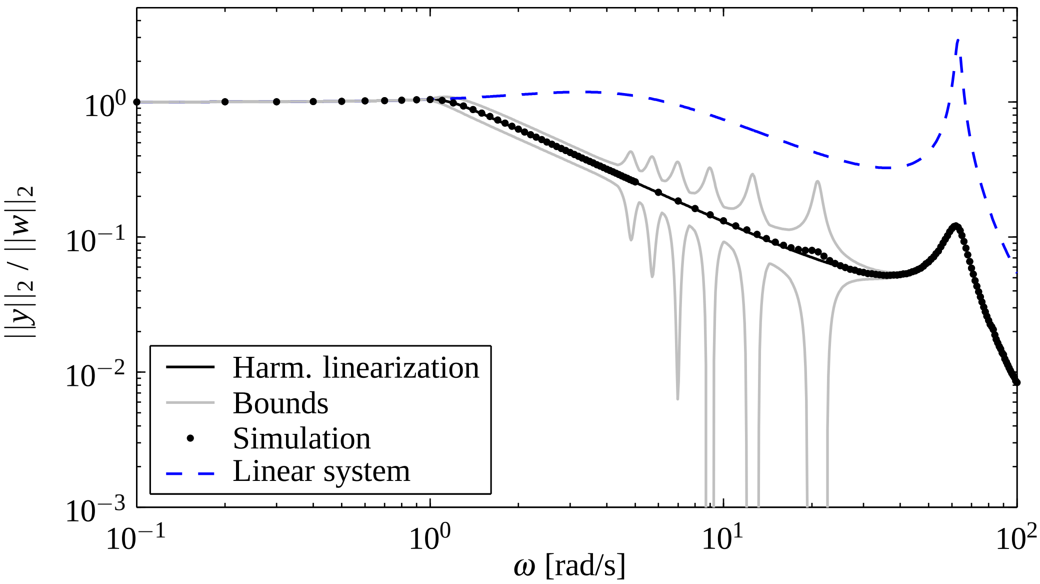

Figure 4.17: Nonlinear FRF and harmonic linearization results for $k_A = 0.5$ and $w_2(t) = \sin(\omega t)$.

anti-windup). Since the harmonic linearization results are based on the same dynamics as in the simulation model, the deviant experimental results are left out here. Figure 4.17 provides valuable information on the frequency domain performance of the system. It clearly shows how output y behaves in steady-state under harmonic input signals with respectively high or low frequencies. Also, it can be seen that the frequency domain behavior of the system with saturation substantially differs from the corresponding linear system. Another interesting observation is that the error bounds on the harmonic linearization contain 'copies' of the resonant peak, i.e. while the resonant peak lies at approximately 62 rad/s, the peaks in the error bounds lie at approximately $\frac{62}{3}, \frac{62}{5}, \frac{62}{7}, \ldots$ rad/s. These 'copies' are a result of the definition of the bounds (see ρ_1 in Section 3.4). Nevertheless, the error bounds lie relatively tight around the exact results as obtained by simulation, from which it can be concluded that the harmonic linearization approach gives a quite accurate description of the frequency domain behavior of this system. Note that a similar plot can be made for the nonlinear sensitivity function ($||w_2 - y||_2$ / $||w_2||_2$) to investigate for example tracking behavior of the system.

Finally note that since this system has a marginally stable plant, in general no finite estimate of the $\mathcal{L}_2$ gain from w_2 to y can be found using a quadratic storage function. However, even if such an $\mathcal{L}_2$ gain estimate can be found, for example by using another approach, it would only be a horizontal line in this plot, i.e. an upper bound for the frequency domain performance. For a convergent system as considered here, both the simulation based approach and the harmonic linearization approach provide more detailed information on the frequency domain behavior of the system. Nevertheless, it should be remarked that the result in Figure 4.17 only holds for a harmonic reference signal with amplitude $b = 1$, and although similar plots can be constructed for different harmonic reference signals, the superposition principle does not hold here, since the considered system is nonlinear. For periodic reference signals that are not harmonic (e.g.

multi-harmonic signals), the simulation-based approach can still be used to determine the exact steady-state response to such a reference signal. The harmonic linearization approach, on the other hand is not applicable for such reference signals.

4.6 Discussion

In this chapter a theorem was presented with sufficient conditions to guarantee uniform convergency for externally forced Lur'e systems with a saturation nonlinearity and marginally stable linear part. The theorem was shown to be also applicable to a class of anti-windup systems with a marginally stable plant. The presented result is both new in the field of convergent systems and in the field of anti-windup design.

In the research field of convergent systems, most approaches are based on finding quadratic Lyapunov functions, leading in turn to quadratic convergency conditions. The presented theorem is new in the way that it leads to conditions for uniform convergency, which is less restrictive. This result may also be useful to prove uniform convergency for systems other than those presented in this chapter, for example Lur'e systems with a different nonlinearity. For this purpose, it may also be valuable to take into account the approach and results of [9, 20, 47], in which synchronization of Lur'e systems is studied in the presence of strongly oscillatory external signals.

For the design of anti-windup schemes, most approaches are based on guaranteeing some form of (incremental) $\mathscr{L}_2$ stability of the system. The approach described in this chapter, on the other hand, is based on guaranteeing uniform convergency of the system, i.e. obtaining a unique limit solution which is independent of the initial conditions. This solution can easily be analysed, for example by simulation, to find the exact steady-state performance of the system. The convergency-based approach for the performance analysis of anti-windup systems with a marginally stable plant was illustrated using two case studies, in which both simulation and experimental results were presented to support the theoretical findings.

The convergent systems approach is currently only suitable for *evaluation* of the system's steady-state performance for a given controller, but not for controller *synthesis* and performance *optimization*, except for some small cases such as the case study in Section 4.4. An interesting property of convergent systems, however, is that simulation is a reliable performance analysis tool. This property may be further exploited in order to obtain a simulation-based performance optimization tool, which is able to optimize (in some sense) the performance of the limit solution within the boundaries of the conditions for convergency. This possibility might be interesting to investigate in future work. Another possibility to strengthen the result of the convergent system approach, is to exploit it in combination with existing synthesis or optimization algorithms. An example of such a combination was given in Section 4.3, where it was shown that an existing anti-windup design [90] also results in a uniformly convergent systems under some minor additional constraints. By combination of these ideas, a stronger conclusion was obtained.

The results obtained in this chapter are used in the following chapter to construct a feedback controller for manufacturing machines.

Chapter 5

Feedback Control of Manufacturing Machines

Abstract This chapter deals with the problem of controlling discrete-event manufacturing machines such that a customer demand is tracked while maintaining a low inventory level. To study this problem, a manufacturing machine is first approximated by an integrator which is subject to input saturation as a result of the finite capacity of the machine. For this 'integrator machine', a proportional-integral (PI) controller with anti-windup compensation is proposed to meet the tracking requirements. Results on harmonic linearization and convergent systems theory as presented in Chapters 3 and 4 are applied to evaluate the tracking performance. The proposed continuous-time controller is subsequently implemented in the discrete-event domain and applied to the discrete-event manufacturing machine. The resulting discrete-event controller is also applied for the control of a line of four machines. It is shown for this line that, in order to meet the tracking and low inventory requirements, application of the proposed controller is not sufficient; the reference demands of the first three machines should also be adjusted. For both the single machine and the line of four machines, simulation results are shown which indicate good tracking behavior of the closed-loop system.

5.1 Introduction

The production control of discrete-event manufacturing systems, i.e. how to control the production rates of machines such that the system tracks a certain customer demand while keeping a low inventory level, has been a field of interest for several decades. Early control strategies based on simple push and pull concepts, such as material requirements planning (MRP), enterprise resources planning (ERP), and just-in-time (JIT), see e.g. [34], can provide an adequate solution if the system requirements are not very strict and a fast reaction to possible disturbances/failures is not required (e.g. since such disturbances/failures hardly occur). However, as manufacturing systems become more complex and the system's performance must constantly improve in order to stay competitive in today's global economy, these control strategies become less effective.

A more structured control theory was proposed in 1987 by Ramadge and Wonham under the name of supervisory control theory [73, 74]. This theory, which is based on a discrete-event description of the manufacturing system, has since then been extended by several research groups. However, when it comes to the control of large manufacturing systems (or networks of such systems), supervisory control is not very suitable due to the high level of detail it deals with, which causes the corresponding control problem to grow intractably large. Furthermore, the supervisory control theory does not deal with transient or steady-state performance of a system, but mainly focusses on guaranteeing avoidance of undesired/unsafe behavior, such as deadlock.

Another strategy for the control of manufacturing systems, is to describe the manufacturing systems using so-called flow models, see e.g. [2]. These models, which are based on ordinary differential/difference equations (ODEs), or sometimes partial differential equations (PDEs, see e.g. [45, 97]), form a continuous approximation of the discrete-event manufacturing systems and therefore result in a simpler control problem. Moreover, various (advanced) control theories are already available for ODEs, which makes these models attractive to work with. Most control strategies proposed in literature that use flow models to describe the manufacturing system, are based on the assumption that (an estimate of) the future demand is known, and use some optimization algorithm to find a suitable control signal, see e.g. [28, 85, 105]. In the ODE models, a manufacturing machine is usually interpreted as an integrator, where the cumulative number of finished products is the integral of the production rate. Bounds on the production rate, due to the finite capacity of the machine, are then taken into account in the optimization problem. Disadvantages of these control strategies are that they depend on future demands (which are hard to predict and therefore often inaccurate) and that in general the optimization problem requires much computational effort.

In this chapter, a different strategy is employed for the control of manufacturing machines, which does not depend on future demands and requires less computational effort. For this control strategy, the manufacturing machines are still approximated by an integrator, but the bounds on the production rate are interpreted as a saturation function. A simple proportional-integral (PI) feedback controller with anti-windup compensation is applied to pursue good tracking properties for the closed-loop system. First, the system with a single machine (integrator) is investigated. The tracking behavior of this continuous system is analysed using the harmonic linearization and convergent systems theory as presented in Chapters 3 and 4. In particular, the tracking behavior for customer demands with periodic fluctuations[1] is investigated. The controller as designed for the continuous approximation model is subsequently implemented in the discrete-event domain to control the discrete-event machine, and simulation results are compared with those of the continuous approximation. Finally, the control problem is extended to a line of four manufacturing machines. In this case, each machine is controlled by a PI controller with anti-windup to set its production rate. In addition, a coupling relation between the machines is defined to set the reference demands for the first three machines.

It should be noted that the ideas and results as presented in this chapter are only the first findings in the development of this control strategy for discrete-event manufacturing systems. Many other aspects (see Section 5.4) should be investigated before it can become clear if this control strategy is suitable for the control of complex manufacturing systems in practice. Nevertheless, for the simple systems as considered in this chapter the control strategy shows promising results.

The remainder of this chapter is organized as follows. In Section 5.2 the control of a single manufacturing machine is discussed for both the continuous and the discrete-event domain. Section 5.3 deals with the control of a manufacturing line consisting of four machines. Finally, Section 5.4 gives a discussion on the results obtained in this chapter.

5.2 Feedback control of a single machine

In this section a simple feedback controller is derived for a single discrete-event manufacturing machine. For this purpose, the discrete-event machine is first approximated by a continuous model, i.e. an integrator with input saturation. Then, a feedback controller is derived for this continuous model, such that the closed-loop system has satisfactory tracking behavior. After analysing the system's tracking performance in the continuous domain, the controller is implemented in the discrete-event domain and simulation results are presented that show the tracking performance of the discrete-event system.

Continuous approximation

Consider a manufacturing machine (Figure 5.1) that produces items with production rate $u_{\mathrm{p}}(t)$. It is assumed that there is always sufficient raw material to feed the machine, i.e. the machine never starves. The total amount of items produced by the machine is indicated by $y(t)$ and is related to production rate $u_{\mathrm{p}}(t)$ according to the relation

$$\dot{y}(t) = u_{\mathrm{p}}(t).$$

[1] In [7] a similar control problem with a *constant* customer demand rate has been considered.

That is, the machine can be interpreted as an integrator. In order to let the total production $y(t)$ follow a certain customer demand $y_{\mathrm{d}}(t)$ a feedback controller can be used to set the production rate $u_{\mathrm{p}}(t)$. However, in case of a manufacturing machine, one should take into account the fact that the production rate of a machine cannot be negative and has a certain maximum (capacity of the machine), i.e. the production rate is constrained by the following bounds

$$0 \leq u_{\mathrm{p}}(t) \leq u_{\mathrm{p,max}}. \tag{5.1}$$

In order to deal with these constraints, one can either build a controller that takes these bounds into account, or build a controller that initially does not take into account the bounds and add some modification to the controller for the times that the control signal exceeds a bound. An example of the former control method is model predictive control (MPC), in which the bounds on the control signal can be explicitly taken into account in the optimization problem. For cases in which the control signal only rarely exceeds the bounds, the latter control method is often preferred due to its simplicity. Here, the latter control method is used, since this results in a simpler controller and no knowledge of the future demand is required (whereas for MPC such knowledge is required).

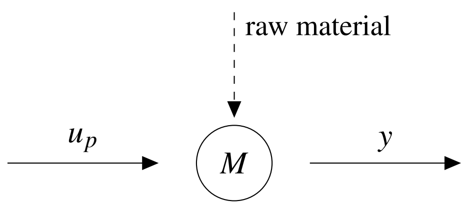

Figure 5.1: Manufacturing machine M with production rate u_{p}.

PI controller with anti-windup modification

Assume that the manufacturing machine should follow a reference production signal

$$y_{\mathrm{d}}(t) = y_{\mathrm{d0}} + u_{\mathrm{d}}t + r(t) \tag{5.2}$$

where y_{d0} is the desired production at $t = 0$, u_{d} is a constant that represents the average desired production rate, and $r(t)$ represents a fluctuation around this average as a result of (for instance seasonal) market fluctuation. Throughout this chapter, the fluctuation $r(t)$ is assumed to be harmonic. This assumption makes it possible to use harmonic linearization to analyse the tracking performance of the system. For fluctuations other than harmonic, performance analysis using harmonic linearization as presented in Chapter 3 is not possible, but the analysis can still be performed using simulation (provided the system is convergent for this reference $r(t)$).

First a controller is selected for the linear system, i.e. the integrator without the saturation nonlinearity. The simplest feedback controller that is able to make the machine follow (to some extent) a reference production signal like (5.2), is a proportional integral (PI) controller, i.e.

$$u(t) = k_{\mathrm{P}} e(t) + k_{\mathrm{I}} \int_0^t e(\tau) d\tau$$

with $e(t) = y_{\mathrm{d}}(t) - y(t)$. For the linear system it holds that $u_{\mathrm{p}} = u$. For $r(t) \equiv 0$, this controller with parameters $k_{\mathrm{P}} > 0$ and $k_{\mathrm{I}} > 0$ drives the error $y - y_{\mathrm{d}}$ to zero as $t \to \infty$ for arbitrary constants $y_{\mathrm{d}0}$ and u_{d}, as follows by the final value theorem from linear control theory, see e.g. [21]. For a harmonic fluctuation $r(t)$, the tracking performance can be determined in terms of the sensitivity or complementary sensitivity function, which are defined in the Laplace domain. For a closed-loop system as shown in Figure 5.2, the sensitivity function $S(s)$ and complementary sensitivity function $T(s)$ are given by

$$S(s) = \frac{Y_{\mathrm{d}}(s) - Y(s)}{Y_{\mathrm{d}}(s)} = \frac{1}{1 + G(s)C(s)}, \qquad T(s) = 1 - S(s) = \frac{Y(s)}{Y_{\mathrm{d}}(s)} = \frac{G(s)C(s)}{1 + G(s)C(s)}$$

where $C(s)$ and $G(s)$ are the transfer functions of respectively the controller and the machine, while $Y(s)$ and $Y_{\mathrm{d}}(s)$ are the Laplace transforms of respectively $y(t)$ and $y_{\mathrm{d}}(t)$. Due to the so-called waterbed effect this controller cannot achieve good tracking behavior of $r(t)$ for all frequencies. The waterbed effect, which is based on the Bode sensitivity integral [5], implies roughly speaking that by decreasing the sensitivity in a certain frequency range (due to some changes in the controller parameters), the sensitivity is increased in another frequency range. Nevertheless, considering certain performance requirements on the (complementary) sensitivity function, one can try to find the 'best' possible parameters k_{P} and k_{I} for the system. Other controllers may be considered as well to investigate if they are more suitable to control the manufacturing machine. Here, however, only the application of a PI controller is investigated.

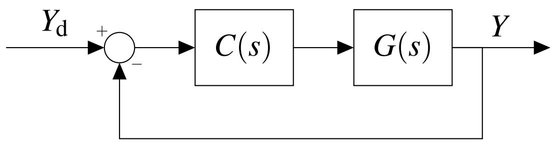

Figure 5.2: Closed-loop control system.

The second step in the design of the controller is to construct an anti-windup compensator to deal with the constraints on the production rate. In order to be able to apply a standard static anti-windup compensator as discussed in Section 4.3 the following coordinate transformation is performed. Take $k = u_{\mathrm{p,max}}/2$ and rewrite the constraints in (5.1) as

$$-k \leq u_{\mathrm{p}} - k \leq k.$$

Now $u_{\mathrm{p}} - k$ is the output of a saturation function $\mathrm{sat}_k(u) = \mathrm{sign}(u) \min(k, |u|)$, and thus the actual production rate is given by

$$u_{\mathrm{p}} = \mathrm{sat}_k(u) + k$$

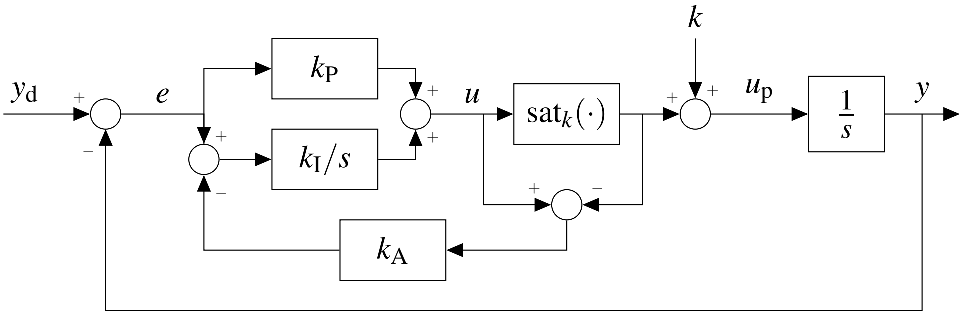

Figure 5.3: Anti-windup system with integrator plant.

where u is the output of the controller. After the application of a static anti-windup compensator, the closed-loop system becomes as depicted in Figure 5.3, in which $s = \frac{d}{dt}$ is a differential operator. The dynamics of this system can be described by

$$\begin{aligned} \dot{y}(t) &= \mathrm{sat}_k(u(t)) + k, \\ u(t) &= k_{\mathrm{P}}e(t) + k_{\mathrm{I}} \int_0^t e(\tau)d\tau + k_{\mathrm{I}}k_{\mathrm{A}} \int_0^t (\mathrm{sat}_k(u(\tau)) - u(\tau))\, d\tau, \\ e(t) &= y_{\mathrm{d}}(t) - y(t). \end{aligned} \tag{5.3}$$

In the following subsection, the performance of this system is evaluated using convergent systems theory and the harmonic linearization method. The convergent systems theory requires the input to be bounded, and the harmonic linearization method requires a harmonic input. Therefore, the linear part of the reference signal, i.e. $y_{\mathrm{d}0} + u_{\mathrm{d}}t$, is subtracted from both y_{d} and y, so that the system with harmonic input $r(t)$ can be investigated. It is obvious that $y_{\mathrm{d}}(t) - y_{\mathrm{d}0} - u_{\mathrm{d}}t$ equals $r(t)$. For the subtraction of $y_{\mathrm{d}0} + u_{\mathrm{d}}t$ from $y(t)$, the following holds:

$$y(t) - y_{\mathrm{d}0} - u_{\mathrm{d}}t = z(t),$$

where $z(t)$ is defined to be the new output. For the system with this new notation (see Figure 5.4) the closed-loop dynamics can be described by

$$\begin{aligned} \dot{z}(t) &= \mathrm{sat}_k(u(t)) + k - u_{\mathrm{d}}, \\ u(t) &= k_{\mathrm{P}}e(t) + k_{\mathrm{I}} \int_0^t e(\tau)d\tau + k_{\mathrm{I}}k_{\mathrm{A}} \int_0^t (\mathrm{sat}_k(u(\tau)) - u(\tau))\, d\tau, \\ e(t) &= r(t) - z(t), \end{aligned} \tag{5.4}$$

or, in state-space notation, by

$$\begin{aligned} \dot{x} &= Ax + B\mathrm{sat}_k(u) + Fw \\ u &= Cx + Dw \\ z &= Hx \end{aligned} \tag{5.5}$$

with $w = [k - u_{\mathrm{d}}, r]^T$ and

$$A = \begin{bmatrix} 0 & 0 \\ -(1-k_A k_P) & -k_I k_A \end{bmatrix}, \quad B = \begin{bmatrix} 1 \\ k_A \end{bmatrix}, \quad F = \begin{bmatrix} 1 & 0 \\ 0 & 1 - k_A k_P \end{bmatrix},$$

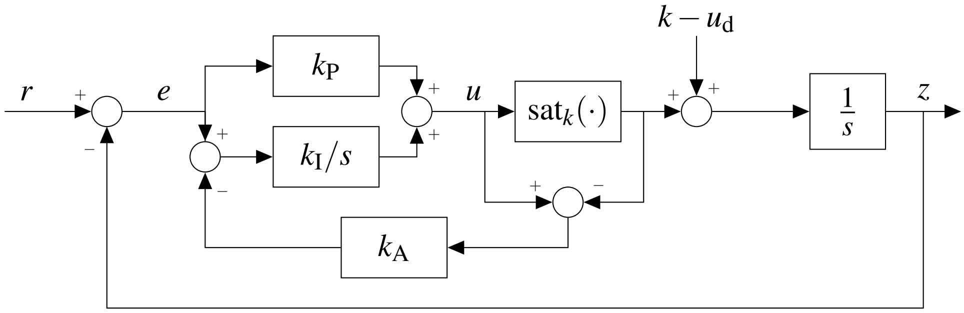

Figure 5.4: Anti-windup system with integrator plant, normalized.

$$C = \begin{bmatrix} -k_P & k_I \end{bmatrix}, \quad D = \begin{bmatrix} 0 & k_P \end{bmatrix}, \quad H = \begin{bmatrix} 1 & 0 \end{bmatrix}.$$

Note that since $y_{\mathrm{d}0} + u_\mathrm{d}t$ is subtracted from both y_d and y, the error signal $e(t) = y_\mathrm{d}(t) - y(t) = r(t) - z(t)$ in (5.3) and (5.4) is identical and hence the controller output $u(t)$ is identical for these systems. Therefore, the system response $y(t)$ to the input $y_\mathrm{d}(t)$ can be simply obtained from the system response $z(t)$ by adding $y_{\mathrm{d}0} + u_\mathrm{d}t$ to it.

Performance analysis in continuous domain

Consider the system in Figure 5.4 and note that if $k = 1$ (i.e. $\mathrm{sat}_k = \mathrm{sat}$), then the system is identical to the system in Figure 4.2 with $w_1 = k - u_\mathrm{d}$ and $w_2 = r$. Hence for this case, the system is uniformly convergent if $k_A > 1/k_P$, as stated in Corollary 4.5. The following corollary shows that also for $k \neq 1$, the considered system is uniformly convergent if $k_A > 1/k_P$.

Corollary 5.1. *If $k_A > 1/k_P$ then system* (5.5)*, visualized in Figure 5.4, is uniformly convergent for all $w = [\, w_1,\ w_2 \,]^T = [\, k - u_d,\ r]^T$ that satisfy*
1. $|w_1| < k$,
2. $r(t)$ is a harmonic function of time.

Proof. Note that for any $u \in \mathbb{R}$ it holds that $\mathrm{sat}_k(u) = k \cdot \mathrm{sat}(u/k)$ and therefore (5.5) can be written as

$$\dot{x} = Ax + B_k \mathrm{sat}(C_k x + D_k w) + Fw,$$

where $B_k = kB$, $C_k = C/k$, and $D_k = D/k$. Since $D_k w(t) = \frac{D_c}{k} r(t)$ is uniformly continuous, $|w_1(t)| < k$ implies $|F_1 w(t)| < \alpha_1 |kB_1|$ for some constant $\alpha_1 < 1$, and $A + B_k C_k = A + BC$, one can exactly follow the proof of Corollary 4.5 to prove that the system in Figure 5.4 is uniformly convergent for the class of inputs described in Corollary 5.1 if $k_A > 1/k_P$. $\square$

Since system (5.5) is uniformly convergent for all admissible inputs ($r(t)$, u_d) if an anti-windup gain $k_A > 1/k_P$ is applied, simulation can be used to analyse the frequency domain performance of the system, in terms of a nonlinear frequency response function (nFRF). If furthermore it is

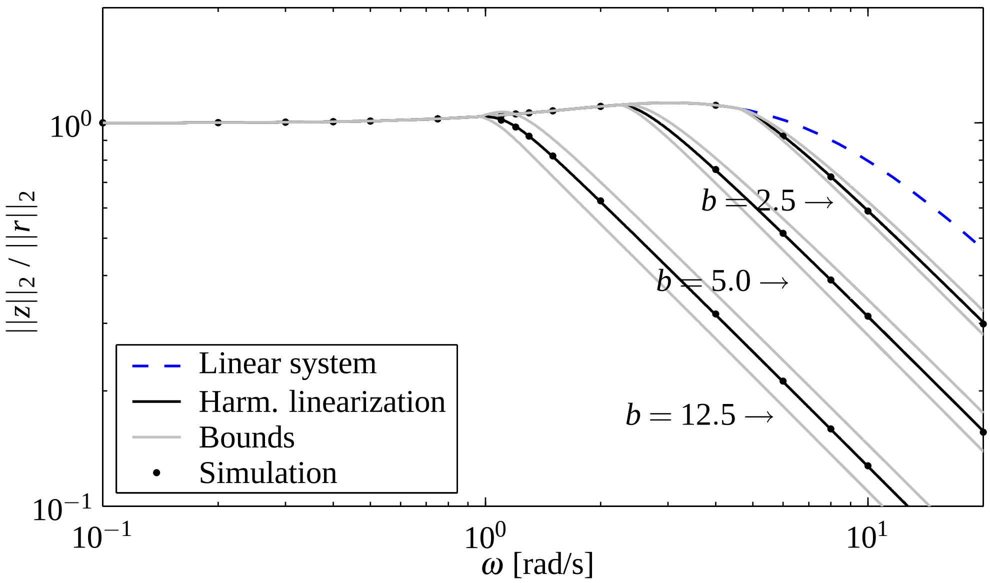

Figure 5.5: Nonlinear complementary sensitivity function for the system in Figure 5.4.

assumed that $u_d = k$, i.e. $w_1 = 0$, then also the harmonic linearization method as described in Chapter 3 can be used to analyse the frequency domain performance of the system. For the analysis of the case in which the average utilization of the machine is not 50%, i.e. $u_d \neq k$, the harmonic linearization method may be modified in a straightforward way. The derivation of such a modification, however, is not of interest here. Moreover, for the case with $u_d \neq k$, the frequency domain performance can also be analysed using simulation.

For the system described below, both simulation and the harmonic linearization method are applied to determine the frequency domain performance of the system.

Consider the PI controlled manufacturing machine (approximated by integrator and saturation) with anti-windup compensation, as depicted in Figure 5.4, and take $k_P = 10$, $k_I = 20$, $k_A = 0.5$, $u_{\mathrm{p,max}} = 25.0$ items/sec, $k = u_{\mathrm{d}} = 12.5$ items/sec, and $r = b\sin(\omega t)$. For amplitudes $b \in \{2.5, 5.0, 12.5\}$ and frequencies $\omega \in [0.1, 20]$ rad/sec, the nonlinear complementary sensitivity function $\mathscr{T}(b,\omega) = ||z||_2/||r||_2$ is plotted in Figure 5.5. For comparison, the complementary sensitivity function for the linear system (i.e. without saturation) is shown as well.

In Figure 5.5 it can be observed that, as mentioned before, the nonlinear FRF is dependent on the amplitude of the reference signal r, unlike linear FRFs.

Furthermore, it can be seen that for $\omega > u_{\mathrm{d}}/b$ the nFRF shows a sudden decrease in performance. Hence, for large amplitudes b this decrease occurs at a low frequency. This is due to the fact that the machine then should produce beyond its capacity, i.e. in order to track the reference signal $y_{\mathrm{d}} = u_{\mathrm{d}}t + b\sin(\omega t)$ the control signal should equal $u_{\mathrm{p}} = \dot{y} = u_{\mathrm{d}} + b\omega\cos(\omega t)$ which for $\omega > u_{\mathrm{d}}/b$ has a maximum and minimum that violate the constraints $0 \leq u_{\mathrm{p}} \leq u_{\mathrm{p,max}}$. For $\omega \leq u_{\mathrm{d}}/b$, on the other hand, one can observe that the closed-loop behavior of the system with saturation is identical to that of the linear system (without saturation). This makes sense, since in this case the controller signal remains within the saturation bounds, and hence the system behaves in a linear way.

Finally, based on the results in Figure 5.5 it is suspected that for low frequencies (roughly below 1 rad/sec) the closed-loop system has good tracking behavior. However, as $||z||_2$ contains no information for example on the phase of z, the data in Figure 5.5 alone is not sufficient to conclude good tracking for these frequencies. Nevertheless, one can conclude from the simulation results shown in the next subsection that for these frequencies the system indeed has good tracking behavior. For reference signals with small enough amplitude b, a resonant peak is visible at approximately 4 rad/sec. For high frequencies (or large reference amplitudes) the closed-loop system is not able to follow the reference signal.

Based on a result like Figure 5.5, one can determine if the controller performs satisfactory. If not, the controller parameters k_P, k_I, k_A can be adjusted, or a new controller can be proposed. Assuming that the reference demand only fluctuates with a relatively small frequency, the current controller performs well enough. The following subsection discusses the implementation and application of the controller in the discrete-event domain.

Implementation and simulation results in discrete-event domain

Before considering the implementation of the controller in the discrete-event domain, first some differences between the continuous time integrator and discrete-event machine are identified. First, it is noted that for the integrator it is possible to produce a total amount of items that is not an integer, e.g. 15.36 items, whereas the discrete-event machine can only produce whole items and thus the total amount of produced items is always a nonnegative integer. Furthermore, the production rate for the integrator can vary in a continuous way, while the discrete-event machine can only produce at full capacity or be idle. Finally, once the discrete-event machine starts processing, it takes a full processing time delay after which the total amount of produced items is increased by one. For the integrator, the production of items is a continuous process without delay, i.e. when the production rate becomes larger than zero, the amount of produced items directly increases (in a continuous way).

As a result of these differences, the continuous time controller cannot achieve the same behavior for the discrete-event machine as for the integrator. Nevertheless, as long as the processing time of the machine is small enough in comparison to the period of harmonic demand fluctuation $r(t)$, the integrator is a good approximation of the discrete-event machine, and in this case the proposed controller is assumed to achieve similar behavior in the discrete-event domain.

In order to apply the controller in the discrete-event domain, some modifications are required. Instead of controlling the production rate of the machine itself, the rate at which items arrive at the machine is controlled. The resulting control structure is depicted in Figure 5.6. Here,

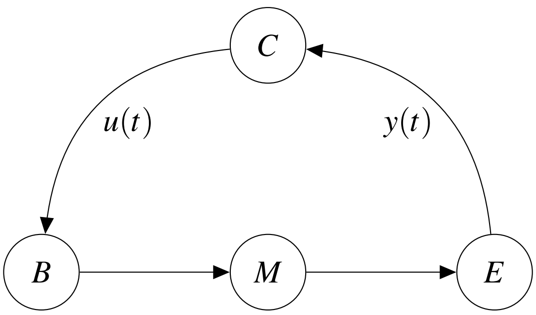

Figure 5.6: Schematic representation of the control structure for a discrete-event machine.

buffer B in front of the machine releases items into the machine according to rate $u(t)$, which is set by controller C. Machine M processes items with a processing time of $t_0 = \frac{1}{u_{\mathrm{p,max}}}$ per item. Exit buffer E receives the completed items and sends the total number of produced items $y(t)$ to the controller. Based on this number $y(t)$ and reference demand $y_{\mathrm{d}}(t)$ the PI controller with anti-windup modification computes production rate $u(t)$ at each sample time t_s (which is relatively small in comparison with t_0). The resulting rate $u(t)$ is sent to buffer B, which then releases items into the machine at this rate. If the machine is busy at the time that the buffer tries to send an item, then the item remains in the buffer until the machine becomes available.

In order to test the controller in the discrete-event domain, several discrete-event simulations have been performed. To do so, the control structure as shown in Figure 5.6 was implemented in χ, a specification language developed at the Eindhoven University of Technology [92]. More details on the implementation can be found in [101]. Here, some results of the discrete-event simulations are shown and discussed.

Consider the system with $k_P = 10$, $k_I = 20$, $u_{\mathrm{p,max}} = 25.0$ items/sec, and $k = u_{\mathrm{d}} = 12.5$ items/sec. The discrete-event simulations were performed in the original coordinates, i.e. with y_d and y, but the results are displayed here using the normalized coordinate $z(t) = y(t) - u_{\mathrm{d}} - y_{\mathrm{d}0}$, since in these coordinates the results are easier to analyse.

In Figures 5.7 and 5.8, the normalized system output $z(t)$ is shown for $r = b\sin(\omega t)$ and respectively $k_{\mathrm{A}} = 0$ (no anti-windup) and $k_{\mathrm{A}} = 0.5$ (i.e. $k_{\mathrm{A}}k_{\mathrm{P}} > 1$). One can observe that the system has properties similar to its continuous approximation system. For $k_{\mathrm{A}} = 0$, the discrete-event system has multiple steady-state solutions, which correspond to the solutions of the continuous approximation system. For $k_A = 0.5$, the solutions with the different initial conditions converge to one steady-state solution. This behavior also corresponds to the behavior of the continuous approximation, which is convergent for $k_A = 0.5$. Since the goal in this chapter is to find a controller with good tracking behavior, only the controller with $k_{\mathrm{A}} = 0.5$ is considered further here.

In Figure 5.5, the frequency domain analysis results for the continuous approximation system (with the same system parameters as considered here) indicate that the tracking behavior can

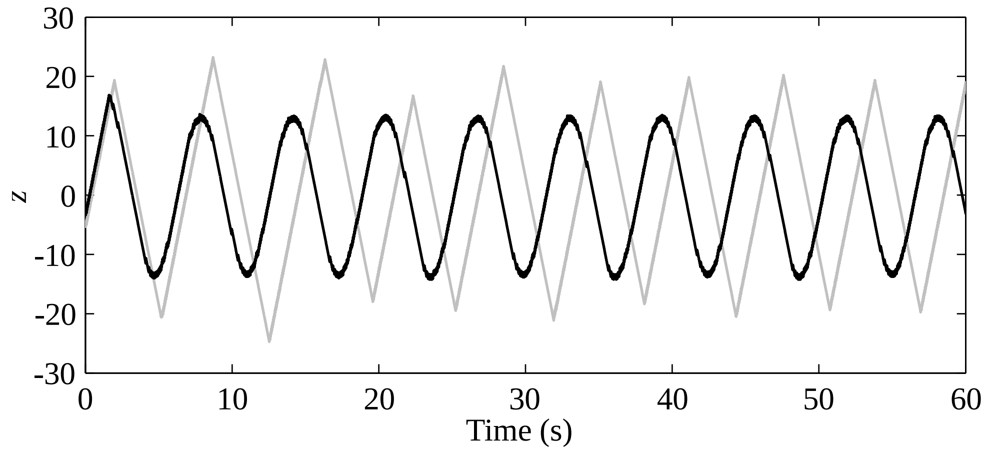

Figure 5.7: System output $z(t)$ for $k_A = 0$ and resp. $z(0) = -3$ and $z(0) = -5$.

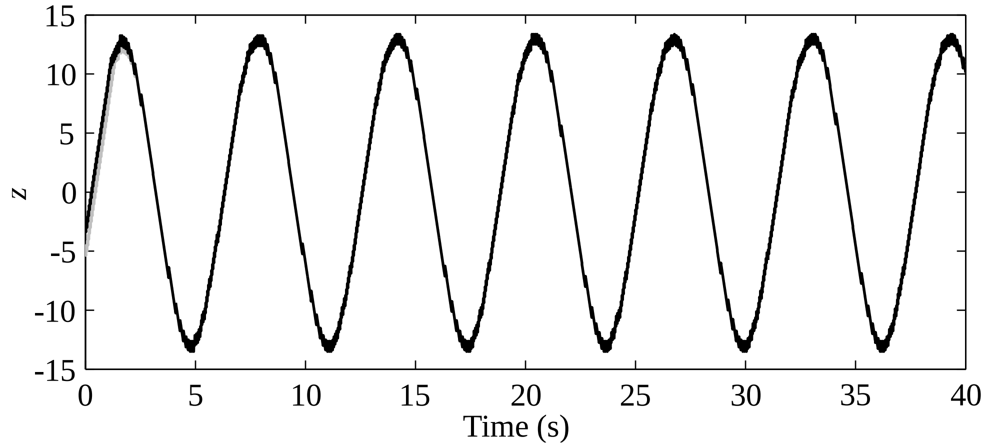

Figure 5.8: System output $z(t)$ for $k_A = 0.5$ and resp. $z(0) = -3$ and $z(0) = -5$.

be roughly divided into three regions: good tracking behavior for frequencies below 1 rad/sec, a resonant peak around 4 rad/sec, and a drop in performance for frequencies above u_d/b. In Figures 5.9–5.11 simulation results are shown for frequencies in each of these regions, i.e. for $\omega = \{0.5, 4.0, 10.0\}$, and $b = 2.5$. The results of the discrete-event simulations are compared to the simulation results of the continuous approximation model. Note that the results are plotted on different time scales: for each frequency the output $z(t)$ is displayed for two periods. After a short transient period (due to well-chosen initial conditions), the steady-state behavior can already be observed in these figures. The 'saw-tooth' like fluctuation around the average trend of the discrete-event simulation results is caused by the integer character of machine output y.

Figure 5.9 shows that, for a low frequency of $r(t)$, the results of the discrete-event simulation and the continuous-time simulation match very well. Furthermore, it can be seen that the machine output $z(t)$ follows, after a short transient time, the demand fluctuation $r(t)$ very well.

For the frequency $\omega = 4.0$ rad/sec (Figure 5.10) the results of the discrete-event simulation and the continuous-time simulation still match very well. Both results show a phase lag and an

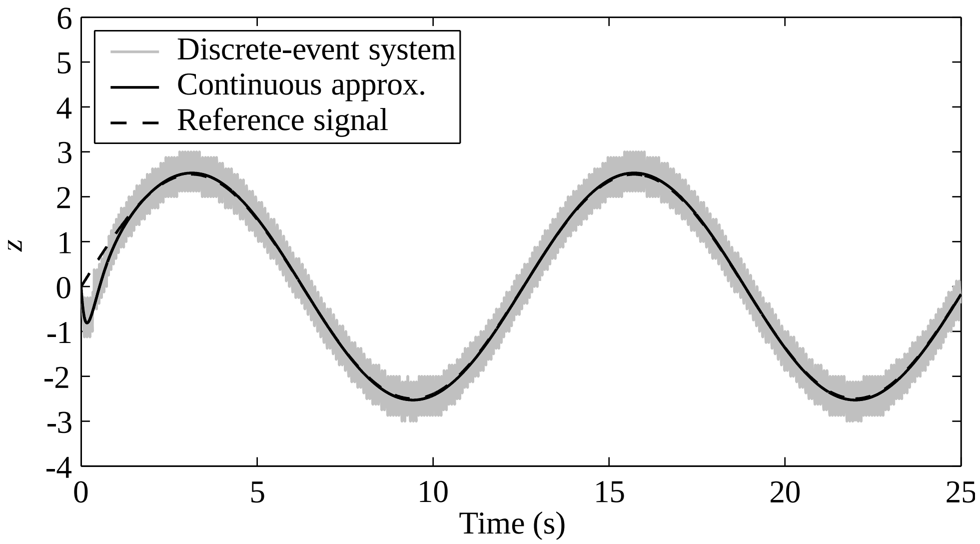

Figure 5.9: System output $z(t)$ for $k_{\mathrm{A}} = 0.5$ and $r(t) = 2.5\sin(0.5t)$.

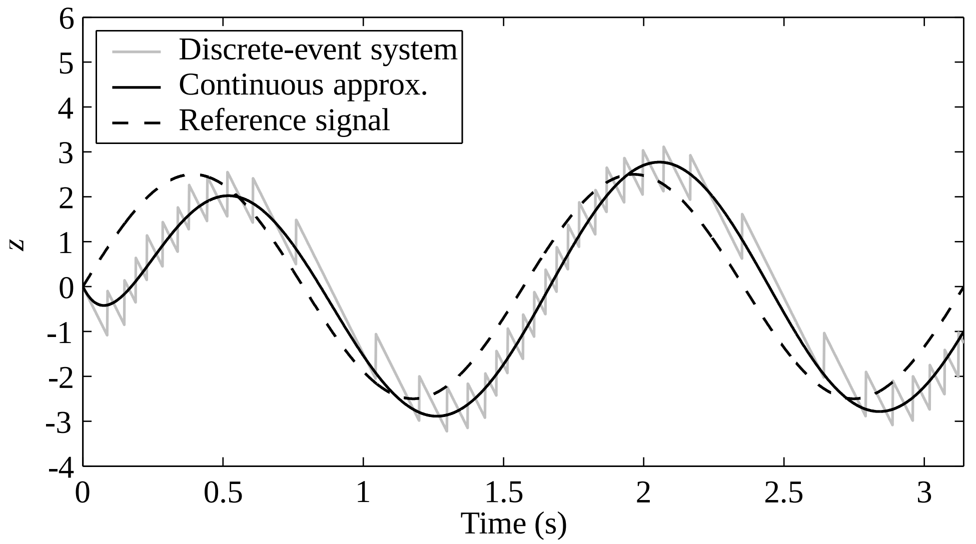

Figure 5.10: System output $z(t)$ for $k_{\mathrm{A}} = 0.5$ and $r(t) = 2.5\sin(4t)$.

increased amplitude for $z(t)$ in comparison with the demand fluctuation $r(t)$. This increase in amplitude is in accordance with the results as shown in Figure 5.5.

Finally, Figure 5.11 shows that for a relatively high frequency, the results of the discrete-event simulation and the continuous-time simulation still match quite well, although the relative deviation due to the integer character of the discrete-event results is obviously larger than in the previous two simulations. Furthermore, both results show a large phase lag and a decreased amplitude for $z(t)$ in comparison with the demand fluctuation $r(t)$. The decrease in amplitude is again in accordance with the results as shown in Figure 5.5.

Concluding, one can state that, as long as the processing time is much smaller than the period

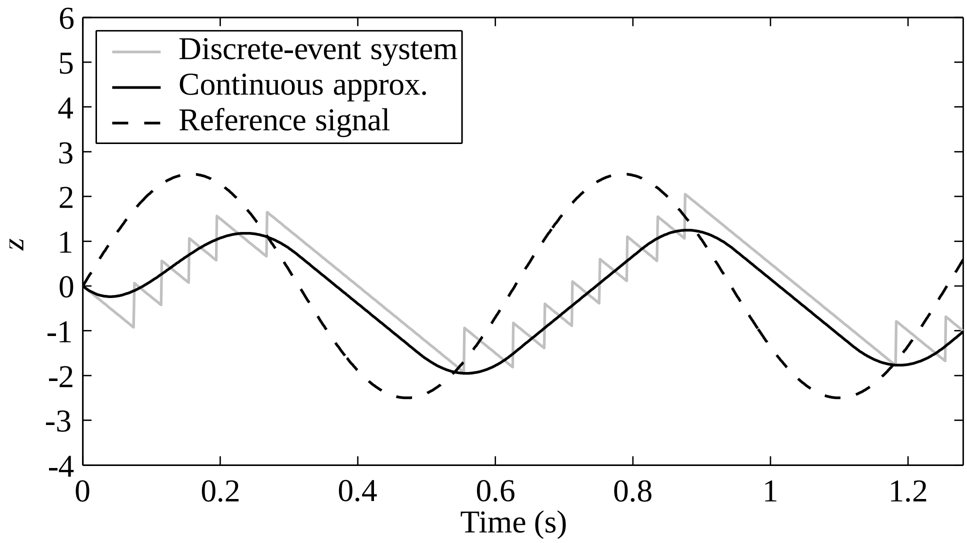

Figure 5.11: System output $z(t)$ for $k_A = 0.5$ and $r(t) = 2.5\sin(10t)$.

of the fluctuation, the proposed controller implementation works satisfactory, and the resulting discrete-event system behaves in a very similar way to its continuous-time approximation system. Furthermore, it was observed that for the proposed PI controller with anti-windup compensation, the system shows good tracking behavior for frequencies roughly below 1 rad/sec.

5.3 Feedback control of a line of machines

In Section 5.2, a tracking problem for a single machine was considered, and a PI controller with anti-windup compensation was proposed to solve this problem. In this section, the control problem is extended to a line of four manufacturing machines. The goal of this control problem is to track a certain reference demand y_d with the last machine in the line, while maintaining a low inventory level in the line.

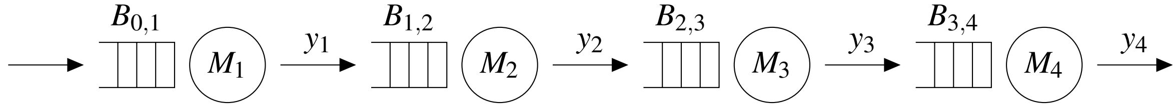

Figure 5.12: A manufacturing line consisting of four identical machines.

The line (see Figure 5.12) that is considered throughout this section consists of four identical manufacturing machines, which are separated by buffers with an infinite capacity. The machines M_i, $i \in \{1,2,3,4\}$ have a maximum production rate $u_{p,\max}$ and the total amount of items produced by machine M_i is indicated by y_i. Machine M_i processes items from buffer $B_{i-1,i}$ and puts them in buffer $B_{i,i+1}$ when finished. Machine M_4 sends the finished items to the exit buffer (not shown in Figure 5.12). The amount of items in the intermediate buffers $B_{i-1,i}$, $i \in \{2,3,4\}$

is indicated by $w_{i-1,i}$ and satisfies the following relation

$$w_{i-1,i} = y_{i-1} - y_i.$$

Since the amount of items in a buffer cannot become negative, machine M_{i+1} cannot produce (i.e. starves) while $w_{i,i+1} = 0$. It is assumed that machine M_1 never starves.

In order to control this line, the production rate $u_i(t)$ of each machine is controlled using the PI-controller with anti-windup compensation as proposed in Section 5.2. Note that as a result of the buffer constraint $w_{i,i+1} \geq 0$, the machines are influenced by each other: if for example machine M_2 needs to process an item according to control signal $u_2(t)$, but buffer $B_{1,2}$ is empty, then it has to wait until machine M_1 has processed a new item. Another issue that has a large influence on the behavior of the manufacturing line, is how to set the reference signal for the first three machines, i.e. when should these machines be authorized to process an item? If these machines are allowed to process continuously at full capacity, then the amount of inventory probably becomes very large, which is undesirable. On the other hand, if these machines do not produce at all, then the fourth machine is not able to follow the reference demand.

In order to address this problem of reference signals, first the continuous approximation system is shortly considered again, in which the machines are replaced by integrators and a saturation function. After that, the feedback controlled manufacturing line is considered in the discrete-event domain, and some simulation results are shown.

Continuous approximation

For each machine in the line, the continuous approximation system with an integrator plant, saturation, a PI controller, and anti-windup compensation is identical to the system in Figure 5.3 (or Figure 5.4 with normalized coordinates) except for the fact that the buffer constraints $w_{i,i+1} \geq 0$ should be taken into account. Figure 5.13 shows the adjusted approximation system for machines M_i, $i \in \{2,3,4\}$, according to the following relations

$$\dot{y}_i(t) = f(u_{\mathrm{p},i}(t), w_{i-1,i}) = \begin{cases} u_{\mathrm{p},i}(t) & \text{if } w_{i-1,i} > 0, \\ 0 & \text{if } w_{i-1,i} = 0. \end{cases}$$

Since machine M_1 is not affected by the buffer constraint, the corresponding continuous approximation system for this machine is identical to the system in Figure 5.3.

As can be seen in Figure 5.13 each machine requires a reference signal $y_{\mathrm{d},i}(t)$ to track. For the fourth machine this reference signal is obviously given by the customer demand, i.e. $y_{\mathrm{d},4}(t) = y_{\mathrm{d}}(t) = y_{\mathrm{d}0} + u_{\mathrm{d}}t + r(t)$. For the first three machines, the choice of an appropriate reference signal is now discussed.

First consider the case in which the reference signal for all machines is given by $y_{\mathrm{d}}(t)$, i.e. $y_{\mathrm{d},1}(t) = y_{\mathrm{d},2}(t) = y_{\mathrm{d},3}(t) = y_{\mathrm{d},4}(t) = y_{\mathrm{d}}(t)$. Since items are processed in the continuous ap-

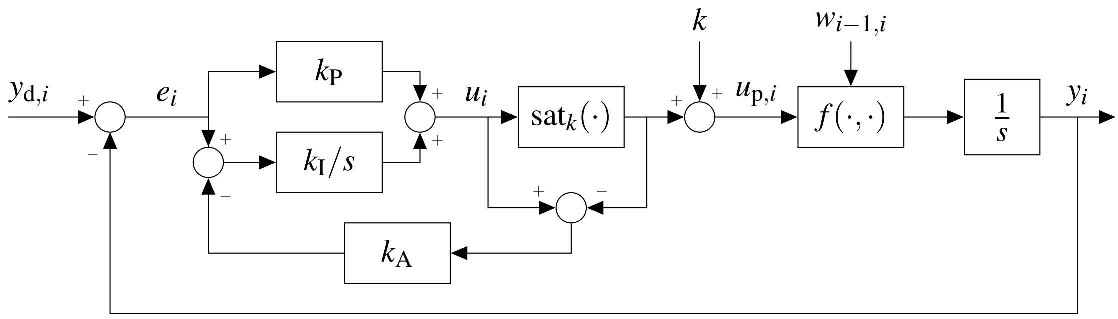

Figure 5.13: Anti-windup system with integrator plant adjusted for buffer constraint.

proximation system without a process delay, at first sight this reference signal seems to work fine: machine M_4 can track the customer demand (provided the frequency of $r(t)$ is below 1 rad/sec), and the buffers remain empty since the other three machines follow the same reference signal. From a practical point of view, however, it is obvious that this solution does not work properly. In practice, the production of an item takes a delay of t_0 seconds. This implies that if machine M_1 starts processing an item at $t = 0$, then machine M_2 cannot start processing this item before $t = t_0$, and so on, which eventually results in the fact that y_4 lags y_1 by at least $3t_0$ seconds. A solution to this problem can be to apply a reference signal to the machine which *leads* the reference signal of its first downstream machine by t_0 seconds. However, this would require future knowledge of the reference signal, which is assumed not to be available. Another reason why the reference signal $y_{\mathrm{d}}(t)$ for the first three machines does not work is that in practice failures may occur at machines and bad products may be thrown away (scrapped). In this case, the upstream machines need to produce extra items to compensate for the scrapped items. However, using a reference signal $y_{\mathrm{d}}(t)$ such compensation does not occur.

In order to be able to deal with issues as production delay and compensation for scrapped items, information on the production error of (at least) the downstream machine M_{i+1} should be incorporated in the reference signal of machine M_i. The following reference signal construction achieves this goal:

$$\begin{cases} y_{d,4} = & y_d \\ y_{d,i} = & y_d + K_{i,i+1} \cdot e_{i+1} \quad , \text{ for } i = 1,2,3 \end{cases} \tag{5.6}$$

where $e_i = y_{\mathrm{d},i} - y_i$ is the production error of machine M_i and $K_{i,i+1}$ is a gain that indicates how much of the error e_{i+1} is added to $y_{\mathrm{d},i}$. The motivation for this reference signal is as follows. Suppose that a downstream machine M_{i+1} has a production error $e_{i+1} > 0$ (due to scrap or production delay). Then, in order to make it possible for this machine to compensate for this error, the production of M_i should also be increased to prevent the intermediate buffer from depleting. In the following subsection the consequences of this reference signal construction and the choice of $K_{i,i+1}$ are discussed further for the system in the discrete-event domain.

Before the discrete-event implementation of this feedback controlled manufacturing line is discussed, a final remark is given on the convergency of this continuous approximation system.

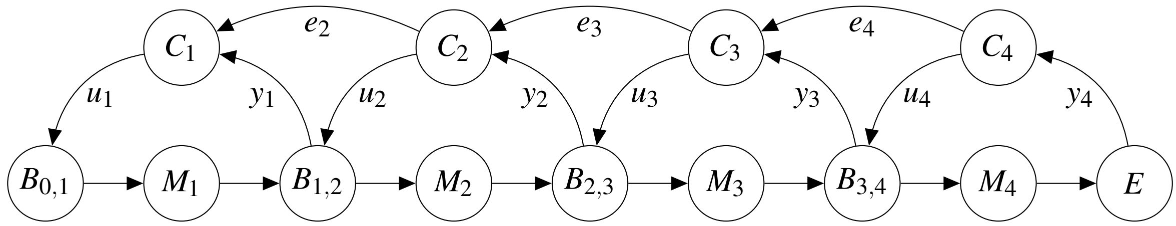

Figure 5.14: Schematic representation of the control structure for the discrete-event manufacturing line.

The continuous manufacturing line with reference signals (5.6) but *without* the positive buffer constraints, can be seen as a cascade of systems. In [72], it is shown that if each of these systems is convergent and in addition certain mild regularity conditions are met (which is the case for the system considered here), then the cascade of these systems is also convergent. A proof of convergency of the cascaded system *with* the positive buffer constraint, however, has not been found so far.

Discrete-event implementation and simulation results

The feedback controlled manufacturing line was implemented in χ, in a similar way to which it was done in Section 5.2, and is only discussed shortly here. More details on this discrete-event implementation can be found in [101].

In the implementation, each machine M_i has its own controller process C_i as depicted in Figure 5.14. This controller process is almost identical to the controller process for the single machine as depicted in Figure 5.6. The only two differences are that the reference signal is now described by (5.6), and that the error signal e_i is sent to the upstream controller.

Several discrete-event simulations have been performed for this system with the reference signal construction as described by (5.6). For these simulations, the parameters of the controller and the machines are the same as in Section 5.2, i.e. $k_\mathrm{P} = 10$, $k_\mathrm{I} = 20$, $k_\mathrm{A} = 0.5$, $u_{\mathrm{p,max}} = 25.0$ items/sec, $k = u_\mathrm{d} = 12.5$ items/sec. The reference demand considered here is $y_\mathrm{d}(t) = u_\mathrm{d}t + b\sin(\omega t)$, with $b = 12.5$ and $\omega = 0.25$, such that a *single* machine with the proposed feedback controller is able to follow the reference signal, see Figure 5.5. With the simulation results shown here, the influence of the value of gain $K_{i,i+1}$ in (5.6) is analysed.

First the case with $K = K_{i,i+1} = 0\ \forall i$ is considered, i.e. the production error of downstream machine M_{i+1} is not communicated to the controller of machine M_i. Figures 5.15 and 5.16 show some discrete-event simulation results for this system. In Figure 5.15 the system output (in normalized coordinates) $z_4(t)$ is shown together with the reference fluctuation $r(t)$. The figure clearly shows an offset between $z_4(t)$ and $r(t)$. The reason for this offset is the lag of $3t_0$ as a result of the production times of the machines, as discussed in the previous subsection. This lag of $3t_0$ is better visible in Figure 5.16 in which the output of the four machines is shown in original coordinates. In this figure, which is zoomed in on the simulation results, it can be seen that machine M_1 follows the desired production quite well, while machines M_2, M_3, and M_4 lag respectively t_0, $2t_0$ and $3t_0$ seconds. From this result, it is concluded that the reference signal with $K = 0$, i.e. $y_{\mathrm{d},i} = y_{\mathrm{d}}$, is unsatisfactory for the first three machines.

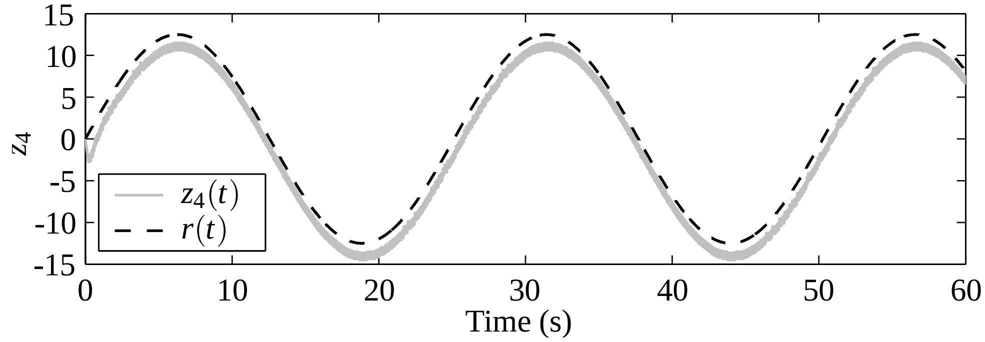

Figure 5.15: System output $z_4(t)$ for $K = 0$.

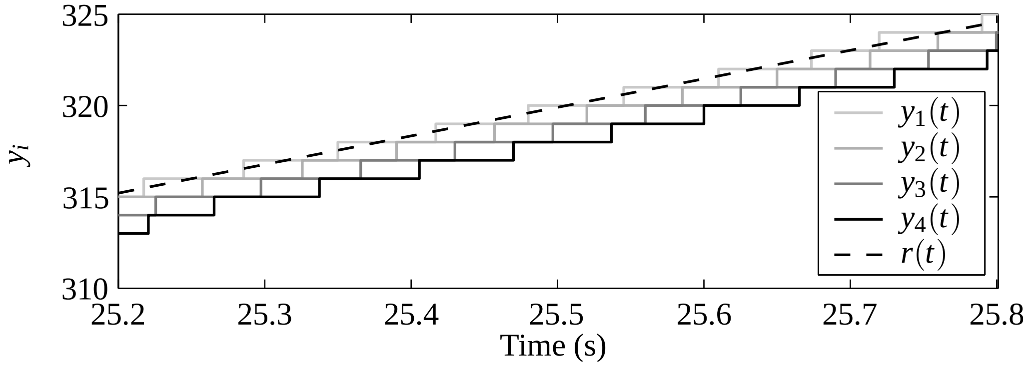

Figure 5.16: System outputs in original coordinates $y_i(t)$, $i \in \{1,2,3,4\}$ for $K = 0$.

In Figures 5.17 and 5.18 the discrete-event simulation results are shown for the system with $K = K_{i,i+1} = 1.0\ \forall i$. In Figure 5.17 one can observe that for this value of K, the offset between $z_4(t)$ and $r(t)$ is much smaller, but the oscillation of z_4 around its mean value is in amplitude larger than the oscillation that is caused by the integer character of the output, as can be seen for example in Figure 5.15. Figure 5.18 shows again detailed results for the four machine outputs y_i, from which this larger oscillation can be explained. In this figure, it can be seen that at $t = 25.2$ the output of machine M_4 is lagging behind the reference output y_{d}. Due to (5.6) with $K = 1.0$, this production error e_4 causes a larger reference signal for machine M_3 and in turn M_2 and M_1. As a result, the machine outputs y_1, y_2, and y_3 start to lead y_{d}, such that at $t = 25.5$ y_4 is able to meet the desired production y_{d}. Now, e_4 is small again and hence $y_3 \approx y_{\mathrm{d}}$, which causes bad tracking performance for machine M_4, due to which e_4 increases again. This explains the observed oscillation around y_{d}.

Apparently, $K = 1.0$ is still too small to guarantee good tracking behavior for machine M_4. After some trial-and-error, a more proper value for gain K was found, i.e. $K = K_{i,i+1} = 3.5\ \forall i$. The discrete-event simulation results for this setting are displayed in Figures 5.19 and 5.20. As

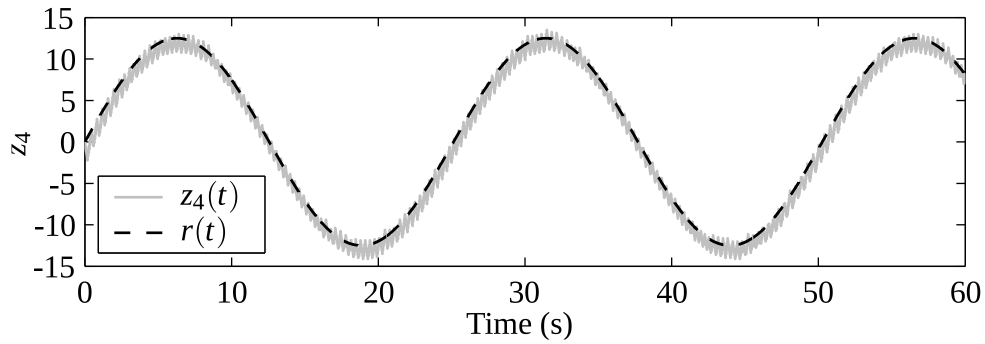

Figure 5.17: System output $z_4(t)$ for $K = 1.0$.

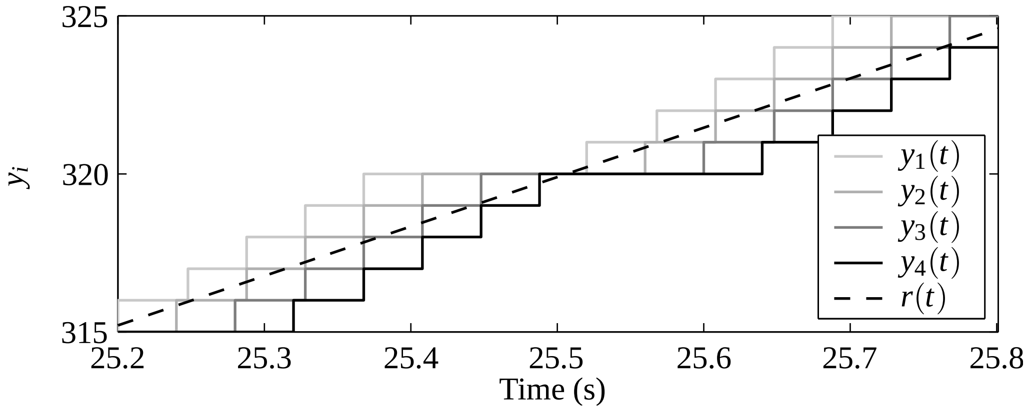

Figure 5.18: System outputs in original coordinates $y_i(t)$, $i \in \{1,2,3,4\}$ for $K = 1.0$.

one can see in Figure 5.19, the system output z_4 now follows the reference signal r very well, and the oscillation of z_4 around its mean value is small again. In Figure 5.20 one can observe that y_4 indeed tracks y_d quite well, and that the outputs y_i of the first three machines all lie well above y_4. Recall that the vertical distance between two adjacent lines in this figure, i.e. $y_i - y_{i+1}$, represents the total number of items in machine M_{i+1} and $B_{i,i+1}$. In this case the total amount of items in the system is quite small. For larger values of K, M_4 still shows a good tracking performance, but the amount of items in the system increases, which is undesirable.

Note that for the presented simulation results, all controllers in the line used the same value for K. Of course, one can try to use a different value of K for each controller, in order to obtain good tracking performance with even less inventory in the system. One may also think of other relations than (5.6) to include the production error of the downstream machine M_{i+1} in the reference signal of machine M_i. Future research must point out if such relations can further decrease the system's inventory while preserving the tracking behavior.

5.4 Discussion

In this chapter, a feedback controller was proposed for the tracking control of a discrete-event manufacturing machine. In order to design this feedback controller, the discrete-event machine

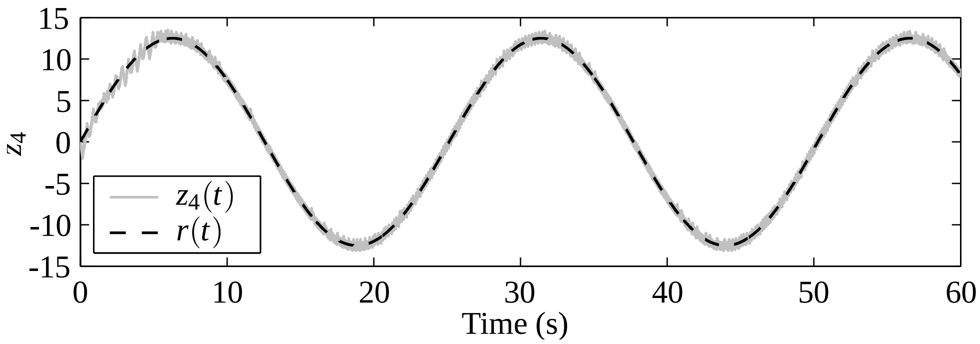

Figure 5.19: System output $z_4(t)$ for $K = 3.5$.

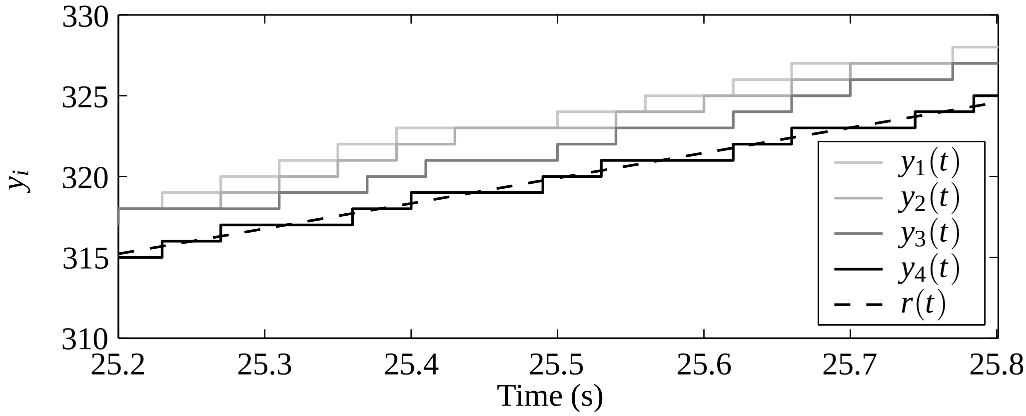

Figure 5.20: System outputs in original coordinates $y_i(t)$, $i \in \{1,2,3,4\}$ for $K = 3.5$.

was first approximated by an integrator with saturation on the ingoing channel. It was shown, by means of the convergent systems theory and the harmonic linearization method, that a PI controller with anti-windup compensation is a simple but effective controller for this continuous approximation of the machine, which achieves the desired tracking performance. The proposed controller was subsequently implemented in the discrete-event domain and applied to the discrete-event machine. Discrete-event simulation results were compared to simulation results of the continuous approximation system. This comparison showed that the PI controller achieves similar tracking behavior in the continuous-time domain and the discrete-event domain, as long as the processing time at the machine is relatively small in comparison with the period of the fluctuation of the reference demand.

Subsequently, the PI controller with anti-windup compensation was applied for the control of a discrete-event manufacturing line consisting of four machines. Besides the tracking requirement, a second requirement for this control problem was to keep the inventory in the line as small as possible. To each machine in the line the controller was applied, and it was shown that in order to solve the given control problem, the reference signals for the first three machines should include some information on the production error of the direct downstream machine. A linear coupling relation was proposed to include this production error in the reference signal, and by means of simulations a proper value of the gain in this relation was found. The application of the developed controller together with the adjusted reference signal for the first three machines resulted in a satisfactory tracking behavior with little inventory in the line, for the given reference signal. However, it did not become clear from the results if this linear coupling relation achieved the best possible result and if it is also applicable for longer manufacturing lines or different reference signals, and hence it is useful to investigate other coupling relations in future research as well.

Another issue that requires more investigation in future research is the applicability of the proposed feedback controller in more complex manufacturing systems. In this chapter, only some preliminary results were shown for a single machine and a short line of machines. Other investigations should point out if the proposed controller is also applicable for manufacturing systems with for example larger lines, assembly lines, multiple parallel machines, batch machines, multiple item machines, stochastic processing times, setup times, and/or multiple products with possible priority rules, or what adjustments should be made to the controller for these cases.

This research may also provide some contribution to the analysis of the bullwhip effect (i.e. demand amplification) in manufacturing lines, see e.g. [26, 44]. For example the frequency domain result in Figure 5.5 clearly indicates an amplification of the reference amplitude for a certain frequency range, which in turn may lead to an even larger output amplitude in upstream machines, due to the coupling relation. Note, however, that although this research may provide some insight in a bullwhip effect that is due to a choice of control policy, many more factors can contribute to the bullwhip effect, which are not described by the system considered in this chapter.

Although it is obvious that more research is required before a feedback controller of this kind may become practically applicable to manufacturing systems, in this chapter the first steps towards this goal have been made and the results obtained so far are promising.

Chapter 6

Performance Analysis of Switched Linear Systems under Specific Switching Rule Design

Abstract Whereas Chapters 3–5 dealt with systems described by linear dynamics and a static (saturation) nonlinearity, this chapter focusses on switched linear systems, i.e. systems that consist of several linear subsystems and a switching rule that governs the switching between these subsystems. Due to the switching, such a system is either linear time-varying (in case of time-dependent switching) or nonlinear (in case of state-dependent switching) and hence the steady-state solution of a switched linear system is in general dependent on the initial conditions. Some switched linear systems, however, are convergent and therefore have a unique steady-state solution. In this chapter it is discussed if, under the assumption that the dynamics of the separate linear submodes are given, a switching rule can be found for which the closed-loop system is convergent. Both a state-dependent switching rule, an (observer-based) output-dependent switching rule, and a time-dependent switching rule are considered. For each of these switching rules, sufficient conditions are found under which the closed-loop system is exponentially convergent. The presented theory is illustrated by means of a case study in which these results are used to analyse the steady-state performance of switched linear systems. This case study is supported by results from both simulation and real-time experiments.

6.1 Introduction

A switched linear system is a system that consists of two or more linear subsystems and a switching rule that decides which of the subsystems is active at a certain moment in time. These systems have received a lot of attention in the last decades, see e.g. [10, 36, 48, 54, 59, 60, 82, 88, 89] and references therein. One of the aspects that makes a switched linear system interesting is that by appropriate switching between the available linear subsystems/controllers, the performance (e.g. transient response) of the closed-loop system can be improved, see e.g. [16]. Most studies in which the performance of switched linear systems is compared to the performance of linear systems are based on time-domain analysis. Frequency domain performance analyses (i.e. using frequency response functions) of switched linear systems, however, are rare. This is due to the fact that the frequency response functions for linear systems cannot be straightforwardly extended to the nonlinear case. Nevertheless, in many cases such a frequency domain performance analysis is an important aspect of the overall performance analysis of a system. For example, for the controller design for a CD/DVD player, it is important to investigate the steady-state response to periodic disturbance inputs [32]. Fortunately, there exist some types of nonlinear systems, such as time-periodic systems (see e.g. [15, 80]) or nonlinear convergent systems (see Section 2.4), which *can* be analysed using frequency response functions. This chapter focusses on the latter type.

By the results of [66] (see also Section 2.4) it is known that for the class of convergent switched linear systems, a frequency domain analysis can be performed which is similar to the frequency response function analysis known from linear systems theory. Evidently, not all switched linear systems are convergent. Recent research provides LMIs to analyse if a certain switched linear system is quadratically convergent [65]. Furthermore, in [13] an approach is given to design a linear feedback matrix for a switched linear system with a fixed switching rule in such a way that the closed-loop system is convergent.

This chapter provides a different starting point for the design of a convergent switched linear system. That is, the dynamics of all linear subsystems are assumed to be given (in contrast to the situation in [13], in which the switching rule is given). For this situation, a switching rule is proposed and sufficient conditions are found under which this switching rule results in a convergent closed-loop system. In particular, two switching rules are considered. Firstly, the case is considered in which the switching rule depends on state feedback. Secondly, the case is considered in which full state information is not available. For this case a switching rule is discussed that is based on an observer of the system. Finally, the use of time-dependent switching rules is also briefly discussed.

The remainder of this chapter is organized as follows. Section 6.2 introduces the considered switched linear system and discusses the different investigated switching rules. Section 6.3 describes a case study that illustrates the presented theory and shows how this theory can be used to analyse the steady-state performance of switched linear systems. Finally, Section 6.4 gives a discussion on the results obtained in this chapter.

6.2 Convergent system design using switching rules

In this section, first the switched linear system is introduced that is considered throughout the chapter. Then, the idea of designing a switching rule that renders the closed-loop system convergent, is explained further. Subsequently, the use of a state-dependent switching rule is discussed for the case that full state information is available. Finally, the case is considered in which only some part of the state information is available for feedback. For this case an observer-based switching rule is presented.

Consider the switched linear system

$$\begin{aligned} \dot{x}(t) &= A_i x(t) + B_i w(t) \\ y(t) &= C_i x(t) \end{aligned} \qquad i = 1, \ldots, k \tag{6.1}$$

where $x(t) \in \mathbb{R}^n$ is the state, $y(t) \in \mathbb{R}^l$ is the output, and $w(t) \in \overline{\mathbb{PC}}^m$ is the input. Here $\overline{\mathbb{PC}}^m$ is the class of bounded piecewise continuous inputs $w(t) : \mathbb{R} \to \mathbb{R}^m$. The dynamics in (6.1) can for example represent the behavior of a switched linear control system as visualized in Figure 6.1. It is assumed that the collections of matrices $\{A_1, \ldots, A_k\}$, $\{B_1, \ldots, B_k\}$, and $\{C_1, \ldots, C_k\}$ are given, which implies that the dynamics of the linear subsystems are fixed. The general problem that is considered in this section is to find a *switching rule* for which the closed-loop system is exponentially convergent.

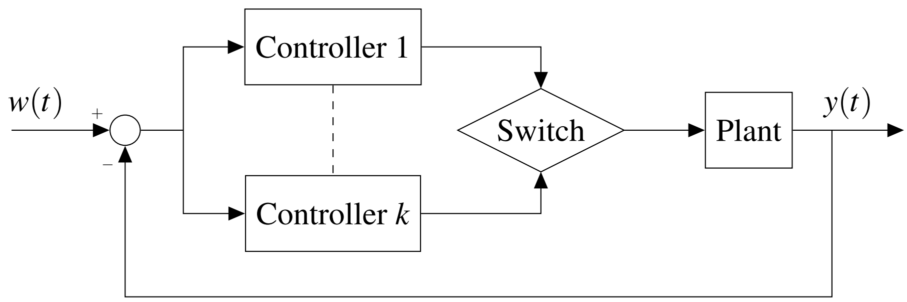

Figure 6.1: Switched linear control system.

Note that it is always possible to find a switching rule that makes the system exponentially convergent whenever there is at least one exponentially stable mode. That is, a ‘switching’ rule that keeps the system in only one (exponentially stable) mode, results in a system that is in fact linear, and thus exponentially convergent. Here, this trivial case is ignored: only switching rules are considered that take into account all modes, in order to obtain a convergent *switched* linear system. Of course, it may occur that for a certain solution of the system the switching rule *selects* only one mode (as a result of the given dynamics in the different modes, the input signal and the initial condition), but in this selection all other modes are involved as well.

For a time-dependent switching rule, i.e. a switching rule that changes the active mode of the system at fixed time instances regardless of the values of the state and input, it can easily be seen that the existence of a common matrix $P = P^T > 0$ that satisfies

$$A_i^T P + PA_i < 0, \ \forall i = 1, \dots, k \tag{6.2}$$

is a sufficient condition for quadratic convergency. That is, for an arbitrary time-dependent switching rule and a Lyapunov function $V = (x_1 - x_2)^T P(x_1 - x_2)$, where x_1 and x_2 are two arbitrary solutions of system (6.1), the derivative $\dot{V}$ is at each time instance smaller then $-\alpha V$ for some fixed $\alpha > 0$, because the active mode is always the same for x_1 and x_2. The inequality $\dot{V} < -\alpha V$ implies that the system is quadratically convergent.

For state-dependent switching rules, on the other hand, the existence of a common matrix $P = P^T > 0$ satisfying (6.2) may not be sufficient for quadratic convergency of system (6.1), as is demonstrated in the following example, which is based on results in [65].

Example 6.1. Consider the following system with a state-dependent switching rule

$$\dot{x}(t) = \begin{cases} -3x(t) + w(t) & \text{if } |x| \le 2 \\ -2x(t) + w(t) & \text{if } |x| > 2 \end{cases} \tag{6.3}$$

of which the dynamics are schematically depicted in Figure 6.2. For $w(t) \equiv 0$, it is easy to conclude, using a common quadratic Lyapunov function $V = x^2$, that the system is globally exponentially stable. However, for other (e.g. constant) input signals $w(t)$, it can be deduced from Figure 6.2 that the steady-state solution of the system can depend on the initial condition. For example, if $w(t) = 5$ for all time, then the solutions $x(t)$ with initial conditions $x(0) = 0$ and $x(0) = 4$ stabilize at respectively $x = 5/3$ and $x = 5/2$. Hence, the system is not convergent even though a common quadratic Lyapunov function exists for this system.

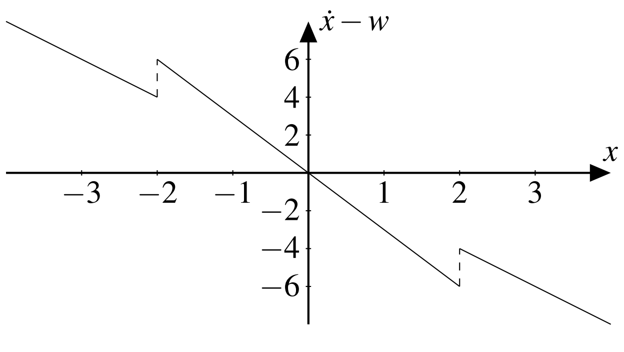

Figure 6.2: Schematic representation of the dynamics of system (6.3).

△

Since the existence of a common Lyapunov function does not guarantee that a switched linear system is convergent under an arbitrary state-dependent switching rule, it is not trivial to find a state-based switching rule that renders system (6.1) exponentially convergent. In the remainder of this section, two kinds of switching rules are discussed, i.e. a switching rule based on state feedback and a switching rule based on output feedback, and sufficient conditions are derived under which these switching rules render the closed-loop system exponentially convergent.

State-dependent switching rule

Consider the following switching rule for system (6.1)

$$\sigma(x,w) = \arg\ \min_i \{x^T Z_{ix} x + x^T Z_{iw} w\} \tag{6.4}$$

in which Z_{ix} and Z_{iw} are matrices to be defined. The following theorem provides sufficient conditions under which this switching rule makes system (6.1) quadratically convergent.

Theorem 6.2. *If for system* (6.1) *the following conditions hold*

1. *a common Lyapunov matrix $P = P^T > 0$ exists that satisfies*

$$A_i^T P + PA_i < 0, \ \ \forall i = 1, \dots, k, \tag{6.5}$$

2. *matrices $Z_{1w}, \dots, Z_{kw}$ are given by $Z_{iw} = 2PB_i$, $i = 1, \dots, k$,*

3. *matrices $Z_{1x}, \dots, Z_{kx}$ exist such that*

$$Z_{ix} \neq Z_{jx} \text{ and/or } Z_{iw} \neq Z_{jw} \quad \forall i, j \leq k,\ i \neq j \tag{6.6}$$

and for some $\varepsilon > 0$

$$\begin{bmatrix} PA_i + A_i^T P & -(A_i^T P + PA_j) \\ -(A_j^T P + PA_i) & PA_j + A_j^T P \end{bmatrix} + \begin{bmatrix} -(Z_{ix} - Z_{jx}) & 0 \\ 0 & Z_{ix} - Z_{jx} \end{bmatrix} \leq -\varepsilon \begin{bmatrix} I_n & -I_n \\ -I_n & I_n \end{bmatrix} \quad \forall i, j \leq k,\ i \neq j. \tag{6.7}$$

Then switching rule (6.4) *with matrices Z_{ix} and $Z_{iw} = 2PB_i$, $i = 1, \dots, k$ makes system* (6.1) *quadratically convergent.*

Proof. First note that condition (6.6) assures the existence of a solution in the sense of Filippov for the closed-loop system. Consider the Lyapunov function

$$V(x_1,x_2) = (x_1 - x_2)^T P (x_1 - x_2) \tag{6.8}$$

in which $x_1(t)$ and $x_2(t)$ are two arbitrary solutions of system (6.1) with input $w(t)$, and $P = P^T > 0$ satisfies (6.5). Let $\sigma(x_1,w) = p$ and $\sigma(x_2,w) = q$, such that the derivative of (6.8) becomes

$$\begin{aligned} \dot{V} = {} & x_1^T (A_p^T P + PA_p) x_1 + x_2^T (A_q^T P + PA_q) x_2 \\ & - x_1^T (A_p^T P + PA_q) x_2 - x_2^T (PA_p + A_q^T P) x_1 \\ & + 2x_1^T P (B_p - B_q) w + 2x_2^T P (B_q - B_p) w. \end{aligned} \tag{6.9}$$

If $p = q$, i.e. the active mode for solution $x_1(t)$ equals the active mode for solution $x_2(t)$ at time t, then the inequality

$$\dot{V} \leq -\alpha V, \ \ \alpha > 0$$

is obviously satisfied. For the case that $p \neq q$, this inequality also holds for some $\alpha > 0$ if condition (6.7) is met, which is proven using the following reasoning.

Switching rule (6.4) implies the following constraints for mode p

$$G_1(x,w) = x_1^T(Z_{px} - Z_{qx})x_1 + x_1^T(Z_{pw} - Z_{qw})w \leq 0$$

and for mode q

$$G_2(x,w) = x_2^T(Z_{qx} - Z_{px})x_2 + x_2^T(Z_{qw} - Z_{pw})w \leq 0.$$

The system is quadratically convergent if for some $\varepsilon > 0$ it holds that

$$\dot{V} \leq -\varepsilon \begin{bmatrix} x_1 \\ x_2 \end{bmatrix}^T \begin{bmatrix} I_n & -I_n \\ -I_n & I_n \end{bmatrix} \begin{bmatrix} x_1 \\ x_2 \end{bmatrix}$$

for all (x,w) that satisfy $G_1(x,w) \leq 0$ and $G_2(x,w) \leq 0$. Using the S-procedure (see Section 2.2), the previous condition is satisfied if the following inequality holds

$$\dot{V} - G_1 - G_2 \leq -\varepsilon \begin{bmatrix} x_1 \\ x_2 \end{bmatrix}^T \begin{bmatrix} I_n & -I_n \\ -I_n & I_n \end{bmatrix} \begin{bmatrix} x_1 \\ x_2 \end{bmatrix}.$$

This inequality is equivalent to (6.7). □

Remark 6.3. If the conditions of Theorem 6.2 hold, then the closed-loop system is well-posed in the sense of Filippov, i.e. existence, right uniqueness, and continuous dependence on initial conditions of solutions are assured. The right uniqueness and continuous dependence on initial conditions of solutions follow from the fact that the system is quadratically convergent, similar to Theorem 2.10.1 in [17].

Remark 6.4. Note that (6.5) and (6.7) are LMIs with design variables P and $Z_{1x}, \ldots, Z_{kx}$, which can be solved efficiently using available LMI toolboxes.

Although Theorem 6.2 gives sufficient conditions for quadratic convergency, it does not give insight for what collection of matrices $\{A_1, \ldots, A_k\}$ a switching law can be found. In the case that both Z_{ix} and Z_{iw} are defined in advance for all $i = 1, \ldots, k$, i.e.

$$Z_{ix} = \frac{1}{2}\left(A_i^T P + PA_i\right), \quad Z_{iw} = 2PB_i \tag{6.10}$$

then Theorem 6.2 can be simplified as follows.

Corollary 6.5. *If there exists a common Lyapunov matrix $P = P^T > 0$ such that conditions* (6.5) *and* (6.6) *are satisfied and in addition*

$$P(A_i - A_j) - (A_i - A_j)^T P = 0 \quad \forall i, j \leq k \tag{6.11}$$

then switching rule (6.4) *with matrices $Z_{1x}, \ldots, Z_{kx}$ and $Z_{1w}, \ldots, Z_{kw}$ as defined in* (6.10) *makes system* (6.1) *quadratically convergent.*

Proof. The proof of this corollary is based on the proof of Theorem 6.2. Substituting $Z_{ix} = \frac{1}{2}\left(A_i^T P + PA_i\right)$ and using condition (6.11) gives

$$\dot{V} - G_1 - G_2 \leq \frac{1}{2}(x_1 - x_2)^T (Z_{px} + Z_{qx})(x_1 - x_2).$$

Since $Z_{px} + Z_{qx} \leq -\varepsilon I_n$ for some $\varepsilon > 0$, it follows that system (6.1) is quadratically convergent. □

Remark 6.6. Note that condition (6.11) is an equality constraint and therefore the LMI problem corresponding to Corollary 6.5 is harder to solve (using LMI toolboxes) than the LMI problem corresponding to Theorem 6.2. On the other hand, condition (6.11) is very useful since it provides direct insight in the fact that the LMI problem is solvable for *symmetric* Hurwitz matrices A_i, $i = 1, \ldots, k$, using $P = I_n$. This insight could not be gained directly from Theorem 6.2.

Switching rule (6.4) as used in Theorem 6.2 and Corollary 6.5 is based on the fact that full state information is available for feedback. In the following subsection the case is discussed in which only a part of the state is available for feedback.

Observer-based switching rule

Consider the case in which only some system output $C_i x$ is available for feedback, instead of the entire state. For this case, an observer is constructed for system (6.1)

$$\dot{\hat{x}}(t) = A_i \hat{x}(t) + B_i w(t) + L_i C_i (x - \hat{x}), \quad i = 1, \ldots, k \tag{6.12}$$

where $\hat{x}$ is the estimate of state x and $L_i \in \mathbb{R}^{n \times l}$ is the observer gain matrix. The following observer-based switching rule is proposed

$$\sigma(\hat{x}, w) = \arg \min_i \{\hat{x}^T Z_{ix} \hat{x} + \hat{x}^T Z_{iw} w\} \tag{6.13}$$

in which Z_{iw} and Z_{ix} are matrices to be defined.

Theorem 6.7. *If for system* (6.1) *all conditions of Theorem 6.2 hold, and in addition there exist a matrix $P_2 = P_2^T > 0$ and matrices L_i for $i = 1, \ldots, k$, such that*

$$(A_i - L_i C_i)^T P_2 + P_2 (A_i - L_i C_i) < 0, \quad \forall i = 1, \ldots, k \tag{6.14}$$

then observer-based switching rule (6.13) *with matrices Z_{ix} and $Z_{iw} = 2PB_i$, $i = 1, \ldots, k$ makes system* (6.1) *exponentially convergent.*

Proof. First it is proven that the state $x(t)$ of system (6.1) either lies in a positive invariant compact set or converges exponentially in time to this set. Consider the Lyapunov function

$$V(x) = x^T P x.$$

Since there exists a common P such that (6.5) is satisfied, it follows that

$$\dot{V}(x) \leq -\alpha V + \beta^* |x||w| \leq -\alpha V + \beta \sqrt{V}$$

for some positive constants α, β^*, and β, and bounded input $w \in \overline{\mathbb{PC}}^m$. Here, $|\cdot|$ represents the Euclidean norm. Note that there exists a level set

$$\Omega = \left\{ x \;\middle|\; V(x) \leq \frac{\beta^2}{\alpha^2} \right\}$$

outside of which $\dot{V} < 0$. This implies that if initial condition $V(x(0))$ lies within this level set, then $V(x(t))$ remains within this set for all $t > 0$. If $V(x(0))$ lies outside this set, then $V(x(t))$ converges exponentially in time to this set as can be seen from

$$\dot{V} \leq -\alpha V + \beta \sqrt{V} \leq -\alpha \left(V - \frac{\beta^2}{\alpha^2} \right).$$

Since V is a quadratic function of $x(t)$, it can be concluded that $x(t)$ also converges exponentially to the positively invariant compact set Ω.

Secondly it is proven that the estimation error $e(t) = x(t) - \hat{x}(t)$ decreases exponentially towards zero as $t \to \infty$ if (6.14) holds. Since both the observer (6.12) and system (6.1) use the same switching rule (6.13) the error dynamics become

$$\dot{e} = \begin{cases} (A_1 - L_1 C_1)e & \text{for } \sigma(\hat{x}, w) = 1 \\ \qquad \vdots & \\ (A_k - L_k C_k)e & \text{for } \sigma(\hat{x}, w) = k \end{cases}$$

If there exists a common Lyapunov matrix P_2 for all $(A_i - L_i C_i)$, $i = 1, \ldots, k$, i.e. condition (6.14) is satisfied, then the equilibrium point $e = 0$ is globally exponentially stable.

Finally consider the Lyapunov function and its derivative given in respectively (6.8) and (6.9). Let $\sigma(\hat{x}_1, w) = p$ and $\sigma(\hat{x}_2, w) = q$. The observer-based switching rule (6.13) implies the following constraints for mode p

$$G_1(\hat{x}, w) = \hat{x}_1^T (Z_{px} - Z_{qx}) \hat{x}_1 + \hat{x}_1^T (Z_{pw} - Z_{qw}) w \leq 0$$

and for mode q

$$G_2(\hat{x}, w) = \hat{x}_2^T (Z_{qx} - Z_{px}) \hat{x}_2 + \hat{x}_2^T (Z_{qw} - Z_{pw}) w \leq 0.$$

Substituting $\hat{x}_i$ by $x_i - e_i$ gives

$$\begin{aligned} G_1(\hat{x}_1, w) &= G_1(x_1, w) + G_1(e_1, w) - f(e_1, x_1), \\ G_2(\hat{x}_2, w) &= G_2(x_2, w) + G_2(e_2, w) + f(e_2, x_2), \end{aligned}$$

with

$$f(e_i, x_i) = x_i^T(Z_{qx} - Z_{px})e_i + e_i^T(Z_{qx} - Z_{px})x_i.$$

Subsequently, the S-procedure is applied to obtain

$$\dot{V} - G_1(\hat{x}_1, w) - G_2(\hat{x}_2, w) \leq -\alpha_1 V + g$$

with

$$g = -G_1(e_1, w) - G_2(e_2, w) + f(e_1, x_1) - f(e_2, x_2).$$

Since $e_i(t)$ tends exponentially towards zero as $t \longrightarrow \infty$, $x_i(t)$ lies in Ω or converges exponentially in time towards this set for $i = 1, 2$, and $w(t)$ is bounded, function g tends exponentially towards zero as a function of time. Thus, using switching rule (6.13) the following inequality is true

$$\dot{V} \leq -\alpha_1 V + \gamma e^{-\alpha_2 t} \tag{6.15}$$

where α_1, α_2, γ are some positive constants. Using for example the comparison principle (see e.g. [40]) it can be shown that (6.15) implies that $V(x_1(t) - x_2(t))$ reduces exponentially towards zero as $t \longrightarrow \infty$ and therefore that system (6.1) is exponentially convergent. This completes the proof. □

Remark 6.8. Since there exists a common P for all A_i, $i = 1, \ldots, k$, condition (6.14) can always be met (take e.g. $L_i = 0$).

Remark 6.9. Condition (6.14) is not an LMI because of the product of design matrices $P_2 L_i$. However, replacing $P_2 L_i$ by matrices Q_i leads to an LMI with design matrices P_2 and Q_i. Once the LMI is solved the matrices L_i can be obtained from $L_i = P_2^{-1} Q_i$. The inverse of P_2 always exists since P_2 is positive definite.

It has been shown in this section that both time-dependent, state-dependent and output-dependent switching rules can be defined that lead to an exponentially convergent closed-loop system, provided this system satisfies some conditions. In the remainder of this chapter, these results are illustrated by means of a case study.

6.3 Case study: Performance analysis of a switched linear system

In this case study the following switched linear system is investigated

$$\begin{aligned} \dot{x} &= A_i x + B_i w(t) \\ y &= Cx \end{aligned} \qquad i = 1, 2 \tag{6.16}$$

in which $x(t) \in \mathbb{R}^3$ is the state, $w(t) \in \overline{\mathbb{PC}}$ is the input, and

$$
\begin{aligned}
A_1 &= \begin{bmatrix} -5 & -8 & 3 \\ 10 & -2 & 0 \\ 9 & -1 & -6 \end{bmatrix}, \quad B_1 = \begin{bmatrix} 14 \\ -6 \\ 7 \end{bmatrix}, \\
A_2 &= \begin{bmatrix} -8 & -5 & -8 \\ 13 & -8 & 2 \\ -2 & 1 & -4 \end{bmatrix}, \quad B_2 = \begin{bmatrix} 20 \\ -16 \\ 8 \end{bmatrix}, \\
C &= \begin{bmatrix} 1 & 0 & 0 \end{bmatrix}.
\end{aligned}
$$

For this system, first a state-dependent switching rule is applied to obtain a quadratically convergent system. Subsequently, the steady-state performance of this convergent system is analysed in the frequency domain and compared to the performance of the two corresponding linear systems. In the second part of the case study it is assumed that only some output y can be measured. For this case an observer-based switching rule is applied to render the system exponentially convergent. The results presented in this section are obtained using both real-time experiments and simulation. The real-time experiments are of special interest here, since they can provide insight in how the switching rules (which allow sliding modes) operate in a real-time environment (with only a finite sampling rate). The experimental setup that was used for the real-time experiments is described below.

Experimental setup

The experimental setup that is used to investigate the behavior of system (6.16) with state-dependent switching rule (6.4) is shown schematically in Figure 6.3. The hardware of this experimental setup is identical to the hardware described in Section 4.4 (see Figures 4.3 and 4.4). The software, on the other hand, here consists of a reference signal generator, two subsystems (controllers) with linear dynamics, a block that computes the switching signal according to switching rule (6.4), and a switch that performs the actual switching between the available subsystems. Directly after the switch, signal $\dot{x}$ is divided into two parts: $\dot{x}_1$ and $[\,\dot{x}_2,\ \dot{x}_3\,]^T$. The first part, i.e. $v = \dot{x}_1$, is the reference velocity that is sent to the actuator, which drives a rotating rigid body. The sensor (an incremental encoder) measures rotation angle x_1. The second part, i.e. $[\,\dot{x}_2,\ \dot{x}_3\,]^T$, is integrated numerically and the resulting $[\,x_2,\ x_3\,]^T$ is fed back into the two subsystems together with the measured x_1. Note that in order to realize the dynamics as described in (6.16) the integrator in the software cannot be incorporated in the subsystems, since at the moment of switching only $\dot{x}$ should be changed, while state x keeps its value. If the integrator would be incorporated in the subsystems then part of the state, i.e. x_2 and x_3, would also change at the moment of switching.

For the investigation of the behavior of system (6.16) with *observer*-based switching rule (6.13), the software of the experimental setup as described in Figure 6.3 is extended with an observer,

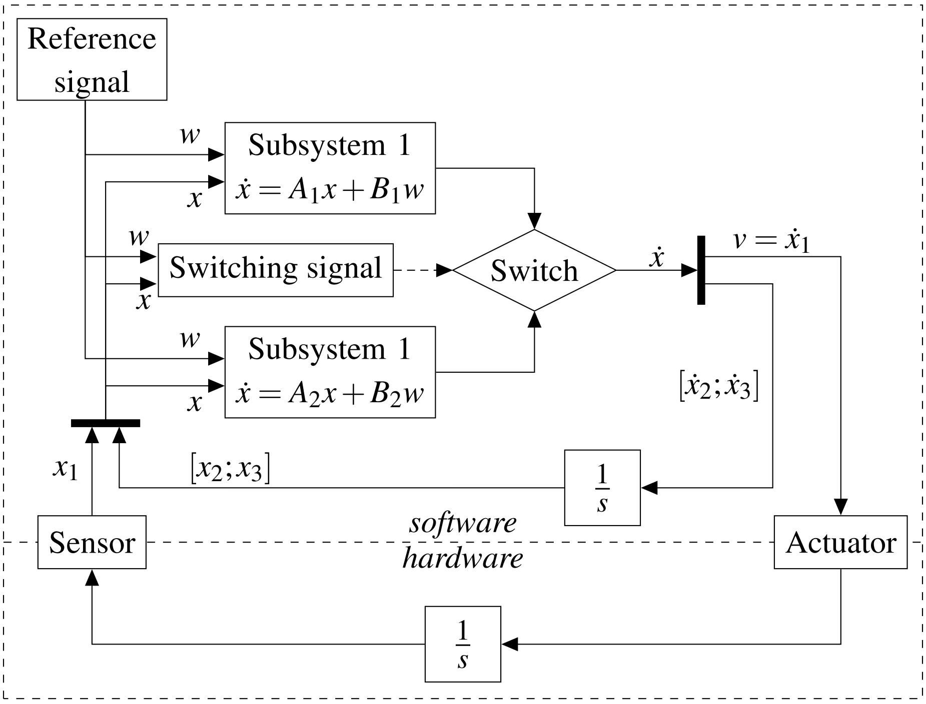

Figure 6.3: Schematic representation of the experimental setup with state-dependent switching.

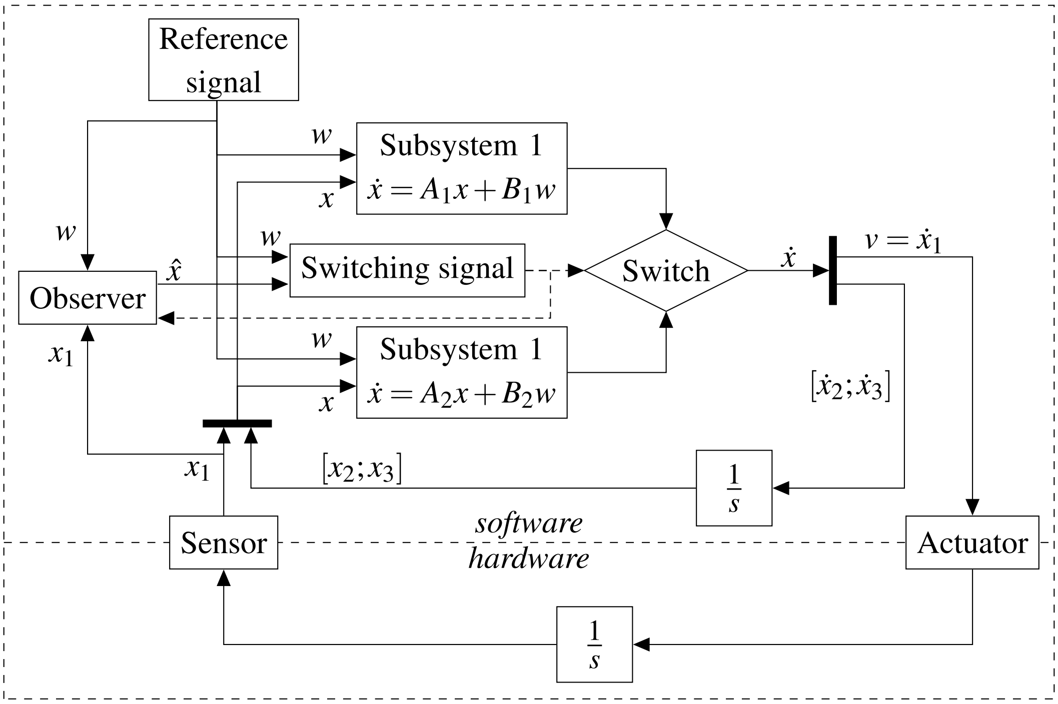

Figure 6.4: Schematic representation of the experimental setup with observer-based switching.

as visualized in the schematic representation in Figure 6.4. This observer contains a copy of the subsystems (with an additional term $L_i(x_1 - \hat{x}_1)$), a switch and a numerical integrator, such that it describes the dynamics as given in (6.12).

State-dependent switching

Consider system (6.16) with the given matrices and state-dependent switching rule (6.4). Using an LMI toolbox the following matrices can be found

$$P = \begin{bmatrix} 0.1033 & -0.0084 & 0.0032 \\ -0.0084 & 0.0880 & -0.0070 \\ 0.0032 & -0.0070 & 0.1015 \end{bmatrix} > 0 \tag{6.17}$$

$$Z_{1x} - Z_{2x} = \begin{bmatrix} 0.3702 & -0.3670 & 1.1471 \\ -0.3670 & 0.5676 & -0.2548 \\ 1.1471 & -0.2548 & -0.1539 \end{bmatrix} \tag{6.18}$$

that in combination with $Z_{1w} = 2PB_1$ and $Z_{2w} = 2PB_2$ satisfy conditions (6.5)–(6.7) with $\varepsilon = 0.4415$. Here, Z_{1x} and Z_{2x} can be chosen freely within the restrictions of (6.6) and (6.18). Since all conditions of Theorem 6.2 are met, one can conclude that switching rule (6.4) with the matrices as defined above makes system (6.16) quadratically convergent, i.e.

$$\begin{aligned} \dot{V} &\leq -0.4415(x_1 - x_2)^T(x_1 - x_2) \\ &\leq -3.9782(x_1 - x_2)^T P(x_1 - x_2) \\ &\leq -3.9782V. \end{aligned}$$

In order to determine how fast a solution converges to the limit solution $\bar{x}(t)$, the following calculation can be made. First note that

$$\begin{aligned} (x_1 - x_2)^T P(x_1 - x_2) &\geq \lambda_{\min}(P)|x_1 - x_2|^2 \\ (x_1 - x_2)^T P(x_1 - x_2) &\leq \lambda_{\max}(P)|x_1 - x_2|^2 \end{aligned}$$

where $\lambda_{\min}(P)$ and $\lambda_{\max}(P)$ denote respectively the minimum and maximum eigenvalue of P. An upper bound on the exponential convergency of solutions can now be expressed as

$$\begin{aligned} |x_1(t) - x_2(t)| &\leq \sqrt{\frac{\lambda_{\max}(P)}{\lambda_{\min}(P)}}\, |x_1(0) - x_2(0)|\, e^{\frac{-3.9782}{2}t} \\ &\leq 1.1580\, |x_1(0) - x_2(0)|\, e^{-1.9891t}. \end{aligned} \tag{6.19}$$

Note that for different matrices P and $Z_{1x} - Z_{2x}$ (that also satisfy all conditions of Theorem 6.2), a *different* upper bound can be found for $|x_1(t) - x_2(t)|$. However, as the main interest here lies with the steady-state performance of the switched linear system, this transient performance and for example the possibility of optimizing the upper bound on the exponential convergency is not discussed further here.

In order to analyse the steady-state performance of this switched linear system, both simulation and real-time experiments were used. As explained in Section 2.4, simulation is (experiments are) a reliable way for convergent systems to determine the limit solution of the system. The steady-state response of the switched linear system is compared to the steady-state response of the two corresponding linear systems, i.e. $\dot{x} = A_1x + B_1w(t)$ and $\dot{x} = A_2x + B_2w(t)$, for harmonic input signals

$$w(t) = \sin(\omega t), \quad \omega \in [10^{-2}, 10^3].$$

By means of simulation the limit solutions of all three systems have been determined and a nonlinear sensitivity function ($\mathscr{S} = ||w-y||_2/||w||_2$, see Section 2.4) has been computed. This nonlinear sensitivity function is shown in Figure 6.5.

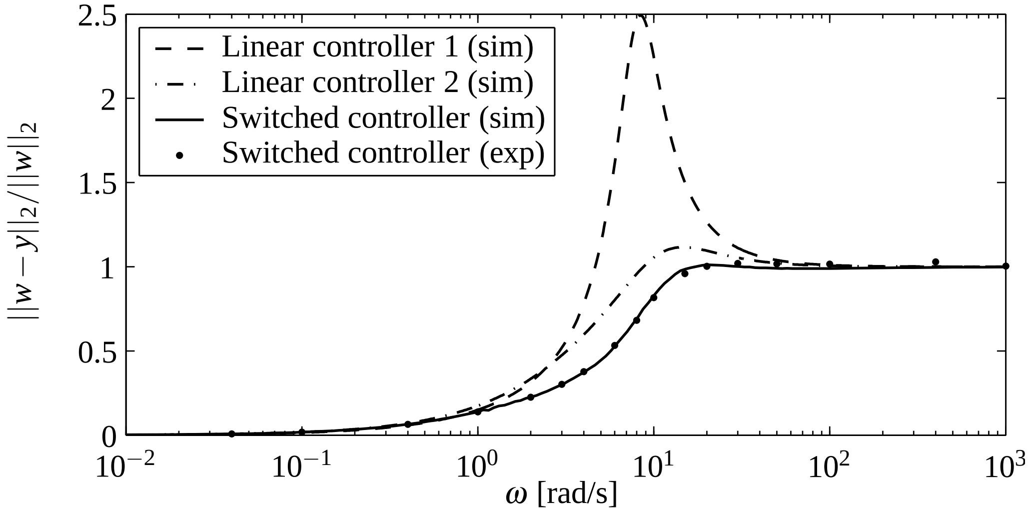

Figure 6.5: Nonlinear sensitivity function.

In Figure 6.5 it can be observed that for the considered nonlinear sensitivity function the switched linear system performs better than the linear systems for the input range $\omega \in [10^0, 10^2]$. This implies that besides improvement of transient behavior (see e.g. [16]), the use of switched linear control instead of linear control may also provide better steady-state behavior. A more important observation, however, is that the performance of the switched linear system *can* be compared to the performance of the linear systems in the frequency domain, something which is not trivial for switched linear systems in general.

Note that the nonlinear sensitivity function for the linear systems as depicted in Figure 6.5 is *not* the same as the magnitude of the linear sensitivity function. Due to the definition of the nonlinear sensitivity function a difference in phase between input w and output y also results in a positive value of the nonlinear sensitivity, even if the amplitude of w and y are identical.

The nonlinear sensitivity function of the switched linear system is also determined by means of experiments on the experimental setup as described in the previous subsection. These results are indicated in Figure 6.5 with dots. One can observe that the results of the experiments correspond quite well with the simulation results, especially for low frequencies. For higher frequencies, the deviation between the experimental and simulation results becomes larger. This is to be expected, since the sampling rate (1000 Hz) here forms an obvious limitation. Another observation, which was made during the execution of the experiments, is that for some input frequencies the system goes through a short time of ‘chattering’ in every period. This 'chattering' is caused by very fast switching between the two subsystems, which is visualized in Figures 6.6 and 6.7 for the system with $w(t) = \sin(0.4t)$. In these figures both output y and switching signal $\sigma(x,w)$ are shown as a function of time. Since fast switching implies that the system is subject to large forces, such a switching policy may not be suitable for every type of system. Nevertheless, for systems that do allow such a switching policy, the nonlinear sensitivity may be improved as suggested in Figure 6.5.

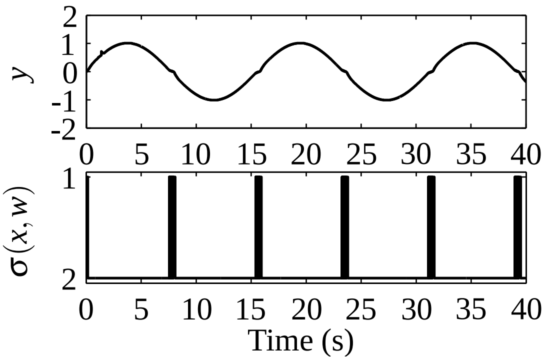

Figure 6.6: Experimental result: $x_1(t)$ for system with $w(t) = \sin(0.4t)$.

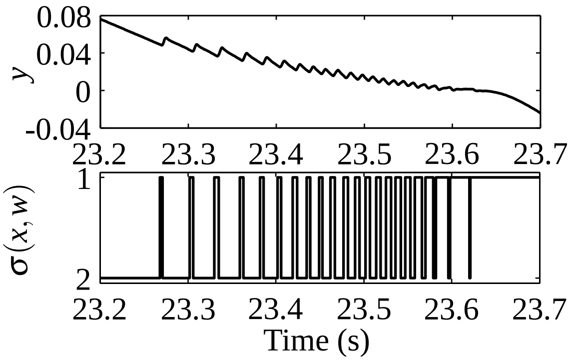

Figure 6.7: Experimental result: $x_1(t)$ for system with $w(t) = \sin(0.4t)$, zoomed in.

Observer-based switching

In this subsection the effect of observer-based switching as opposed to state-based switching is shown. Consider again system (6.16) with the given matrices and consider (6.12) with gain matrices

$$L_1 = \begin{bmatrix} 10 \\ 5 \\ 10 \end{bmatrix}, \quad L_2 = \begin{bmatrix} 5 \\ 10 \\ -10 \end{bmatrix}$$

which are chosen in such a way that condition (6.14) can be satisfied for some P_2. Since matrices (6.17) and (6.18) as used in the previous subsection can still be applied, all conditions in Theorem 6.7 are satisfied, which implies that system (6.16) with observer-based switching rule (6.13) is exponentially convergent for any input $w \in \overline{\mathbb{PC}}$. In Figure 6.8 the convergent behavior of system output y as obtained by simulation is visualized for $x(0) = [0;0;0]$, $w = \sin(5t)$, and initial estimation errors $e(0) = \{[-10;-10;-10],[-100;100;0],[100;0;-10]\}$ (respectively the dashed, dash-dotted, and dotted line). Furthermore, the output of the system with state-based switching is plotted (solid line) to make a comparison with the observer-based switching. One can observe that for the different initial estimation errors, output y converges to the unique steady-state solution that was also obtained using the state-dependent switching rule.

The experiment as described above is repeated in real-time on the experimental setup as shown schematically in Figure 6.4. The results as obtained by these real-time experiments (gray solid lines) are given in Figure 6.9 together with the results obtained by simulation (black dashed

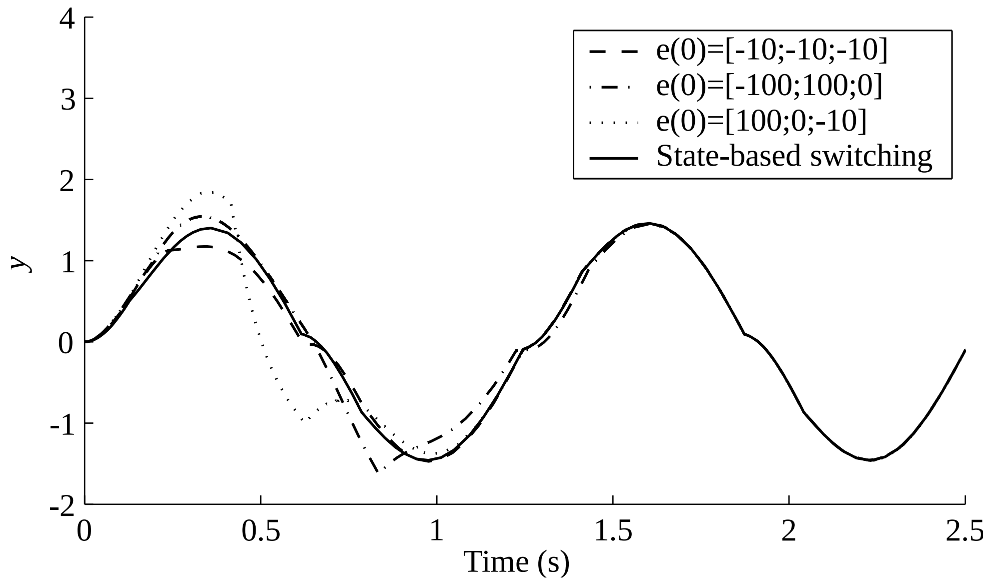

Figure 6.8: Observer-based versus state-based switching.

lines). As one can observe, the experimental results do not match with the simulation results during the transient part of the solutions, but the limit solution corresponds very well. The fact that the transient parts of the experimental results deviate from the simulation results is most likely caused by unmodeled dynamics in the experimental setup, such as the dynamics of the velocity controller. Nevertheless, after some time all solutions are converged to the limit solution, which indicates that the observer-based switching rule can also be applied successfully in real-time for this case.

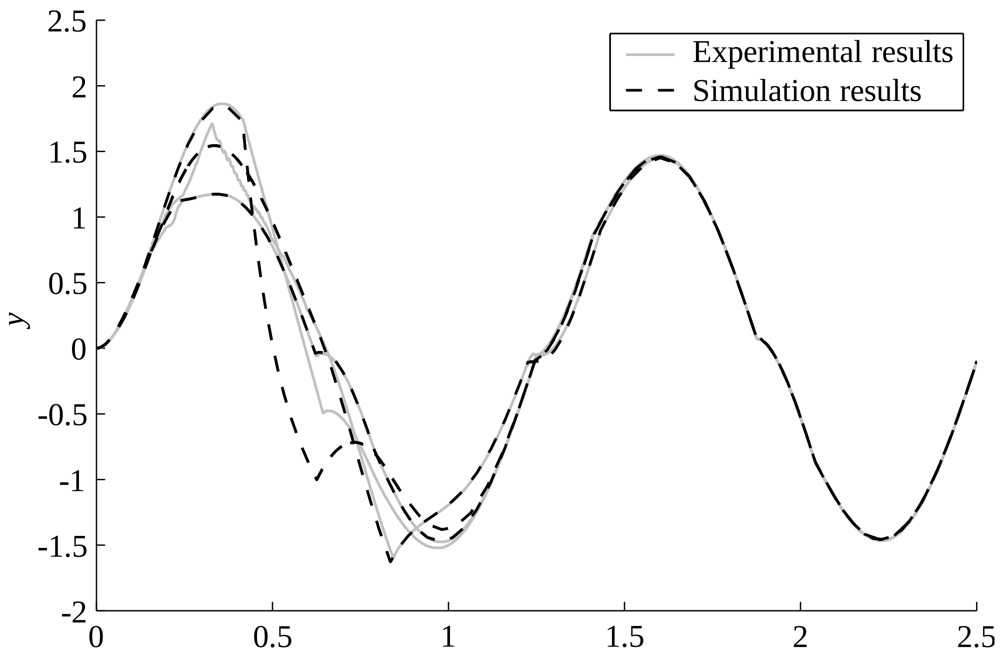

Figure 6.9: Experimental results versus simulation results.

Finally note that only the transient part of the solution is influenced by the choice of switching (i.e. state-dependent or observer-based), the limit solution is identical for both types of switching. Therefore, if the performance analysis of the previous subsection would be repeated for the observer-based switching rule, then the results would be identical to those in Figure 6.5.

6.4 Discussion

In contrast to general switched linear systems, the steady-state performance of a convergent switched linear system can be evaluated using (nonlinear) frequency response functions. As a result, the limit behavior of these systems can also be easily compared in the frequency domain to the limit behavior of linear systems. This allows one to better understand the value of switched linear systems in comparison with linear systems. In this chapter, it was shown for the case that the dynamics of all subsystems are given a priori, one can define a time-dependent, state-dependent, or observer-based switching rule that renders the closed-loop system exponentially convergent if some sufficient conditions are satisfied. By means of a case study the use of the state-dependent and observer-based switching rule was illustrated, and a comparison was made between the limit behavior of the switched system and the corresponding individual linear subsystems, for the case in which the system is externally forced with a harmonic signal.

The limit behavior as analysed in the case study was determined using simulation and experiments. The harmonic balance method, which was used in Chapters 4 and 5 as an alternative to determine the limit behavior of a system with harmonic excitation, could not be directly applied in the case study in this chapter. For a switched linear system with time-dependent switching, the harmonic balance method *can* be used, as demonstrated in e.g. [46]. However, for the state-dependent and output-dependent switching rules as presented in this chapter, this method cannot be straightforwardly applied, since the switching rule depends on both a (multi-dimensional) state x (or $\hat{x}$) and input w.

Furthermore, in this chapter only switched linear systems were considered. Switched affine systems, i.e. systems of the form $\dot{x}(t) = A_i x(t) + B_i w(t) + F_i$, where F_i is a constant matrix, were not discussed, but the results presented in this chapter can be easily extended towards this case.

Finally, it should be mentioned that although the existence of a common Lyapunov matrix, see e.g. (6.5), is not sufficient for state-dependent switching rules *in general* to guarantee an exponentially convergent system, for *some* state-dependent switching rules such a common Lyapunov matrix may not even be necessary. For systems with a *time-dependent* switching rule it is obvious that a common quadratic Lyapunov matrix is not necessary to prove exponential convergency, since roughly speaking only the average matrix $\bar{A} = (t_1 A_1 + t_2 A_2 + \ldots + t_k A_k)/\sum_{i=1}^{k} t_i$ needs to be Hurwitz, while all individual matrices A_i may have eigenvalues with a positive real part. Also, a 'switching' rule that dictates the system to remain in one exponentially stable mode, does not require a common Lyapunov matrix condition. More research is required, however, to find other *state-dependent* switching rules and less conservative conditions under which the closed-loop system is exponentially convergent.

Chapter 7

Conclusions and Recommendations

7.1 Conclusions

In this thesis, several contributions were made to the research on performance analysis of externally forced nonlinear systems, using the notion of convergent systems. These contributions are summarized in this section, and can be roughly divided into four themes: conditions for convergent systems, computationally efficient performance analysis, applications, and experimental validation. These themes correspond to the four research objectives defined in Section 1.3.

Conditions for convergent systems

In previous research, it has already been demonstrated that convergent systems, in contrast to nonlinear systems in general, have specific properties due to which detailed steady-state performance analysis (e.g. using nonlinear frequency response functions) is possible. The available results that provide sufficient conditions to prove that a system is convergent, however, are still limited. In this thesis, two new contributions were made to this field, i.e. sufficient conditions were found to prove uniform convergency for Lur'e systems, and sufficient conditions were found to prove exponential convergency for switched linear systems.

The Lur'e system that was considered, is an externally forced Lur'e system with a saturation nonlinearity and marginally stable linear part. In Chapter 4, a theorem was presented with sufficient conditions to guarantee that such a system is uniformly convergent, i.e. within a given compact set, the system is convergent with an exponential rate. The theorem was shown to be also applicable to a class of anti-windup systems with a marginally stable plant, as discussed further in subsection 'Applications'.

For the switched linear systems with external inputs, it was assumed that the dynamics of all subsystems are given a priori. For this setting, switching rules and accompanying conditions were discussed in Chapter 6 that guarantee an exponentially convergent closed-loop system. Both state-dependent, observer-based (output-dependent), and time-dependent switching rules were shown to be applicable to guarantee a convergent system under some additional conditions.

Computationally efficient performance analysis

Although simulation can be used for convergent systems to analyse the system's steady-state performance, this can be very time-consuming. In Chapter 3 of this thesis, a computationally efficient approach was presented to approximate nonlinear frequency response functions (nFRFs) for Lur'e systems with forced harmonic excitation. This approach is based on the method of harmonic linearization, and provides both a linear approximation of the nFRF and an upper bound on the error between the approximative nFRF and the true nFRF.

This computationally efficient alternative for the computation of nFRFs was illustrated by means of three examples. These examples made clear that the proposed frequency domain analysis based on harmonic linearization can provide an accurate approximation of the nFRF, and is much more time-efficient than the exact simulation-based analysis. Furthermore, the examples showed that this approximative analysis often provides more detailed information on the considered system than the often used $\mathscr{L}_2$ gain. It was also shown that for some systems, such a (finite) $\mathscr{L}_2$ gain estimate cannot even be found using a quadratic storage function (as described in Section 2.3), while the harmonic linearization approach still can provide detailed results. Finally, it was observed that the method of harmonic linearization can sometimes be misleading: if the harmonic balance equation has a unique solution, the corresponding nonlinear system can still have multiple distinct steady-state solutions, as demonstrated in Example 3.11.

Applications

In this thesis, the theoretical results on uniform convergency of Lur'e systems have been further exploited in two application fields: anti-windup systems with a marginally stable plant, and anti-windup control for discrete-event manufacturing systems.

The proof of uniform convergency for Lur'e systems as presented in Chapter 4 was shown to be also applicable to a class of anti-windup systems with a marginally stable plant. It was shown that in comparison with the performance results as obtained by existing anti-windup methods, the convergency-based performance analysis can in some cases provide more detailed information on the steady-state behavior of the system. Two case studies were performed to illustrate how the theory on uniform convergency can be applied to analyse the steady-state performance of anti-windup systems. In the first case study, which focused on a PI controlled integrator plant with actuator saturation and static anti-windup gain, the theory was used to show that the closed-loop system is convergent if the anti-windup gain is large enough. Both the case in which the system is not convergent and the case in which it is convergent were illustrated by means of simulations, and for the convergent system an nFRF was constructed, using both simulation and the method of harmonic linearization. In the second case study, which dealt with a PI controlled 'mass-spring-damper' plant with actuator saturation and static anti-windup gain, the system was shown to be uniformly convergent for a range of anti-windup gains and again an nFRF was constructed.

In Chapter 5, a PI controller with anti-windup compensation was proposed for the tracking control of a discrete-event manufacturing machine. Advantages of such a controller over existing MPC strategies are that no estimates of future customer demands are required, and that it requires less computational effort. In order to design this feedback controller, the discrete-event machine was approximated by an integrator that is preceded by a saturation nonlinearity. Using the results of Chapters 3 and 4, the use of the proposed controller was shown to result in a convergent closed-loop system with desired tracking performance. The proposed controller was subsequently implemented in the discrete-event domain and applied to the discrete-event machine. Discrete-event simulation results were compared to simulation results of the continuous approximation system, which indicated a good match between the results, as long as the processing time of the machine is relatively small in comparison with the period of the fluctuation of the reference demand. The controller was also applied for the tracking and inventory control of a discrete-event manufacturing line consisting of four machines. It was shown that in order to solve the given control problem, the reference signals for the first three machines should include some information on the production error of the direct downstream machine. A linear coupling relation was proposed to include this production error in the reference signal, which together with the anti-windup controller resulted in satisfactory tracking behavior with little inventory in the line, for the considered reference signal.

Experimental validation

Besides the simulation-based validation of the theoretical results in Chapters 4 and 6, also real-time experiments were performed. For this purpose an electromechanical setup was constructed. This experimental setup was used to generate real-time results for the case studies described in Chapter 4, in order to illustrate the (non-)convergent behavior of the system and to construct an nFRF of the considered anti-windup systems. The results were shown to match well with the simulation results in general, although for high frequencies of the input signal some mismatches were observed, which are probably caused by unmodeled dynamics. The electromechanical setup was also used to generate real-time results for the case study described in Chapter 6. In this case study, the proposed state-dependent and observer-based (output-dependent) switching rules were applied to a switched linear control system, and the exponentially convergent behavior was indicated using both simulation and real-time experiments. It was observed that the considered switching rules, which in theory allow infinitely fast switching (sliding mode), still performed well in a real-time environment, in which the sample frequency is limited. Finally, an nFRF was constructed, and it was observed that the experimental results match well with the simulation results, except for high frequencies of the input signal; here, the effect of the finite sample time of the experimental setup becomes significant.

7.2 Recommendations for future research

In the 'Discussion' sections of Chapters 3-6 several suggestions were made to extend the results obtained in this thesis. This section summarizes the main recommendations for future research.

- Currently, the notion of convergent systems is only used to *analyse* the steady-state performance of nonlinear systems. It would be very interesting to investigate if the convergent systems approach can also be extended so that it can be used to *design* for performance. One way to approach this problem can be to develop a simulation-based optimization tool, which is able to optimize certain system parameters with respect to some performance index, while preserving the conditions that are required for convergent systems. For example, in the case study in Section 4.4, it was shown that the considered system is uniformly convergent if parameter k_{A} is larger than $1/k_{\mathrm{P}}$. Using such a simulation-based optimization tool, one can determine an optimal value of k_{A}, that still satisfies $k_{\mathrm{A}} > 1/k_{\mathrm{P}}$. If the considered performance index is based on some nFRF, then instead of only simulation, one can also use the method of harmonic linearization as presented in Chapter 3, which may lead to a more time-efficient tool. Finally, another possibility to strengthen the result of the convergent system approach, is to exploit it in combination with existing synthesis or optimization algorithms. An example of this was given in Section 4.3, where by combination of an existing anti-windup design method and the proof of convergency, a stronger conclusion was obtained on the performance of the system.

- In the research field of convergent systems, most approaches are based on finding quadratic Lyapunov functions, leading in turn to quadratic convergency conditions. The theorem presented in Chapter 4 is new in the way that it leads to conditions for uniform convergency, which are less restrictive. This result may be extended in future research to prove uniform convergency for other (similar) systems. For this purpose, it may also be valuable to take into account the approach and results of [9, 20, 47], in which synchronization of Lur'e systems is studied in the presence of strongly oscillatory external signals.

- In Chapter 5 only some preliminary results were obtained in the research on anti-windup control for manufacturing systems. Other investigations should point out if the proposed controller is also applicable to more complex manufacturing systems, with for example a different structure (e.g. assembly points, networks) or different type of machines (e.g. batch machines, stochastic processing times, setup times), or what adjustments should be made to the controller for such systems. One part of the control structure that requires additional investigation is the construction of the reference signal for the upstream machines. In this thesis, the reference signal was assumed to be linearly dependent on the production error of the direct downstream machine, which resulted in satisfactory behavior of a small manufacturing line. However, it should be investigated if such a reference signal construction is also suitable for more complex manufacturing systems, starting with longer manufacturing lines.

- As mentioned in Chapter 6, the existence of a common Lyapunov function is not sufficient for state-dependent switching rules *in general* to guarantee an exponentially convergent system. However, for *some* state-dependent switching rules such a common Lyapunov function is not even necessary. For example, a ‘switching’ rule that dictates the system to remain in one exponentially stable mode, does not require this condition. Future research may lead to other state-dependent switching rules and less conservative conditions under which the closed-loop system is (exponentially) convergent.

Bibliography

[1] L.Ya. Adrianova. *Introduction to Linear Systems of Differential Equations*. American Mathematical Society, Providence, 1995.

[2] R. Alvarez-Vargas, Y. Dallery, and R. David. A study of the continuous flow model of production lines with unreliable machines and finite buffers. *Journal of Manufacturing Systems*, 13(3):221–234, 1994.

[3] D. Angeli. A Lyapunov approach to incremental stability properties. *IEEE Trans. Automatic Control*, 47(3):410–421, March 2002.

[4] D.P. Atherton. *Nonlinear Control Engineering*. Van Nostrand Reinhold, London, student edition, 1982.

[5] H.W. Bode. *Network Analysis and Feedback Amplifier Design*. Van Nostrand, Princeton, New Jersey, 1945.

[6] S. Boyd, L. El Ghaoui, E. Feron, and V. Balakrishnan. *Linear Matrix Inequalities in System and Control Theory*. SIAM Studies in Applied Mathematics, Philadelphia, 1994.

[7] A. Bradshaw and Y. Erol. Control policies for production-inventory systems with bounded input. *International Journal of Systems Science*, 11(8):947–959, 1980.

[8] M.L. Cartwright and J.E. Littlewood. On nonlinear differential equations of the second order, I: the equation $\ddot{y}+k(1-y^2)\dot{y}+y = b\lambda k\cos(\lambda t+a)$, k large. *J. London Math. Soc.*, 20:180–189, 1945.

[9] M.Yu. Churilova. Conditions of stabilization of nonlinear systems by a harmonic external action. *Automation and Remote Control*, 55(3):356–360, 1994.

[10] R.A. DeCarlo, M.S. Branicky, S. Pettersson, and B. Lennartson. Perspectives and results on the stability and stabilization of hybrid systems. *Proceedings of the IEEE*, 88(7): 1069–1082, 2000.

[11] B.P. Demidovich. Dissipativity of a nonlinear system of differential equations. *Vestnik Moscow State University, Ser. Mat. Mekh.* Part I–6 (1961) 19-27; Part II–1 (1962) 3-8 (in Russian).

[12] B.P. Demidovich. *Lectures on Stability Theory*. Nauka, Moscow, 1967.

[13] A. Doris, N. van de Wouw, and H. Nijmeijer. Disturbance attenuation for a periodically excited piece-wise linear beam system. *Proceedings of the 5th EUROMECH Nonlinear Oscillations Conference (ENOC), The Netherlands*, 2005.

[14] M.A. Dornheim. Report pinpoints factors leading to yf-22 crash. *Aviation Week and Space Technology*, 137:53–54, 1992.

[15] A. Feuer. Periodic control of linear time-invariant systems - a critical point of view. *Proceedings of the 12th IFAC World Congress*, pages VIII–145, 1993.

[16] A. Feuer, G.C. Goodwin, and M. Salgado. Potential benefits of hybrid control for linear time invariant plants. *Proceedings of American Control Conference, New Mexico, USA*, pages 2790–2794, 1997.

[17] A.F. Filippov. *Differential Equations with Discontinuous Right Hand Sides*. Kluwer Academic, Dordrecht, 1988.

[18] A.L. Fradkov. Conic S-procedure and constrained dissipativity. *ArXiv.org, math/0509718*, 2005.

[19] A.L. Fradkov and V.A. Jakubovic. The S-procedure and a duality relations in nonconvex problems of quadratic programming. *Vestnik Leningrad Univ. Math.*, 6:101109, 1979.

[20] A.L. Fradkov, G.A. Leonov, and H. Nijmeijer. Frequency-domain conditions for global synchronization of nonlinear systems driven by a multiharmonic external signal. *Proceedings of 5th European Control Conference, Karlsruhe, Germany*, 1999.

[21] G.F. Franklin, J.D. Powell, and A. Emami-Naeini. *Feedback Control of Dynamic Systems*. Addison Wesley, New York, third edition, 1994.

[22] V. Fromion and G. Scorletti. About incremental stability interest when analysing anti-windup control law performance. *14th international conference on mathematical theory of networks and systems, Perpignan*, 2000. available at `http://www.univ-perp.fr/mtns2000/articles/B228.pdf`.

[23] V. Fromion, S. Monaco, and D. Normand-Cyrot. Asymptotic properties of incrementally stable systems. *IEEE Trans. Automatic Control*, 41(5):721–723, 1996.

[24] S. Galeani and A.R. Teel. On a performance-robustness trade-off intrinsic to the natural anti-windup problem. *Automatica*, 42:1949–1861, 2006.

[25] S. Galeani, A.R. Teel, and L. Zaccarian. Constructive nonlinear anti-windup design for exponentially unstable linear plants. *43rd IEEE Conference on Decision and Control*, pages 5028–5033, 2004.

[26] S. Geary, S.M. Disney, and D.R. Towill. On bullwhip in supply chains – historical review, present practice and expected future impact. *International Journal of Production Economics*, 101(1):2–18, 2006.

[27] R. Genesio and A. Tesi. Harmonic balance methods for the analysis of chaotic dynamics in nonlinear systems. *Automatica*, 28(3):531–548, 1992.

[28] S.B. Gershwin. Hierarchical flow control: A framework for scheduling and planning discrete events in manufacturing systems. *Proceedings of the IEEE*, 77(1):195–208, 1989.

[29] G. Grimm, J. Hatfield, I. Postlethwaite, A.R. Teel, M.C. Turner, and L. Zaccarian. Antiwindup for stable linear systems with input saturation: An lmi-based synthesis. *IEEE Trans. Automatic Control*, 48:1509–1525, 2003.

[30] W. Hahn. *Stability of Motion*. Springer-Verlag, Berlin-Heidelberg, 1967.

[31] C. Hayashi. *Nonlinear Oscillations in Physical Systems*. Princeton University Press, Princeton, 1964.

[32] M. Heertjes, E. Pastink, N. van de Wouw, and H. Nijmeijer. Experimental frequency-domain analysis of nonlinear controlled optical storage drives. *IEEE Transactions on Control Systems Technology*, 14(3):389 – 397, 2006.

[33] J.M. Holtzman. *Nonlinear System Theory, A Functional Analysis Approach*. Prentice Hall, New Jersey, 1970.

[34] W.J. Hopp and M.L. Spearman. *Factory physics: Foundations of manufacturing management*. Irwin/McGraw-Hill International Editions, Singapore, second edition, 2000. ISBN 0-07-116378-6.

[35] J.C. Hsu and A.U. Meyer. *Modern Control Principles and Applications*. McGraw-Hill, New York, 1968.

[36] M. Johansson and A. Rantzer. Computation of piecewise quadratic Lyapunov functions for hybrid systems. *IEEE Trans. Automatic Control*, 43(4):555–559, 1998.

[37] U.T. Jönsson, Chung-Yao Kao, and A. Megretski. Analysis of periodically forced uncertain feedback systems. *IEEE Transactions on circuits and systems–I: fundamental theory and applications*, 50(2):244–258, 2003.

[38] D.W. Jordan and P. Smith. *Nonlinear Ordinary Differential Equations, An Introduction to Dynamical Systems*. Oxford University Press, third edition, 1999.

[39] N. Kapoor, A.R. Teel, and P. Daoutidis. An anti-windup design for linear systems with input saturation. *Automatica*, 34(5):559–574, 1998.

[40] H.K. Khalil. *Nonlinear Systems*. Prentice Hall, New Jersey, third edition, 2002.

[41] M.V. Kothare, P.J. Campo, M. Morari, and C.N. Nett. A unifed framework for the study of anti-windup designs. *Automatica*, 30(12):1869–1883, 1994.

[42] N. Krylov and N. Bogolioubov. *Introduction to Nonlinear Mechanics*. Acad. Sci. USSR, 1937. (English translation: Princeton: Princeton University Press 1947.).

[43] J.P. LaSalle and S. Lefschetz. *Stability by Liapunov's direct method with applications*. Academic press, New York, 1961.

[44] H.L. Lee, V. Padmanabhan, and S. Whang. The bullwhip effect in supply chains. *Sloan Management Review*, 38(3):93–102, 1997.

[45] E. Lefeber, R.A. van den Berg, and J.E. Rooda. Modelling manufacturing systems for control: a validation study. In *Networks of interacting machines: production organization in complex industrial systems and biological cells*, pages 101–126. World Scientific, 2005. ISBN 981-256-498-5.

[46] D. Leith, R. Shorten, W. Leithead, W. Mason, and P. Curran. Issues in the design of switched linear control systems: A benchmark study. *Int. Jnl. of Adaptive Control*, 17: 103–118, 2003.

[47] G.A. Leonov. A frequency criterion of stabilization of nonlinear systems by a harmonic external action. *Automatika i Telemekhaniba*, (1):169–174, 1986. in Russian.

[48] D. Liberzon and A.S. Morse. Basic problems in stability and design of switched systems. *IEEE Control Systems Magazine*, 19(5):59–70, 1999.

[49] W. Liu, Y. Chitour, and E. Sontag. On finite gain stabilizability of linear systems subject to input saturation. *SIAM Journal on Control and Optimization*, 34(4):1190–1219, 1996.

[50] LMI-lab. Matlab toolbox for control analysis and design. Website. `http://www.mathworks.com/`, 2008.

[51] J. Löfberg. YALMIP. Website. `http://control.ee.ethz.ch/~joloef/yalmip.php`, 2007.

[52] W. Lohmiller and J.J.E Slotine. On contraction analysis for nonlinear systems. *Automatica*, 34(6):683–696, 1998.

[53] A. Loria, E. Panteley, D. Popovic, and A.R. Teel. A nested Matrosov theorem and persistency of excitation for uniform convergence in stable nonautonomous systems. *IEEE Trans. Automatic Control*, 50(2):183–198, 2005.

[54] A.S. Matveev and A.V. Savkin. *Qualitative Theory of Hybrid Dynamical Systems*. Birkhauser, Boston, 2000.

[55] A.I. Mees. Describing functions: ten years on. *IMA Journal of Applied Mathematics*, 32:221–233, 1984.

[56] A.I. Mees and A.R. Bergen. Describing functions revisited. *IEEE Transactions on Automatic Control*, AC-20(4):473–478, 1975.

[57] A. Megretski and A. Rantzer. System analysis via integral quadratic constraints. *IEEE Trans. Automatic Control*, 42(6):819 – 830, 1997.

[58] A. Megretski and S. Treil. Power distribution inequalities in optimization and robustness of uncertain systems. *Journal of Mathematical Systems, Estimation and Control*, 3(3): 301–319, 1993.

[59] A.S. Morse. Supervisory control of families of linear set-point controllers–part 1: Exact matching. *IEEE Trans. Automatic Control*, 41(10):1413–1431, 1996.

[60] K.S. Narendra and J. Balakrishnan. Adaptive control using multiple models. *IEEE Trans. Automatic Control*, 42(2):171–187, 1997.

[61] D.E. Newland. On the methods of Galerkin, Ritz, and Krylov- Bogoliubov in the theory of nonlinear vibrations. *International Journal of Mechanical Sciences*, 7:159–172, 1965.

[62] E. Panteley, A. Loria, and A.R. Teel. Relaxed persistency of excitation for uniform asymptotic stability. *IEEE Trans. Automatic Control*, 46(12):1874–1886, 2001.

[63] A. Pavlov, A. Pogromsky, N. van de Wouw, and H. Nijmeijer. Convergent dynamics, a tribute to Boris Pavlovich Demidovich. *Systems and Control Letters*, 52:257–261, 2004.

[64] A. Pavlov, N. van de Wouw, and H. Nijmeijer. *Uniform Output Regulation of Nonlinear Systems: a Convergent Dynamics Approach*. Birkhauser, 2006. ISBN 0-8176-4445-8.

[65] A. Pavlov, A. Pogromsky, N. van de Wouw, and H. Nijmeijer. On convergence properties of piecewise affine systems. *International Journal of Control*, 80:1233–1247, 2007.

[66] A. Pavlov, N. van de Wouw, and H. Nijmeijer. Frequency response functions for nonlinear convergent systems. *IEEE Trans. Automatic Control*, 52(6):1159–1165, 2007.

[67] A. Pavlov, N. van de Wouw, A. Pogromsky, M.F. Heertjes, and H. Nijmeijer. Frequency domain performance analysis of nonlinearly controlled motion systems. *Proceedings of the 46th IEEE Conference on Decision and Control, New Orleans, USA*, 2007.

[68] I.R. Petersen, V.A. Ugrinovskii, and A.V. Savkin. *Robust Control Design Using H-infinity Methods*. Springer-Verlag, London, 2000.

[69] V.A. Pliss. *Nonlocal Problems of the Theory of Oscillations*. Academic Press, London, 1966.

[70] A.Y. Pogromsky. Passivity based design of synchronizing systems. *International Journal of Bifurcation and Chaos*, 8(2):295–319, 1998.

[71] A.Y. Pogromsky, R.A. van den Berg, and J.E. Rooda. Performance analysis of harmonically forced nonlinear systems. *Proceedings of 3rd IFAC Workshop "Periodic Control Systems", St.Petersburg, Russia*, 2007.

[72] A.Y. Pogromsky, R.A. van den Berg, and J.E. Rooda. On cascade interconnections of convergent systems with application to control of manufacturing systems. *Submitted to the 47th IEEE Conference on Decision and Control, Cancun, Mexico*, 2008.

[73] P.J. Ramadge and W.M. Wonham. Supervisory control of a class of discrete-event systems. *SIAM Journal on Control and Optimization*, 25:206–230, 1987.

[74] P.J. Ramadge and W.M. Wonham. The control of discrete event systems. *IEEE Proceedings*, 77(1):81–98, 1989.

[75] A. Rantzer and A. Megretski. Analysis of rate limiters using integral quadratic constraints. *Proceedings of IFAC Nonlinear Control Systems Design Symp., Enschede, The Netherlands*, pages 696–700, 1998.

[76] A. Rantzer and A. Megretski. Harmonic analysis of nonlinear and uncertain systems. *Proceedings of the American Control Conference, Philadelphia, Pennsylvania, USA*, pages 3654–3658, 1998.

[77] B.G. Romanuchuk and M.C. Smith. Incremental gain analysis of linear systems with bounded controls and its application to the anti-windup problem. *Proceedings of the 35th conference on Decision and Control, Japan*, 1996.

[78] E.N. Rosenwasser. *Oscillations of Nonlinear Systems*. Nauka, Moscow, 1969. in Russian.

[79] N. Rouche, P. Habets, and M. Laloy. *Stability Theory by Liapunov's Direct Method*, volume 22. Springer-Verlag, New York, 1977.

[80] H. Sandberg, E. Mllerstedt, and B. Bernhardsson. Frequency-domain analysis of linear time-periodic systems. *IEEE Trans. Automatic Control*, 50(12):1971–1983, 2005.

[81] S.S. Sastry. *Nonlinear Systems: Analysis, Stability, and Control*. Springer-Verlag, New York, 1999.

[82] A.V. Savkin and R.J. Evans. *Hybrid dynamical systems, Controller and Switching Sensor Problems*. Birkhäuser, Boston, 2002.

[83] A.V. Savkin and I.R. Petersen. Structured dissipativeness and absolute stability of non-linear systems. *International Journal of Control*, 62(2):443–460, 1995.

[84] SeDuMi. Website. `http://sedumi.mcmaster.ca/`, 2006.

[85] A. Sharifnia. Stability and performance of distributed production control methods based on continuous-flow models. *IEEE Transactions on Automatic Control*, 39(4):725–737, 1994.

[86] C.A. Shifrin. Sweden seeks cause of gripen crash. *Aviation Week and Space Technology*, 139:78–79, 1993.

[87] S. Skogestad and I. Postlethwaite. *Multivariable Feedback Control: Analysis and Design*. John Wiley & Sons, Chichester, second edition, 2005.

[88] Z. Sun. A robust stabilizing law for switched linear systems. *Int. J. Control*, 77(4): 389–398, 2004.

[89] Z. Sun and S.S. Ge. Analysis and synthesis of switched linear control systems. *Automatica*, 41:181–195, 2005.

[90] A.R. Teel and N. Kapoor. The L_2 anti-windup problem: its definition and solution. *Proceedings of the 4th European Control Conference, Brussels, Belgium*, 1997.

[91] TUeDACS. Website. `http://www.tuedacs.nl/`, 2008.

[92] D.A. van Beek, K.L. Man, M.A. Reniers, J.E. Rooda, and R.R.H. Schiffelers. Syntax and consistent equation semantics of hybrid chi. *Journal of Logic and Algebraic Programming*, 68(1-2):129–210, 2006.

[93] R.A. van den Berg, A.Y. Pogromsky, G.A. Leonov, and J.E. Rooda. Design of convergent switched systems. In *Lecture Notes in Control and Information Sciences 336: Group Coordination and Cooperative Control*, pages 291–311. Springer Verlag, 2006.

[94] R.A. van den Berg, A.Y. Pogromsky, and J.E. Rooda. Convergent systems design: Anti-windup for marginally stable plants. *Proceedings of the 45th IEEE Conference on Decision and Control, San Diego, USA*, 2006.

[95] R.A. van den Berg, A.Y. Pogromsky, and J.E. Rooda. Convergent design of switched linear systems. *Proceedings of 2nd IFAC Conference on Analysis and Design of Hybrid System, Alghero, Sardinia*, 2006.

[96] R.A. van den Berg, A.Y. Pogromsky, and J.E. Rooda. Well-posedness and accuracy of harmonic linearization for Lur'e systems. *Proceedings of the 46th IEEE Conference on Decision and Control, New Orleans, USA*, 2007.

[97] R.A. van den Berg, E. Lefeber, and J.E. Rooda. Modeling and control of a manufacturing flow line using partial differential equations. *IEEE Transactions on Control Systems Technology*, 16(1):130–136, 2008.

[98] R.A. van den Berg, A.Y. Pogromsky, and J.E. Rooda. Uniform convergency for anti-windup systems with a marginally stable plant. *Submitted to a journal*, 2008.

[99] R.A. van den Berg, A.Y. Pogromsky, and J.E. Rooda. Frequency domain performance analysis of marginally stable LTI systems with saturation. *Proceedings of the 6th EUROMECH Nonlinear Oscillations Conference (ENOC), St.Petersburg, Russia*, 2008.

[100] R.A. van den Berg, A.Y. Pogromsky, and J.E. Rooda. A new perspective on anti-windup design based on experimental results. *Proceedings of 17th IFAC World Congress, Seoul, Korea*, 2008.

[101] W.A.P. van den Bremer. Feedback control of manufacturing systems using anti-windup. Master's thesis, Eindhoven University of Technology, 2008.

[102] W.A.P. van den Bremer, R.A. van den Berg, A.Y. Pogromsky, and J.E. Rooda. Anti-windup based approach to the control of manufacturing machines. *Proceedings of 17th IFAC World Congress, Seoul, Korea*, 2008.

[103] B. van der Pol. The nonlinear theory of electric oscillations. *Proceedings of the Institute of Radio Engineers*, 22(9):1051–1086, 1934.

[104] B. van der Pol and J. van der Mark. Frequency demultiplication. *Nature*, 120(3019): 363–364, 1927.

[105] F.D. Vargas-Villamil, D.E. Rivera, and K.G. Kempf. A hierachical approach to production control of reentrant semiconductor manufacturing lines. *IEEE Transactions on Control Systems Technology*, 11(4):578–587, 2003.

[106] S. Wiggins. *Introduction to Applied Nonlinear Dynamical Systems and Chaos*. Springer, New York, second edition, 2003.

[107] V.A. Yakubovich. Minimization of quadratic functionals under the quadratic constraints and the necessity of a frequency condition in the quadratic criterion for absolute stability of nonlinear control systems. *Soviet Mathematics Doklady*, 14:593–597, 1973.

[108] V.A. Yakubovich. Nonconvex optimization problem: The infinite-horizon linear-quadratic control problem with quadratic constraints. *Systems and Control Letters*, 19 (1):13–22, 1992.

[109] V.A. Yakubovich. Matrix inequalities in stability theory for nonlinear control systems: I. absolute stability of forced vibrations. *Autom. and Remote Control*, 7:905–917, 1964.

[110] T. Yoshisawa. *Stability Theory by Liapunov's Second Method*. The Mathematical Society of Japan, Tokio, 1966.

Appendix A

Experimental Setup: System Identification

This appendix describes the identification of the dynamics of the 'mass-spring-damper' construction in the experimental setup as discussed in Section 4.5.

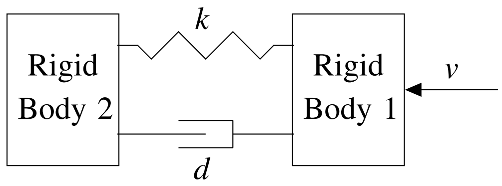

Figure A.1: Schematic representation of the 'mass-spring-damper' plant.

The 'mass-spring-damper' plant of the considered experimental setup, see Figure 4.12, consists of two rotating rigid bodies connected by an element that has a certain stiffness and damping. The dynamics of this plant are assumed to be linear, i.e. the effect of nonlinear elements (such as Coulomb friction or nonlinear spring/damper behavior) is assumed to be negligible. As a result, the dynamics of the plant, as represented schematically in Figure A.1, can be described by the following equations

$$\begin{bmatrix} \dot{r}_1 \\ \dot{r}_2 \\ \ddot{r}_2 \end{bmatrix} = \begin{bmatrix} 0 & 0 & 0 \\ 0 & 0 & 1 \\ \frac{k}{J_2} & -\frac{k}{J_2} & -\frac{d}{J_2} \end{bmatrix} \begin{bmatrix} r_1 \\ r_2 \\ \dot{r}_2 \end{bmatrix} + \begin{bmatrix} 1 \\ 0 \\ \frac{d}{J_2} \end{bmatrix} v \tag{A.1}$$

where r_1 and r_2 are the rotation angles of respectively body 1 and body 2, J_2 is the moment of inertia of body 2 with respect to its rotation axis, k is the spring constant, d is the damping constant, and v is the rotational velocity at which body 1 is driven.

As one can conclude from (A.1), only two parameters need to be estimated in order to identify the dynamics of the plant, i.e. $p_1 = \frac{k}{J_2}$ and $p_2 = \frac{d}{J_2}$. For several harmonic input signals v with different frequencies, the response (rotation angle) of body 2 was measured. Subsequently, a least-squares fit was computed on the obtained experimental data, see Figure A.2, which resulted in the following estimates of the required parameters:

$$\begin{aligned} p_1 &= \frac{k}{J_2} = 3.9 \cdot 10^3 \ \ (1/\mathrm{s}^2), \\ p_2 &= \frac{d}{J_2} = 10.7 \ \ (1/\mathrm{s}). \end{aligned}$$

These estimates are used for the case study in Section 4.5.

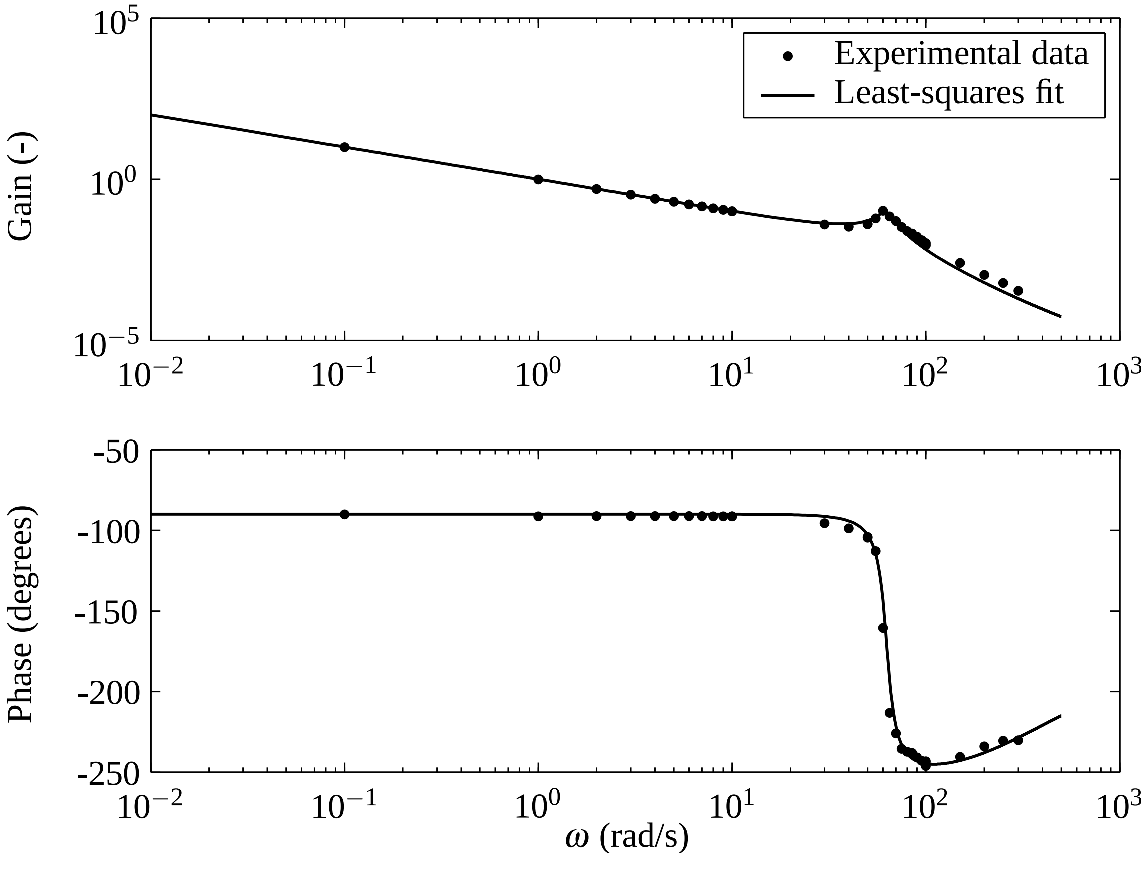

Figure A.2: Experimental data and least-squares fit with $k/J_2 = 3.9 \cdot 10^3$ and $d/J_2 = 10.7$.

Samenvatting

Prestatieanalyse is een belangrijk aspect binnen het ontwerpen van dynamische (regel)systemen. Zonder een degelijke analyse van het gedrag van een systeem, kan men onmogelijk garanderen dat een bepaald ontwerp voldoet aan de gestelde systeemeisen. Voor lineaire tijdsinvariante systemen is het relatief eenvoudig om nauwkeurige prestatieanalyses te maken. Als een gevolg hiervan zijn in het verleden ook al veel lineaire ontwerpmethodes voor (regel)systemen verschenen. Voor niet-lineaire systemen, daarentegen, zijn dit soort nauwkeurige prestatieanalyses en ontwerpmethodes over het algemeen niet beschikbaar. Een belangrijke reden hiervoor is dat niet-lineaire systemen meerdere steady-state oplossingen kunnen hebben, in tegenstelling tot lineaire tijdsinvariante systemen. Door het bestaan van meerdere steady-state oplossingen is het veel lastiger om een nauwkeurige prestatieindex te definiëren. Bepaalde niet-lineaire systemen, d.w.z. de zogenaamde convergente niet-lineaire systemen, worden echter gekarakteriseerd door een *unieke* steady-state oplossing. Deze oplossing kan wel afhankelijk zijn van de ingangssignalen (bijv. referentiesignalen) van het systeem, maar is onafhankelijk van de begincondities van het systeem. In het verleden is al gebleken dat de notie van convergente systemen erg nuttig kan zijn bij de prestatieanalyse van niet-lineare systemen met ingangssignalen.

In dit proefschrift worden nieuwe resultaten gepresenteerd op het gebied van prestatieanalyse van niet-lineaire systemen met ingangssignalen, gebaseerd op de notie van convergente systemen. Een deel van dit proefschrift is gericht op de vraag “hoe kan de prestatie van een convergent systeem geanalyseerd worden?” Omdat het gedrag van een convergent systeem onafhankelijk is van de begincondities (na een transiënte tijd), kan simulatie gebruikt worden om de unieke steady-state oplossing, die correspondeert met een bepaald ingangssignaal, te bepalen. Een dergelijke simulatie kan echter tijdrovend zijn. In dit proefschrift wordt een rekentijd-efficiëntere methode gepresenteerd voor het schatten van de steady-state prestatie van harmonisch aangedreven Lur’e systemen, in termen van niet-lineaire frequentie-responsfuncties (nFRFs). Deze methode is gebaseerd op de methode van harmonisch lineariseren. De methode resulteert in een lineaire benadering van de nFRF en een bovengrens van de fout tussen deze lineaire benadering en de werkelijke nFRF. Verschillende voorbeelden laten zien

dat de benadering van de nFRF nauwkeurig is en dat zij meer gedetailleerde informatie verschaft over het beschouwde systeem dan de veelgebruikte '$\mathscr{L}_2$ gain' prestatieindex. Verder is geobserveerd dat de methode van harmonisch lineariseren soms 'misleidend' kan zijn voor Lur'e systemen met een saturatie niet-lineariteit: het is aangetoond dat, in het geval dat de harmonische balansvergelijking een unieke oplossing heeft, het bijbehorende niet-lineaire systeem toch meerdere verschillende steady-state oplossingen kan hebben.

Een ander deel van het proefschrift is gericht op de vraag "onder welke condities is een systeem met ingangssignalen gegarandeerd convergent?" Twee typen systemen zijn onderzocht: geschakelde lineaire systemen en Lur'e systemen met een saturatie niet-lineariteit en een marginaal stabiel lineair gedeelte.

Voor de geschakelde lineaire systemen is het aangenomen dat de dynamica van de afzonderlijke lineaire subsystemen vastligt. Er is onderzocht of het mogelijk is, onder deze omstandigheden, een schakelwet te definiëren (die aangeeft wanneer er tussen de beschikbare subsystemen geschakeld moet worden), zodat het totale systeem convergent is. Zowel een toestandsafhankelijke, een waarnemerafhankelijke, als een tijdsafhankelijke schakelwet zijn gevonden die gegarandeerd tot een convergent systeem leiden, mits de dynamica van de lineaire subsystemen aan enkele voorwaarden voldoet.

Het tweede soort systemen dat onderzocht is, zijn Lur'e systemen met een saturatie niet-lineariteit en een marginaal stabiel lineair gedeelte. Het onderzoeksdoel voor dit type systemen was om voldoende voorwaarden te vinden waaronder het systeem convergent is. Vanwege het marginaal stabiele gedeelte is het echter niet mogelijk een kwadratisch convergent systeem te verkrijgen. In plaats daarvan zijn voldoende voorwaarden gevonden om uniforme convergentie van het systeem te garanderen. Het is vervolgens aangetoond dat de verkregen theorie ook toepasbaar is voor een klasse van anti-windup systemen met een marginaal stabiele machine. Voor deze klasse van systemen zijn de resultaten van de convergentie-gebaseerde prestatieanalyse vergeleken met de analyseresultaten van bestaande anti-windup methoden. Hierbij is geobserveerd dat de convergentie-gebaseerde prestatieanalyse in sommige gevallen meer gedetailleerde informatie verschaft over het steady-state gedrag van het systeem.

De resultaten van uniforme convergentie voor anti-windup systemen zijn ook toegepast in het gebied van productie- en voorraadbeheersing van discrete-event fabricagesystemen. Aangezien een productiemachine een beperkte capaciteit heeft en niet met een negatieve snelheid kan werken, kan deze machine gezien worden als een integrator (ingang: productiesnelheid, uitgang: aantal bewerkte producten) vooraf gegaan door een saturatie functie. Voor deze marginaal stabiele machine is een regelaar ontworpen, zodanig dat het totale systeem uniform convergent is. De regelaar is vervolgens geïmplementeerd in het discrete-event domein en de resultaten van discrete-event simulaties zijn vergeleken met de resultaten van continue-tijd simulaties. Op dezelfde wijze is de regelaar ook toegepast voor de productie- en voorraadbeheersing van een lijn van vier productiemachines. Voor zowel de enkele machine als de lijn van vier machines is aangetoond dat de resulterende geregelde discrete-event systemen het gewenste tracking gedrag hebben.

Naast de genoemde theoretische en numerieke resultaten zijn ook experimentele resultaten gepresenteerd in dit proefschrift. Met behulp van een elektromechanische constructie zijn verschillende experimentele resultaten verkregen. Deze resultaten zijn gebruikt om de theoretische resultaten voor zowel de geschakelde lineaire systemen als de anti-windup systemen te valideren.

Curriculum Vitae

Roel van den Berg was born on Februari 18, 1980 in Roosendaal, The Netherlands. After finishing Gymnasium at the Norbertus college in Roosendaal in 1998, he studied Mechanical Engineering at the Eindhoven University of Technology, The Netherlands. Under supervision of professor J.E. Rooda (Systems Engineering Group), he performed his graduation project on the topic 'partial differential equations in modeling and control of manufacturing systems'. After receiving the Master of Science degree cum laude in 2004, he started his PhD project in the same group. During this project he also participated in several international conferences and paid a scientific visit to professor A.L. Fradkov (Institute of Problems of Mechanical Engineering) and professor G.A. Leonov (State University, Mathematics and Mechanics Faculty), both in St. Petersburg, Russia. The main results of his PhD research are described in this thesis.